

# The osteology and affinities of *Eotyrannus lengi*, a tyrannosauroid theropod from the Wealden Supergroup of southern England (#21595)

1

First submission

## Editor guidance

Please submit by **29 Dec 2017** for the benefit of the authors (and your \$200 publishing discount).



### Structure and Criteria

Please read the 'Structure and Criteria' page for general guidance.



### Author notes

Have you read the author notes on the [guidance page](#)?



### Raw data check

Review the raw data. Download from the [materials page](#).



### Image check

Check that figures and images have not been inappropriately manipulated.

Privacy reminder: If uploading an annotated PDF, remove identifiable information to remain anonymous.

## Files

Download and review all files from the [materials page](#).

28 Figure file(s)

7 Table file(s)

2 Other file(s)



## Structure your review

The review form is divided into 5 sections.

Please consider these when composing your review:

### 1. BASIC REPORTING

### 2. EXPERIMENTAL DESIGN

### 3. VALIDITY OF THE FINDINGS

4. General comments

5. Confidential notes to the editor

 You can also annotate this PDF and upload it as part of your review

When ready [submit online](#).

## Editorial Criteria

Use these criteria points to structure your review. The full detailed editorial criteria is on your [guidance page](#).





### BASIC REPORTING

-  Clear, unambiguous, professional English language used throughout.
-  Intro & background to show context. Literature well referenced & relevant.
-  Structure conforms to [PeerJ standards](#), discipline norm, or improved for clarity.
-  Figures are relevant, high quality, well labelled & described.
-  Raw data supplied (see [PeerJ policy](#)).

### EXPERIMENTAL DESIGN

-  Original primary research within [Scope of the journal](#).
-  Research question well defined, relevant & meaningful. It is stated how the research fills an identified knowledge gap.
-  Rigorous investigation performed to a high technical & ethical standard.
-  Methods described with sufficient detail & information to replicate.

### VALIDITY OF THE FINDINGS

-  Impact and novelty not assessed. Negative/inconclusive results accepted. *Meaningful* replication encouraged where rationale & benefit to literature is clearly stated.
-  Data is robust, statistically sound, & controlled.
-  Conclusions are well stated, linked to original research question & limited to supporting results.
-  Speculation is welcome, but should be identified as such.

# Standout reviewing tips

3



The best reviewers use these techniques

## Tip

**Support criticisms with evidence from the text or from other sources**

## Example

*Smith et al (J of Methodology, 2005, V3, pp 123) have shown that the analysis you use in Lines 241-250 is not the most appropriate for this situation. Please explain why you used this method.*

**Give specific suggestions on how to improve the manuscript**

*Your introduction needs more detail. I suggest that you improve the description at lines 57- 86 to provide more justification for your study (specifically, you should expand upon the knowledge gap being filled).*

**Comment on language and grammar issues**

*The English language should be improved to ensure that an international audience can clearly understand your text. Some examples where the language could be improved include lines 23, 77, 121, 128 – the current phrasing makes comprehension difficult.*

**Organize by importance of the issues, and number your points**

1. Your most important issue
2. The next most important item
3. ...
4. The least important points

**Please provide constructive criticism, and avoid personal opinions**

*I thank you for providing the raw data, however your supplemental files need more descriptive metadata identifiers to be useful to future readers. Although your results are compelling, the data analysis should be improved in the following ways: AA, BB, CC*

**Comment on strengths (as well as weaknesses) of the manuscript**

*I commend the authors for their extensive data set, compiled over many years of detailed fieldwork. In addition, the manuscript is clearly written in professional, unambiguous language. If there is a weakness, it is in the statistical analysis (as I have noted above) which should be improved upon before Acceptance.*

# The osteology and affinities of *Eotyrannus lengi*, a tyrannosauroid theropod from the Wealden Supergroup of southern England

Darren Naish <sup>Corresp., 1</sup>, Andrea Cau <sup>2</sup>

<sup>1</sup> Ocean and Earth Science, University of Southampton, Southampton, UK

<sup>2</sup> Dipartimento di Scienze Biologiche Geologiche Ambientali, Università di Bologna, Bologna, Italy

Corresponding Author: Darren Naish

Email address: eotyrannus@gmail.com

*Eotyrannus lengi* Hutt et al. 2001 from the Lower Cretaceous Wessex Formation (part of the Wealden Supergroup) of the Isle of Wight, southern England, is described in detail, compared with other theropods, and evaluated in a new phylogenetic analysis. *Eotyrannus* is represented by a single individual that would have been c. 4.5 m long; it preserves the anterior part of the skull, a partial forelimb and pectoral girdle, various cervical, dorsal and caudal vertebrae, rib fragments, part of the ilium, and hindlimb elements excluding the femur. Lack of fusion as goes both neurocentral and sacral sutures indicates a subadult status. *Eotyrannus* possesses thickened, fused, pneumatic nasals with deep lateral recesses, elongate, tridactyl forelimbs and a tyrannosaurid-like scapulocoracoid. The short preantorbital ramus of the maxilla and nasals that are approximately seven times longer than they are wide show that *Eotyrannus* was not longirostrine. A posterodorsally inclined ridge on the ilium's lateral surface fails to reach the dorsal margin: a configuration seen elsewhere in *Juratyran*. *Eotyrannus* is not arctometatarsalian. Autapomorphies include the presence of curving furrows on the dentary, a block-like humeral entepicondyle, and a distoproximally aligned channel close to the distolateral border of the tibia. Within Tyrannosauroidae, *E. lengi* is phylogenetically intermediate between Proceratosauridae and *Yutyrannus* and the clade that includes *Xiongguanlong*, Megaraptora, *Dryptosaurus* and Tyrannosauridae. We do not find support for a close affinity between *Eotyrannus* and *Juratyran*. Our analysis supports the inclusion of Megaraptora within Tyrannosauroidae and thus increases Cretaceous tyrannosauroid diversity and disparity. A proposal that *Eotyrannus* might belong within Megaraptora, however, is based on character states not present in the taxon. Several theropods from the Wessex Formation are based on material that overlaps with the *E. lengi* holotype but none can be shown to be synonymous with it.

# The osteology and affinities of *Eotyrannus lengi*, a tyrannosauroid theropod from the Wealden Supergroup of southern England

Darren Naish, Andrea Cau

**Abstract** *Eotyrannus lengi* Hutt et al. 2001 from the Lower Cretaceous Wessex Formation (part of the Wealden Supergroup) of the Isle of Wight, southern England, is described in detail, compared with other theropods, and evaluated in a new phylogenetic analysis. *Eotyrannus* is represented by a single individual that would have been c. 4.5 m long; it preserves the anterior part of the skull, a partial forelimb and pectoral girdle, various cervical, dorsal and caudal vertebrae, rib fragments, part of the ilium, and hindlimb elements excluding the femur. Lack of fusion as goes both neurocentral and sacral sutures indicates a subadult status. *Eotyrannus* possesses thickened, fused, pneumatic nasals with deep lateral recesses, elongate, tridactyl forelimbs and a tyrannosaurid-like scapulocoracoid. The short preantorbital ramus of the maxilla and nasals that are approximately seven times longer than they are wide show that *Eotyrannus* was not longirostrine. A posterodorsally inclined ridge on the ilium's lateral surface fails to reach the dorsal margin: a configuration seen elsewhere in *Juratyran*. *Eotyrannus* is not arctometatarsalian. Autapomorphies include the presence of curving furrows on the dentary, a block-like humeral entepicondyle, and a distoproximally aligned channel close to the distolateral border of the tibia. Within Tyrannosauroidae, *E. lengi* is phylogenetically intermediate between Proceratosauridae and *Yutyrannus* and the clade that includes *Xiongguanlong*, Megaraptora, *Dryptosaurus* and Tyrannosauridae. We do not find support for a close affinity between *Eotyrannus* and *Juratyran*. Our analysis supports the inclusion of Megaraptora within Tyrannosauroidae and thus increases Cretaceous tyrannosauroid diversity and disparity. A proposal that *Eotyrannus* might belong within Megaraptora, however, is based on character states not present in the taxon. Several theropods from the Wessex Formation are based on material that overlaps with the *E. lengi* holotype but none can be shown to be synonymous with it.

**Keywords** Tyrannosauroidae *Eotyrannus* Theropoda  anurae Cretaceous Wessex Formation

D. Naish  
Ocean and Earth Science, National Oceanography Centre, University of Southampton,  
Southampton SO14 3ZH, UK

34 e-mail: eotyrannus@gmail.com

35

36 A. Cau

37

38 Dipartimento di Scienze Biologiche Geologiche Ambientali, Alma Mater Studiorum, Università  
39 di Bologna, Via Zamboni 65, I-40127 Bologna, Italy

40 Museo Geologico e Paleontologico “Giovanni Capellini”, Via Zamboni 63, I-40127 Bologna,  
41 Italy

42 e-mail: cauand@gmail.com

43

44

# Introduction

The remains of theropod dinosaurs have been known from the Wessex Formation of the Lower Cretaceous Wealden Group of the Isle of Wight, southern England, since the 1860s. Several names, including *Calamospondylus oweni*, *Aristosuchus pusillus*, *Calamosaurus foxi* and *Thecocoelurus daviesi*, are attached to these specimens. Virtually all are represented by isolated bones: a tendency to report and name additional specimens, and to re-interpret them on a fairly regular basis, has resulted in a complex taxonomy and a list of *nomina dubia* (Naish et al. 2001; Naish 2011). Baryonychine spinosaurids, carcharodontosaurian allosauroids, non-maniraptoran coelurosaurs and maniraptorans are present in the Wessex Formation assemblage. Good associated skeletons of Wessex Formation theropods were unknown prior to 1978 when the holotype of the carcharodontosaurian allosauroid *Neovenator salerii* was discovered (Hutt et al. 1996). This taxon was monographed by Brusatte et al. (2008) and recent phylogenetic work indicates that it is part of a carcharodontosaurian clade that includes diverse allosauroid taxa (Benson et al. 2010a).

A second associated Wessex Formation theropod was discovered on the Isle of Wight in 1997 and described in 2001. Given the large number of Wessex Formation theropod taxa named for fragmentary remains, it was initially assumed that the new specimen would prove referable to one of them. This proved not to be the case and the specimen was found to represent a new taxon, *Eotyrannus lengi* Hutt, Naish, Martill, Barker and Newbery, 2001. Hutt et al.'s (2001) primary contention was that *E. lengi* was a member of the tyrannosaur lineage, and specifically a non-tyrannosaurid tyrannosauroid. *E. lengi* has been discussed and partially illustrated in several publications since the appearance of that original paper (Holtz 2004; Naish et al. 2001; Naish and Martill 2007; Naish 2011) but a comprehensive description and analysis has been absent until now.

*E. lengi* is of substantial interest to those who specialise on the Lower Cretaceous theropods of the UK, those of the Wealden Supergroup in particular. However, its global significance lies in the fact that it provides substantial new information on the early evolution of tyrannosauroids, and potentially on their ecology and interaction with other theropod and dinosaur lineages. Following recognition of the fact that the tyrannosaurids of the Late Cretaceous are not carnosauroids but actually coelurosaurs (Holtz 1994), it became more likely that small "proto-tyrannosaurs" with elongate, tridactyl or tetradactyl forelimbs should await discovery in Jurassic or Lower Cretaceous strata. *E. lengi* validated this prediction, and recent finds show that it is only

one of several non-tyrannosaurid members of the coelurosaurian clade Tyrannosauroida, some of which are as old as Middle Jurassic. Since *E. lengi* was named in 2001, it has been joined by *Aviatyrannis jurassica* from the Kimmeridgian Alcobaça Formation of Portugal (Rauhut 2003a), *Dilong paradoxus* from the Lower Cretaceous Yixian Formation of China (Xu et al. 2004), *Guanlong wucaii* from the Oxfordian Shishugou Formation of China (Xu et al. 2006), *Sinotyrannus kazuoensis* from the Albian Jiufotang Formation of China (Ji et al. 2008) and *Kileskus aristocus* from the Bathonian Itat Formation of Siberia in western Russia (Averianov et al. 2010). It has also become better established that the Late Jurassic *Stokesosaurus*, originally named for the Morrison Formation species *S. clevelandi* from the USA, originally suggested to be an early tyrannosaurid (Madsen 1974), is also an early-diverging tyrannosauroid. The British tyrannosauroid *Juratyran langhami* from the Tithonian Kimmeridge Clay Formation, first described as a new species of *Stokesosaurus* (Benson 2008), is distinct from *S. clevelandi* in several respects, notably possessing a narrow, posterodorsally inclined ridge on the lateral surface of its ilium that stops short of the ilium's dorsal margin. This configuration is present elsewhere (namely in *Eotyrannus*) but is not present in *S. clevelandi* or other tyrannosauroids (Brusatte and Benson 2013). New analyses of *Proceratosaurus bradleyi* from the Bathonian Taynton Limestone Formation of the UK (Rauhut et al. 2010) and *Dryptosaurus aquilunguis* from the Maastrichtian New Egypt Formation of the USA (Brusatte et al. 2011) have established that these taxa are additional members of the tyrannosauroid radiation. Furthermore, both *Xiongguanlong baimoensis* from the Aptian-Albian Xinminpu Group of western China (Li et al. 2009) and *Yutyrannus huali* from the the Lower Cretaceous Yixian Formation of China (Xu et al. 2012) have been recovered as outside the *Dryptosaurus* + Tyrannosauridae clade (Brusatte et al. 2011) while *Appalachiosaurus montgomeriensis* from the Demopolis Formation of the USA (Carr et al. 2005) and *Bistahieversor sealeyi* from the Campanian Kirtland Formation of the USA (Carr and Williamson 2010) are larger-bodied taxa successively closer to Tyrannosauridae and more like tyrannosaurids in cranial and other characters. It has also been proposed that *Bagaraatan ostromi* from the Maastrichtian Nemegt Formation of Mongolia (Osmólska 1996) and *Santanaraptor placidus* from the ?Albian Santana Formation of Brazil (Kellner 1999) might be non-tyrannosaurid tyrannosauroids (Holtz 2004, Choiniere et al. 2010). *Mirisichia asymmetrica*, also from the Santana Formation, has mostly been interpreted as a compsognathid (Naish et al. 2004, Peyer 2006, Rauhut et al. 2010) on the basis of its strong similarity with *Compsognathus*. However, the presence of a similarly proportioned pubis in *Dilong* (where the pubic foot is proportionally long and lacks an expansion anterior to the shaft; Xu et al. 2004), and the presence



of what appears to be a dorsal concavity on the preacetabular process of the ilium (but see Brusatte et al. 2014 for a taphonomic interpretation of that feature) and a concave anterior margin to the pubic peduncle (characters typical of tyrannosauroids; Rauhut 2003a, b, Xu et al. 2004, 2006, Benson 2008, Brusatte and Benson 2013) renders it possible that *Mirisichia* might also be a tyrannosauroid. A few other theropod taxa not typically considered part of Tyrannosauroidea have been hypothesized to be additional members of the group, namely *Tanycolagreus topwilsoni* and *Coelurus fragilis* from the Morrison Formation: both were recovered as early-diverging tyrannosauroids by Senter (2007, 2010). Several additional studies have supported a tyrannosauroid placement of *Tanycolagreus* (Carr and Williamson 2010; Brusatte et al. 2014).

A robust phylogenetic framework now exists for Tyrannosauroidea (Li et al. 2009; Loewen et al. 2013; Brusatte et al. 2010, 2011; Brusatte and Benson 2013; Brusatte and Carr 2016). While conflicting results have led to uncertainty about the topology at the base of the clade, these differences are in part due to incomplete sampling. Holtz (2004) recovered a mostly pectinate arrangement for non-tyrannosaurid tyrannosauroids, and found *E. lengi* to be closer to Tyrannosauridae than were *Bagaraatan*, *Stokesosaurus* and *Dryptosaurus*. Senter (2007, 2010) found *E. lengi* to be closer to Tyrannosauridae than were *Guanlong* and *Dilong*. Li et al. (2009) found *E. lengi* and *Dilong* to form a polytomy with a *Xiongguanlong* + Tyrannosauridae clade, and to be closer to the latter than *Proceratosaurus* and *Guanlong*. Brusatte et al. (2010) and Brusatte and Carr (2016) recovered *E. lengi* as belonging to a clade that also included *Stokesosaurus* and *Juratyran* and was closer to Tyrannosauridae than to *Dilong* and Proceratosauridae, Rauhut et al. (2010, fig. 24) depicted *E. lengi* as part of an unresolved polytomy alongside Proceratosauridae, *Aviatyrannis*, *Stokesosaurus* and a *Dilong* + Tyrannosauridae clade, and Loewen et al. (2013) found *E. lengi* closer to a *Dryptosaurus* + Tyrannosauridae clade than were Proceratosauridae and *Dilong*. Finally, the enigmatic tetanuran clade Megaraptora has recently been placed among non-tyrannosaurid tyrannosauroids by Novas et al. (2013). This controversial hypothesis was further corroborated by the discovery of several tyrannosauroid-like features in a new specimen of *Megaraptor* (Porfiri et al. 2014); these authors also found *Eotyrannus* among megaraptorans, though did note that corroboration was required. The substantial new character information described in the present study allows us to better establish the phylogeny of Tyrannosauroidea.

# Institutional abbreviations

**IWCMS**, Dinosaur Isle Visitor Centre, Isle of Wight County Museums Service, Sandown, UK; **MIWG**, Museum of Isle of Wight Geology, Sandown, UK (collection now incorporated into that of IWCMS); **NHMUK**, The Natural History Museum, London, UK; **UOP**, University of Portsmouth, Portsmouth, UK. NB – IWCMS accession numbers have been published in a number of different ways. Naish et al. (2001) and Hutt (2002) used the convention ‘IWCMS.1997.550’ and Hutt et al. (2001) used the convention ‘IWCMS 1997.550’. The preferred way (D. Pemberton, pers. comm. 2003) is ‘IWCMS : 1997.550’ and this convention is adopted here.

## Context and history of discovery

The *E. lengi* holotype was discovered in September 1997 by amateur collector Gavin Leng approximately 12 m above beach level near Grange Chine on the south-west coast of the Isle of Wight (Fig 1). As is the case for most Isle of Wight dinosaur specimens, it was preserved in a plant debris bed of the Barremian (Allen and Wimbledon 1991) Wessex Formation. The Wessex Formation is a red-bed sequence that comprises varicolored mudstones interbedded with sandstones and subordinate intraformational conglomerates, crevasse splay deposits and plant debris beds (Stewart 1978, 1981; Insole and Hutt 1994). It was deposited on a near-shore floodplain crossed by a large west-to-east meandering river (Radley 1994; Wright et al. 1998). Plant debris beds (sensu Oldham 1976) represent fusain-rich units formed of siltstone and mudstone; they are mostly less than 1 mm thick so the thickness of the bed that yielded *E. lengi* may indicate that it was deposited following an especially large or severe flood event. Stewart (1978, 1981) regarded plant debris beds as representing extrabasinal flood events that carried debris onto the Wessex Formation alluvial plain, but Insole and Hutt (1994) argued that they were the result of local storm events and hence that any incorporated material was of local origin. The rarity of *E. lengi* has led to the speculation that it was not an inhabitant of the floodplain or its immediate surrounds (Naish et al. 2001). Stewart (1978) assigned bed numbers to each of the plant debris beds within the Wessex Formation and *E. lengi* was recovered from L11, the plant debris bed above the Grange Chine Sandstone (Fig 2).

Leng initially recovered only a manual ungual from the site; he took this to S. Hutt (then curator at the Museum of Isle of Wight Geology, Sandown). Hutt realised its significance and (with P. Newbery) visited the site and removed the rest of the skeleton from the outcrop (Hutt et al. 2001; Naish 2001; Hutt 2002). The nature of the matrix in which the specimen was preserved made both initial recovery, and preparation in the laboratory, slow and difficult.

PLACE FIGURE 1 ABOUT HERE

PLACE FIGURE 2 ABOUT HERE

# Systematic Palaeontology

Theropoda Marsh, 1881

Tetanurae Gauthier, 1986

Coelurosauria Huene, 1914

Tyrannosauroida Osborn, 1905

*Eotyrannus lengi* Hutt et al., 2001

**Holotype.** A partial, disarticulated skeleton (IWCMS : 1997.550) consisting of the anterior portion of the skull, a partial forelimb and pectoral girdle, several cervical, dorsal and caudal vertebrae, rib fragments, part of the ilium, and elements of both hindlimbs. The taxon is known from the holotype alone.

**Locality and horizon.** The holotype was recovered from Grange Chine on the south-west coast of the Isle of Wight, from the L11 plant debris bed above the Grange Chine Sandstone of the Wessex Formation of the Wealden Supergroup. It dates to the Barremian.

## The osteology of *Eotyrannus lengi*: general comments

The holotype of *Eotyrannus lengi* is – after the holotype of *Neovenator salerii* Hutt et al., 1996 (NHMUK R10001/MIWG 6348) (Hutt et al. 1996, 2001; Naish et al. 2001; Brusatte et al. 2008) – the most complete theropod yet reported from the Wessex Formation. However, while the *E. lengi* holotype includes a substantial number of bones, many of them are fragmentary and/or broken. The specimen suffers from being embedded within particularly hard sideritic mudstone. Consequently, matrix remains adhered to some of the elements and it should be emphasised that, where matrix obscures part of a given element, the matrix cannot be removed without risk of substantial damage.

The taphonomy of the *E. lengi* holotype was discussed by Hutt et al. (2001, p. 240) and Martill (2001). Several images exist of the specimen prior to its preparation and provide data on the original orientation and disposition of its various bones. Evidently, the skeleton was

substantially disarticulated prior to fossilisation, with elements scattered throughout the area in which the specimen is preserved. None of the vertebrae, for example, are preserved in articulation. Those that are preserved consist of separated neural arches and centra, indicating that the holotype was skeletally immature (Brochu 1996); it is inferred to represent a subadult pending histological analysis. Given that the *E. lengi* holotype represents an individual that we estimate at c. 4.5 m in length (see discussion below), this raises the question as to how large an adult of the species was. While this remains unknown, we suggest on the basis of the subadult condition of the specimen that adult length was not much greater.

The only elements that retain close natural association are the left scapula and coracoid and the left tibia, fibula and metatarsal IV. Much of the skull is preserved, though the bones are mostly disarticulated, broken and/or distorted during diagenesis. Some delicate fragments, including an unidentified fragment of mandibular bone and a palatine, are nevertheless well preserved. Hutt et al. (2001, p. 240) suggested that fractured ends present on some of the bones are indicative of pre-burial trampling. However, there are no clear indications of trampling, such as splintered bone or spiral fractures (Hill 1980; Bilbey 1999). Bones and teeth from a dryosaurid (assumed to be *Valdosaurus* sp. and accessioned as IWCMS : 1997.885) are jumbled among the remains of *E. lengi*. These remains were discussed by Barrett et al. (2011).



## The cranial skeleton

*E. lengi* holotype preserves more cranial material than any other Wessex Formation theropod, including the holotype of *Neovenator salerii*.

Most of the unambiguously identified cranial bones of *E. lengi* belong to the part of the skull anterior to the orbit. However, the right surangular and right quadrate are preserved as well. Some of the description provided here necessarily repeats information previously included within Hutt et al. (2001). For measurements of cranial elements, see Table 1.

## Premaxilla

The right premaxilla of *E. lengi* consists of an almost complete premaxillary body and the base of the nasal process (Fig. 3a–e). The premaxillary ventral margin is mostly complete but its posterior and posterodorsal margins are damaged. Dorsally, the ventral edge of the naris is preserved adjacent to the base of the nasal process, though this is partly obscured by irremovable matrix on the lateral side.

The premaxillary body is slightly longer than it is tall, being 30 mm deep subnarily compared to its length of 36 mm, this resulting in a length/height ratio of 1.2. It appears to be proportionally small relative to the maxilla. As described by Hutt et al. (2001), the premaxillary body is typical for tyrannosauroids in having a high premaxillary angle of 90°. This recalls the condition present in *Guanlong* (Xu et al. 2006), *Proceratosaurus* (Rauhut et al. 2010), tyrannosaurids (Brochu 2003; Currie 2003; Hurum and Sabath 2003) and the premaxilla referred to *Stokesosaurus* by Madsen (1974) (but see Benson (2008)). Reconstructions that show the premaxilla of *E. lengi* as having a sloping anterior border (Naish et al. 2001, text-fig. 9.31; Holtz 2004, fig. 5.25) are inaccurate. As noted by Hutt et al. (2001), the premaxillary body expands mediolaterally as it extends ventrally, thus being shaped like a triangle with the apex oriented dorsally when seen in anterior view. The posterior part of the body adjacent to the maxillary contact is eroded and the maxillary process is absent.

The lateral surface is partly obscured by adhering matrix that covers the region medial to the anteroventral border of the narial fossa. Numerous small foramina are present across the lateral surface of the premaxillary body, the largest of which are situated near the bone's anterior border. Some of the foramina are located within short, shallow canals that are mostly oriented posteroventrally (Hutt et al. 2001). A shallow, indistinct groove housing numerous foramina extends ventrally from the anteroventral corner of the external naris. This structure is likely homologous with similar indistinct grooves present in *Guanlong* (Xu et al 2009) and *Proceratosaurus* (Rauhut et al. 2010).

The nasal process is incomplete, consisting only of its base, and is subtriangular in cross-section. It extends vertically from the premaxillary body and then curves slightly laterally (Fig. 3d–e). This might be due to distortion as there are several cracks at its base. In medial view, the nasal process has a relatively anteroposteriorly long exposure. In lateral view, the anteroposterior exposure is short because the posterior edge of the process is emarginated by a weakly developed narial fossa, part of which is infilled by matrix.

Four subcircular alveoli are present (Fig 3c). These are smaller than those on the dentary and maxilla. With both premaxillae imagined in articulation, the premaxillary arcade is broad and U-shaped (Hutt et al. 2001) and the second tooth would have been located almost as far anteriorly as the first. The third tooth would have been located as far anteriorly as the posterior margin of the second tooth, and the fourth tooth would have been located as far anteriorly as the posterior margin of the third tooth. Distinct interdental plates are not visible on the medial surface of the premaxilla, and they may either have been absent or fused to the medial surface. The latter

scenario is more likely in view of the fact that plates are present in the maxilla and dentaries (Fig 3b). However, a poorly developed vertical groove does appear to correspond to the junction between the second and third plates. Regardless, the medial surface of the premaxillary body dorsal to the plates is perforated by several foramina, the anterior-most of which is located posterodorsal to the first alveolus and close to or at the junction between what appears to be the first plate and the rest of the medial surface. This is also the largest foramen on the medial surface: it is at the anterior end of a line of perhaps four foramina, the most posterior of which is present close to the posterior border of the premaxilla and dorsal to the fourth alveolus. All of these foramina are in a position equivalent to the junction between the fused interdental plates and the rest of the medial surface. The medial surfaces of the plates are covered with far smaller foramina connected by tiny, fine canals. The medial alveolar border is at the same level as the lateral margin of the premaxillary body.

PLACE FIGURE 3 ABOUT HERE

## Maxilla

Only the preantorbital ramus of the left maxilla is preserved (Fig. 3f–i), although a poorly preserved, fragmentary element tentatively identified as a partial right maxilla is preserved within a block where it is held together by matrix. The fragment of left maxilla preserves intact anterior, anterodorsal margins and ventral margins but is broken posterior to the anteriormost rim of the antorbital fossa. Only the base of the nasal ramus is preserved, projecting posterodorsally at approximately 45°. Overall, the preserved portion is 95 mm long and has a maximum height of 72 mm. Posteriorly, the edge of the nasal ramus is continuous with the anterior rim of the bony margin of the antorbital fossa (Fig 3f). Medial to the rim is a dorsally convex posteroventral section of maxilla that would have formed part of the wall of the antorbital fenestra ventral to the maxillary foramen.

The anteroventral rim of the antorbital fossa is sharply delineated and thus comparable to that of a number of other coelurosaurs, including *Proceratosaurus*, *Scipionyx* and members of Compsognathidae and Tyrannosauridae (Currie and Dong 2001; Hwang et al. 2004; Xu et al. 2004; Rauhut et al. 2010; Dal Sasso and Maganuco 2011). The prominence of this rim varies with ontogeny in tyrannosaurids: Carr and Williamson (2004, p. 517) noted it is prominent in juveniles but obliterated during adulthood as the maxilla becomes thicker. Its sharp delineation in *E. lengi* may therefore be an ontogenetic feature.



The body of the maxilla is thick. An anterior ramus, like that present in *Guanlong* (Xu et al. 2006), *Proceratosaurus* (Rauhut et al. 2010) and *Sinotyrannus* (Ji et al. 2009), is absent but a prominent change in the angle of the anterior margin is obvious: the anteriormost margin is inclined at an angle of c 70° relative to the alveolar margin while the anterodorsal section of the margin is inclined at a shallower angle of c 30° relative to the alveolar margin. The overall impression is of a short, truncated preantorbital ramus. This indicates that *E. lengi* was not longirostrine as are such tyrannosauroids as *Guanlong*, *Dilong* and *Xiongguanlong* (Xu et al. 2004, 2006; Li et al. 2009). A furrow on the anteromedial part of the maxilla probably received the maxillary process of the premaxilla like that present in *Kileskus*, *Guanlong* and *Proceratosaurus* (Xu et al. 2006; Averianov et al. 2010; Rauhut et al. 2010) while a slot dorsal to this furrow may have received the premaxillary process of the nasal. The part of the maxilla between these two articular facets is dorsally convex and does not appear to have been overlapped by any bony process. Accordingly, this part of the maxilla probably contributed to the ventral part of the external naris. A long, slender maxillary process that contacts the premaxillary process of the nasal is typical for tyrannosauroids, even in those with an enlarged external naris (Brochu 2003; Xu et al. 2006; Ji et al. 2009; Rauhut et al. 2010; Averianov et al. 2010). A small notch 26 mm dorsal to the lateral alveolar margin appears to mark the position of the subnarial foramen.

The lateral surface of the maxilla is flat. Foramina of diverse sizes are scattered across this surface: a row of tiny foramina are aligned along the ventral margin, adjacent to the alveolar margin, while larger foramina, some of which are at the dorsal ends of short channels (Hutt et al. 2001), are present across the more dorsal part of the surface. A series of deep depressions are arranged in an approximate line some distance dorsal to this margin. Several small foramina are present within these depressions. This line of structures might be homologous with the alveolar row of foramina present in *Guanlong*, *Proceratosaurus* and tyrannosaurids (Currie 2003; Xu et al. 2006; Rauhut et al. 2010). Several poorly differentiated depressions are present in the anteroventral region of the maxilla, one of which is deeper than the others. This is suggestive of the novel maxillary opening present in *Guanlong* (Xu et al. 2006) but is less close to the premaxillary contact. This density of apparently pneumatic structures implies that *E. lengi*'s maxilla was highly pneumatised, at least in its ventral third or so. The ventral alveolar margin of the bone is straight.

On the medial surface, the maxillary shelf is present dorsal to the alveolar margin (Fig 3h). The shelf has a subtle posterodorsal inclination and is only as long as the base of the ascending

process; its posterior end terminates with an irregular break meaning that its full extent is unknown. The shelf's anterior part is smooth medially and forms a concave facet for articulation with (presumably) the palatal shelf of the opposing maxilla: a similar facet was illustrated for *Tarbosaurus bataar* (Hurum and Sabath 2003). The anterior end of the shelf bears a horizontally oriented groove for articulation with the premaxillary palatal process. The short medial extension of the maxillary shelf shows that maxillary contribution to the palate was modest. Dorsomedial to the shelf, five crater-like concavities are present, the largest (*c.* 20 mm long) and most posterior of which probably represents part of a promaxillary recess. It is assumed that these concavities are pneumatic in origin, in which case the dorsomedial part of the preantorbital ramus at least was extensively pneumatised.

Immediately ventral to the palatal shelf, a damaged strip of maxillary wall is marked with a series of poorly defined concavities, at least two of which appear to have a one-to-one correspondence with the more ventrally positioned interdental plates. The homology of these concavities is uncertain but it is possible that they were formed during life by the tips of the dentary teeth: in tyrannosaurid specimens preserved with closed jaws, the dentary teeth are found resting in similar concavities (Currie 2003). Concavities of this sort are known for tyrannosaurids of all main lineages (Currie 2003; Brusatte et al. 2012). Five interdental plates are present, though the anterior three are poorly differentiated from the rest of the maxilla and from one another. The two posterior plates are deep relative to the overall height of the maxilla. They are deeper than they are long and subpentagonal: that is, subrectangular though with ventral edges that taper to a point. Interdental plates of this form are typical for tyrannosauroids (Currie 2003; Brusatte et al. 2011). They are separated by a vertical gap that is confluent at its dorsal end with a subhorizontal fissure – the groove for the dental lamina – that separates the interdental plates from the rest of maxilla. The plates are covered with a slightly different texture from the rest of the maxilla: fine, irregularly oriented anastomosing grooves and small foramina cover their medial surfaces. A texture consisting of tiny pits appears to be typical for tyrannosauroids (Currie 2003; Rauhut et al. 2010; Brusatte et al. 2012); however, anastomosing grooves like those present in *E. lengi* do not otherwise seem to be a tyrannosauroid feature. Interdental plates are typically not fused in tyrannosauroids (e.g. Currie 2003; Hurum & Sabath 2003; Averianov et al. 2010; Rauhut et al. 2010; Brusatte et al. 2011, 2012), though *Tanycolagreus* appears to be an exception (Carpenter et al. 2003).

If the large opening present anterolaterally on the maxilla is the maxillary fenestra, then *E. lengi* lacked a promaxillary fenestra. Though primitively present in Theropoda, this structure was



lost several times (Rauhut 2003b). However, it is also possible that the preserved opening is the promaxillary fenestra, and that the maxillary fenestra was located posterodorsal to it and hence not preserved (Fig 3j). This latter alternative would imply that the promaxillary fenestra of *E. lengi* must have been proportionally large compared to that of *Guanlong*, *Dilong*, *Proceratosaurus*, *Bistahieversor* and tyrannosaurids (Xu et al. 2004, 2006; Carr et al. 2005; Carr and Williamson 2010; Rauhut et al. 2010; Brusatte et al. 2012). The promaxillary fenestra is both comparatively large, and visible in lateral view, in some maniraptorans (Currie and Varricchio 2004). However, the typical condition for tyrannosauroids is that the promaxillary fenestra is smaller than the maxillary fenestra and tucked up against the rim of the antorbital fossa such that it is partly concealed from lateral view (Xu et al. 2004, 2006; Carr et al. 2005; Carr and Williamson 2010; Rauhut et al. 2010; Brusatte et al. 2012). This strengthens the view that the opening preserved in *E. lengi* is the maxillary fenestra, and that the promaxillary fenestra was absent (Fig 3k). It is also possible that the preserved opening is a combined promaxillary-maxillary fenestra. *Monolophosaurus* exhibits only a single opening in the anteroventral part of its antorbital fossa (Zhao and Currie 1993), and while it is in the right place to be a promaxillary fenestra, it appears too large for this, leading Witmer (1997, p. 44) to propose that the two fenestrae had been united by the loss of the promaxillary strut. The presence of this large anterior opening, overlapped ventrolaterally by the lateral surface of the maxilla, is tentatively interpreted as a possible autapomorphy of *E. lengi*: ultimately, poor preservation limits our ability to be confident about the anatomy of this region. The maxillary alveoli are subrectangular, being longer than wide, with thin bony walls separating one alveolus from the next. Five alveoli are present, though the fifth is represented only by its anterior-most 5 mm and only the third and fourth can be measured accurately (Fig 3h).

### Nasals

Both conjoined nasals are known for *E. lengi*. They are thick and dorsally convex in their anterior two-thirds, the two meeting at their suture at a low angle to create a vaulted anatomy. Posteriorly, they are flattened and with raised posterolateral crests. Both nasals are marked on their dorsal surfaces with large foramina. Both are fused into a single unit with an obliterated suture, although this fusion is incomplete posteriorly: here, the two nasals are distinct and separated by a suture on the dorsal side. A keel representing the suture between the two nasals is visible on the ventral surface (Fig 4).

The left nasal is damaged anteriorly and the narial border is absent, only part of the premaxillary process being preserved. The right nasal is more complete, preserving part of the border to the external nasal though the anterior tip of both its premaxillary process and subnarial process are missing. This damage to the anterior parts of both nasals mean that it cannot be determined whether nasal fusion had occurred in this region. Nevertheless, the preserved anterior regions are fully fused. In overall form, the fused nasals are highly similar to those of tyrannosaurids (Hutt et al. 2001; Currie 2003; Currie et al. 2003; Hurum and Sabath 2003; Holtz 2004; Snively et al. 2006; Brusatte et al. 2012) and, to a lesser degree, those of *Guanlong* and *Dilong* (Xu et al. 2004, 2006). The fused nasals of *E. lengi* are far longer, proportionally, than those of *Guanlong* or *Dilong*: in these taxa, the fused nasals are approximately four times longer than they are wide at mid-length (Xu et al. 2004, 2006) whereas the fused nasals of *Eotyrannus* have a far more ‘stretched’ middle section meaning that they are approximately seven times as long as they are wide at mid-length. The latter condition is much like that of tyrannosaurids (Currie 2003; Hurum and Sabath 2003; Brusatte et al 2012). The fact that the fused nasals are not especially slender relative to those of longirostrine tyrannosauroids like *Alioramus* (Brusatte et al 2012) – combined with the shape of the preantorbital ramus of the maxilla – again indicates that *E. lengi* was not longirostrine.

On the right side, the border of the external naris is well preserved and the right ventral premaxillary process is present (though broken), while on the left both structures are absent. At mid-length the fused nasals have a maximum width of 33 mm, and they are widest 15 mm anterior to the posterior end. As noted above, the fused nasals are dorsally convex for most of their length, but the posterior 60 mm or so form a flattened region bounded laterally by low ridges. The nasals are similar in width for the anterior two-thirds or so of their length but widen gradually posteriorly, becoming dorsoventrally flattened as they do so. Five particularly large, asymmetrically arranged dorsal and dorsolateral foramina are present across the middle part of the nasals; the three largest and most prominent are on the right nasal where two are close to the midline and one is closer to the lateral edge (Fig 4c). All of these foramina are deep and subcircular or oval: they have measurements of 6 × 4 mm, 6 × 7 mm, 9 × 4 mm, 8 × 4 mm, and 7 × 5 mm, respectively. A sixth, posteriorly located concavity, positioned on the left nasal and close to the midline, is more elongate anteroposteriorly than these foramina (19 × 3 mm) and may be the result of fusion between two foramina. Some ambiguously shaped concavities cannot be identified as foramina with certainty but probably represent additional examples. Small, widely scattered foramina are common on the nasals of tyrannosauroids (Currie 2003; Hurum and Sabath

2003; Xu et al. 2004; Snively et al. 2006; Brusatte et al. 2012) but no taxon described thus far has foramina that appear as proportionally large as those of *E. lengi*. Some *Tyrannosaurus rex* specimens come closest (Snively et al. 2006).

The premaxillary process of the right nasal diverges laterally as it extends anteriorly (Fig 5b). This indicates that the two medial processes were spread apart to form a V-shaped notch for reception of the dorsal processes of the premaxillae, as is typical for tyrannosauroids. The preserved border of the right external naris describes a portion of an arc that corresponds to a subovoid form but only the shape of the posterior border of the naris can be determined. However, the subnarial process may be slightly displaced dorsomedially, meaning that the naris may originally have been deeper. The latter process extends 10 mm anteroventral to the main body of the right nasal and is square in cross-section. The lateral surface of the premaxillary process bears a flat facet, 6 mm tall dorsoventrally, that continues posteriorly and extends along the lateral surface of the right nasal body for c. 60 mm. The margin of the nasal bearing this facet (for reception of the nasal ramus of the maxilla) is missing from the left side.

Posterior to this facet, the lateral surface of the right nasal possesses a deep subtriangular embayment 53 mm long (Fig. 4b, 5a), here termed the lateral recess. It does not resemble the concave lateral structures seen on the nasals of allosauroids since those are clearly confluent with the antorbital fossa and are not separated from it by a prominent rim (Rauhut 2003b), nor can it be for reception of the lacrimal, as suggested by Hutt et al. (2001, p. 230), since it is positioned too far anteriorly. It appears that the recess in *E. lengi* is dorsal to the antorbital fossa and was not continuous with it. The recess is deepest posteriorly, increasing in height from 3 mm anteriorly to 9 mm posteriorly. Its ventral floor is flat and smooth; the ventral side of the recess, however, bears a sharp, low, lateral ridge that extends the full length of the recess and meets the dorsal margin at an acute angle. The dorsal margin of the recess has a convex lateral edge that is continuous with the dorsal surface of the nasal and marks the junction between the lateral and dorsal surfaces of the nasal. Internal vertical bony struts indicate some form of partitioning of this recess, although damage and matrix infill preclude a full investigation of their morphology. A vertical lamina extends from the floor to the roof of the recess c. 30 mm from the recess's anterior end; what appears to be another lamina is located closer to the posterior end. The lateral recess on the left side is similar but with less well preserved margins, and extends further posteriorly than the recess on the right side, being 70 mm long. At least one vertical lamina is present 36 mm posterior to the recess's anterior end. It is inclined posterodorsally.

Pneumatic recesses of various kinds have been reported in some other theropod nasals. The abelisaurid *Majungasaurus atopus* possesses a subcircular recess, continuous with internal hollows, half-way along each nasal (Sampson et al. 1998; Tykoski and Rowe 2004). Nasal recesses are also present in *Monolophosaurus* and members of Allosauroidea (Madsen 1976; Zhao and Currie 1994) where they occur within the antorbital fossa (e.g. Currie and Zhao 1994, fig. 1). These structures are different in shape to the recesses of *E. lengi* and are assumed to be non-homologous. Within Tyrannosauroidae, *Guanlong* and *Dilong* both possess nasal recesses. Xu et al. (2004, fig. 1A-B) figured two elongate recesses in *Dilong* located dorsal to the anterior half of the antorbital fenestra. They interpreted these as belonging to the laterodorsal part of the maxilla but it actually seems that they belong to the nasals as they do in *E. lengi*. In *Dilong*, the recess is very similar to that of *E. lengi*: it is subtriangular, being deepest posteriorly; a prominent lateral ridge forms its floor and separates it from the antorbital fossa; and a lamina divides it at mid-length into anterior and posterior portions (Xu et al. 2004). *Guanlong* also possesses elongate openings on the lateral surfaces of its nasals (Xu et al. 2006), dorsal to the anterior part of the antorbital fenestra. However, these are located on the sides of the large nasal crest of this taxon, and – if assumed to be homologous to the recesses of other tyrannosauroids – evidently migrated dorsally as the nasals themselves evolved into a tall, laterally compressed crest. Pneumatisation of the nasals is also known for *Proceratosaurus* (Rauhut et al. 2010), although it is unknown whether this taxon possessed lateral recesses. It may therefore be that pneumatic nasals are ubiquitous among early tyrannosauroids, but were lost in the *Xiongguanlong* + Tyrannosauridae clade (Li et al. 2009).

PLACE FIGURE 4 ABOUT HERE

Posterior to the lateral recess, the lateral edges of each nasal is convex and smooth. This contrasts with the tyrannosaurid condition where transverse ridges and grooves are present (Hurum and Sabath 2003, p. 169). There are no distinct lateral facets for reception of the dorsal end of the lacrimal or the prefrontal. Dorsolaterally, the edges of both nasals form low, blunt ridges that (as measured on the more complete left side) are 60 mm long. In dorsal view, the ridges diverge posterolaterally away from the skull's midline. The ridges do not describe perfectly straight lines, but are slightly curved, being convex laterally. At their anterior ends, both ridges grade into the convex dorsal surfaces of the more anterior parts of the nasals, but for most of their length they are taller than the adjacent flattened medial portions of the nasals. The result

is a Y-shaped arrangement of raised surfaces on the fused nasals: the exact same configuration is present in *Dilong* (Xu et al. 2004), the primary difference being that *Dilong*'s nasals are so much shorter relative to their width. Posterolaterally, the ridges of *E. lengi* extend posteriorly as prong-like structures separate from the rest of the nasals (Fig. 4c, 5c), though this is only preserved on the left side. These structures are superficially similar to the lacrimal processes identified in some tyrannosaurids (Hurum and Sabath 2003) as well as in *Carnotaurus* (Bonaparte et al. 1990, fig. 2), *Ceratosaurus* (Madsen and Welles 2000, plate 3) and some allosauroids (Currie and Zhao 1994, fig. 5) where they key into the dorsal process of the lacrimal. However, because the prong-like structures in *E. lengi* are continuous with the posterolaterally located nasal ridges and located far posteriorly on the nasals, they are likely not homologous with the lacrimal processes discussed by Hurum and Sabath (2003). In fact, based on comparison with *Dilong* (Xu et al. 2004), the structures in *E. lengi* must have been located posterior to the descending ramus of the lacrimal. It remains unknown whether these prong-like structures had any direct relationship with the lacrimals.

Posteriorly, and between the nasal ridges, a concave area is present which is continuous with paired, posteromedial processes that would have met with the frontals (Fig. 4c, 5c). Together, these give the posterior end of the fused nasals a breadth of 43 mm. As mentioned above, an open suture separates the posterior ends of the nasals and extends anteriorly for about 40 mm, or half the length of the nasal ridges. The paired posteromedial processes are large: they have subparallel medial and lateral margins but rounded (albeit incompletely preserved) posterior edges. In life, both would have overlapped the frontals: the amount of overlap appears to have been quite extensive, the nasals forming an Y-shaped region dorsal to the anterior edges of the frontals. This amount of overlap is confirmed by the scarified ventral surfaces of the posteromedial processes. A mid-line lappet of bone emerging from the nasals – as is seen in some tyrannosaurids (Currie 2003) – is not present. The ventral surface of the fused nasals reveals little detail: it is flat, the internasal suture forming a low keel that extends for most of its length (Fig 4d). Foramina occur irregularly along this surface. This contrasts with the condition reported for tyrannosaurids (Hurum and Sabath 2003, p. 169) where the ventral surface is smooth and transversely concave.

PLACE FIGURE 5 ABOUT HERE

# **Lacrimal and possible prefrontal**

The right lacrimal of *E. lengi* consists of a descending ramus and an incomplete anterior process (the lateral surface of which is mostly obscured by irremovable matrix) that would have been parallel to the side of the nasal (Fig 6). As preserved, the bone has a height of 95 mm. In dorsal view the lacrimal is subrectangular and flat (Fig 6a), with no trace of a dorsally inflated region, ridge or cornual process like those present in *Applachiosaurus* and tyrannosaurids (Carr et al. 2005). *Guanlong* and *Dilong* also possess the same type of lacrimal as *E. lengi* (Xu et al. 2004, 2006).

The anterior and descending rami of *E. lengi* meet at an angle of approximately 90°, giving the lacrimal the form of an inverted ‘L’: this more recalls the condition present in *Guanlong*, *Dilong* and the majority of tyrannosauroids and theropods (Xu et al. 2004, 2006) than the ‘7-shaped’ lacrimal present in several tyrannosaurids (Brusatte et al. 2012). However, the ventral edge of the preserved fragment of jugal (which articulates tightly with the ventral end of the lacrimal’s descending ramus) indicates that the lacrimal was arranged in life such that the descending ramus was posterodorsally inclined somewhat. This matter is discussed further below.


The dorsolateral part of the lacrimal is obscured by matrix: it is assumed that a pneumatic foramen was present here since this is the plesiomorphic state for Tetanurae (Serenio et al. 1994, 1996; Witmer 1997; Rauhut 2003b), being absent only in ornithomimosaurids and most maniraptorans. The medial surface of the dorsal end is slightly concave but it is not possible to articulate the lacrimal with the lateral surface of the right nasal.

Viewed anteriorly, the incomplete anterior process of the lacrimal is mediolaterally narrow, being 6 mm wide at most. What appears to be a concave furrow at its anterodorsal extremity may have received an articular process from the nasal. The ventral edge of the anterior process joins the anterior edge of the descending ramus via a continuous curved border, this defining the posterodorsal edge of the antorbital fossa.

The descending ramus is straight (Fig. 6b-e), not bowed anteriorly as it is in *Applachiosaurus* and tyrannosaurids (Russell 1970; Carr 1999; Brochu 2003; Currie 2003; Hurum and Sabath 2003; Carr et al. 2005). *Guanlong* and *Dilong* are, again, like *E. lengi* in this regard (Xu et al. 2004, 2006). The descending ramus is formed of distinct lateral and medial laminae. In lateral view, the lateral lamina obscures the medial lamina except ventrally, close to the bone’s contact with the jugal. Here, the medial lamina is exposed and the anterior edge of the lateral lamina is directed posteroventrally. In this respect, the lacrimal of *E. lengi* is like that of *Dilong*, *Proceratosaurus* and tyrannosaurids (Hurum and Sabath 2003; Xu et al. 2004; Rauhut et al. 2010;



Brusatte et al. 2012) more than that of *Guanlong* where the medial lamina is more extensively exposed laterally (Xu et al. 2006). The descending ramus of *Guanlong* also appears more robust than it is in other tyrannosauroids (Xu et al. 2006). In anterior view, the descending ramus of *E. lengi* is deeply concave, with a dorsoventral furrow extending along its length (Fig 6e), the lateral and medial boundaries of which are formed from the anterior edges of the lateral and medial laminae. Several foramina and recesses are located within this furrow. An especially large, ovoid concavity, the edges of which are obscured by irremovable matrix and broken bone, is present at the dorsal end of the furrow. It appears to be homologous to the pneumatic foramen, presumably associated with the lacrimal canal, present in the same position in tyrannosaurids (Currie 2003; Brusatte et al. 2012). Ventral to this large opening, a series of smaller foramina are present, at least two of the more ventrally positioned of which are associated with dorsoventrally aligned grooves. These structures indicate that the descending ramus was extensively pneumatised: foramina positioned within this groove have been described in tyrannosaurids (Currie 2003; Brusatte et al. 2012) but they do not extend as far ventrally as they do in *E. lengi*. Currie (2003, fig. 19) referred to these foramina as lacrimal ducts but this may be incorrect given that they appear to be pneumatic.


The medial surface of the descending ramus bears two gonally oriented, ventrally descending ridges that extend from the posterodorsal region of the ramus to its anteroventral third. They may be the anterior and posterior margins of a single elongate facet that extends for much of the length of the descending ramus. Ridges on the medial surface of the descending process of the lacrimal are a typical feature of tyrannosauroids and have been reported in *Appalachiosaurus* (Carr et al. 2005) and several tyrannosaurids (Currie 2003; Brusatte et al. 2012): Carr et al. (2005) termed the medial ridge in *Appalachiosaurus* the orbitonasal ridge and noted that it functioned in separating the “orbit and paranasal cavity” (p. 124). An alternative and complementary possibility is that it provided mechanical strength (Currie 2003, p. 201). These ridges differ in position and form among taxa. In *E. lengi*, the ridges are more associated with the posterior edge of the ramus than the anterior one. In *Appalachiosaurus* and *Alioramus*, the ridge is a feature of the anterior edge of the ramus (Carr et al. 2005; Brusatte et al. 2012) while in *Albertosaurus* it is close to the posterior edge. The thickness of the ridge is known to be variable with ontogeny (Brusatte et al. 2012), so it is conceivable that its orientation and position may have varied as the animal matured. In *E. lengi* there are at least two foramina on the medial surface of the descending ramus, posterolateral to these ridges.

Ventrally, the descending ramus flares anteroposteriorly so that the ventralmost part would have been *c.* 30 mm long, and thus far wider than the shaft is at mid-height. Viewed anteriorly, the ventralmost end curves slightly medially. The ventral termination of the bone is damaged; however, some of the bone shards here are preserved adhering to the dorsal edge of the partial jugal, meaning that both can be articulated with a good degree of fit.

PLACE FIGURE 6 ABOUT HERE

What might be a damaged prefrontal is preserved in association with the dorsomedial part of the lacrimal, immediately dorsal to the ascending ramus, though it is difficult to determine if cracking of the periosteum simply creates the impression of a separate ossification (Fig 6c). It appears to be a block-shaped bone, separated from the lacrimal by a curving, dorsally convex line that could represent a suture. In tyrannosaurids, the prefrontal is a crescentic element that separates the lacrimal from the posterolateral part of the nasal and anterolateral part of the frontal, distinct prefrontal facets on the dorsomedial lacrimal being anterior to a contact zone with the frontal (Currie 2003; Brusatte et al. 2012). The fragmented structure present in *E. lengi* is in the right position for this; furthermore, the presence of an articulated prefrontal is consistent with the fact that a facet is not visible on the lacrimal.

## Jugal

Two incomplete sections of the body of the right jugal (66 mm long) are preserved as deep, dorsoventrally flattened plates with slightly concave lateral surfaces. The larger fragment is 66 mm long and 36 mm tall while the smaller one is 36 mm long and 29 mm tall. The fragments do not articulate well and additional portions of the bone are clearly missing. They provide little information but the ventral edge of the larger fragment bears a 23 mm long facet, shaped like an inverted  and separated from the lateral surface by a convex longitudinal ridge. A similar ridge is present on the lateral surface of the smaller fragment which also possesses part of a V-shaped facet along its ventral border. It is assumed that both of these facets were originally continuous, and presumably for articulation with the maxilla. It is also assumed on the basis of comparison with articulated tyrannosauroid skulls that this facet was aligned subparallel to the skull's long axis. Accordingly, the articulated jugal and lacrimal must originally have been oriented such that the descending ramus of the lacrimal was posterodorsally inclined relative to the alveolar margin. A cross-sectional view of the smaller fragment reveals that its medial and lateral walls form the



sides of a 6 mm wide internal cavity. The larger section fits well against the broken ventral end of the lacrimal (Fig 6b).

PLACE TABLE 1 ABOUT HERE

# **Palatine**

An incomplete palatine, 88 mm long as preserved, is preserved on a block of matrix (Fig 7). A similar but far less complete element appears to represent the posterior part of the element from the other side. It is not possible to determine which side either element belongs to. The more complete palatine consists of a flattened, subrectangular body 19-24 mm wide, with four short processes, two at each end. Two processes that are on the same side are broken and would originally have projected as far longer structures; the two on the other side are shorter and appear near complete. It is therefore suggested that the two longer processes represent the vomeropterygoid and pterygoid processes. The shorter, more complete processes therefore represent the maxillary and jugal processes. Overall, *E. lengi*'s palatine is elongate and shallow relative to the palatines of *Appalachiosaurus* and tyrannosaurids (Carr et al. 2005, fig. 11). Little data on non-tyrannosaurid tyrannosauroid palatines is available but the palatine of *E. lengi* appears similar to that of *Guanlong* (Xu et al. 2006), albeit longer and with a longer, straighter dorsal margin.

The middle of the palatine body is damaged but the remnants of what appear to be several openings are present. These are presumably palatine recesses homologous to those present in tyrannosaurids, allosauroids and other tetanurans (Witmer 1997). If so, they show that the exposed surface is the lateral one. The assumed anterior end of the palatine is deeply concave: this concave edge (representing the posterior border of the choana) is mostly formed by the anteriorly concave, anteriorly projecting maxillary process, the anterior tip of which forms a pointed projection. This projection comes to a natural termination that does not extend anteriorly any further than the base of the vomeropterygoid process. This condition contrasts with that in *Appalachiosaurus* (Carr et al. 2005) and tyrannosaurids where the maxillary process extends anterior to the vomeropterygoid process (Currie 2003; Hurum and Sabath 2003; Brusatte et al. 2012). The condition in non-tyrannosaurid tyrannosauroids is not clear due to poor preservation and a lack of good disarticulated cranial material (Xu et al. 2004; Li et al. 2009; Rauhut et al. 2010) but the palatine of *Guanlong* appears similarly proportioned to that of *E. lengi* (Xu et al.

2006). It is typical in theropods for the vomeropterygoid process of the palatine to be longer than the maxillary process (Dal Sasso and Maganuco 2011).

Much of the ventral edge of the maxillary process is broken but it appears to be continuous with the ventral edge of the palatine body, as is typical. The broad base of the vomeropterygoid process projects anterodorsally but terminates with a jagged break. What is preserved shows that it projected at an angle of approximately 40° relative to the palatine's long axis. The vomeropterygoid process of *E. lengi* is unusual in that a sinuous ridge, approximately perpendicular to the skull's long axis, extends across the base. The part of the process dorsal to this ridge is inset or embayed relative to the ventral part: the latter part is continuous with the palatine body. A ridge of this sort has not been described in any other tyrannosauroid, to our knowledge, and thus it may be an autapomorphy of *E. lengi*.

The dorsal margin of the palatine is subparallel to the ventral margin, a relatively long and straight edge existing between the vomeropterygoid process and posteromedially projecting pterygoid process. This condition is unusual relative to other tyrannosauroids, all of which possess a far shorter, dorsally concave edge between the vomeropterygoid and pterygoid processes (Currie 2003; Carr et al. 2005; Xu et al. 2006; Brusatte et al. 2012). The long, straight dorsal palatine edge of *E. lengi* may, therefore, also be autapomorphic.

A fan-shaped process extends posteriorly from the palatine body and probably represents the medial or pterygoid process. At its base it is 11 mm wide but it expands to 27 mm posteriorly. It lies in the same plane as the palatine body; it cannot be determined if this is natural or the result of compaction. The ventral margin of this process describes a wide, shallow arc. The broken surface of the fragile pterygoid process reveals little anatomical detail and its dorsal end is damaged and incomplete.

PLACE FIGURE 7 ABOUT HERE

## Quadrates

The single preserved quadrate of *E. lengi* was briefly described by Hutt et al. (2001, pp. 231-232) where it was provisionally identified as a left quadrate; it is reidentified here as a right quadrate. It is mostly complete though the head and the adjacent part of the shaft are missing (Fig 8). The gracile shaft has subparallel medial and lateral margins in posterior view. The lateral side of the shaft immediately dorsal to the lateral condyle is expanded mediolaterally forming a prominent lateral flange that articulated with the quadratojugal (which is not preserved). The

dorsal margin of this flange forms a shoulder where it abruptly grades into the dorsal half of the lateral margin of the quadrate shaft. A shallow, dorsoventrally elongate concavity is present near the middle of the shaft's posterior surface. The quadratojugal contact area is limited to the ventral part of the quadrate: the quadrate fenestra is positioned in between the quadrate shaft and the (unknown) quadratojugal, as is the case in other tyrannosauroids (Carr 1999; Carpenter et al. 2003; Li et al. 2009; Rauhut et al. 2010; Brusatte et al. 2012). The medial embayment of the quadrate's lateral shaft dorsal to the quadratojugal contact area further shows that the quadrate fenestra was large and dorsoventrally elongate and thus similar to the quadrate fenestrae of *Xiongguanlong* (Li et al. 2009) and tyrannosaurids (Carr 1999; Brusatte et al. 2012). The fenestra of *Proceratosaurus* (Rauhut et al. 2010) is much smaller.

A flattened, laterally directed area on the lateral side of the quadratojugal flange, measuring *c.* 18 mm deep dorsoventrally and 9 mm anteroposteriorly, represents the facet for the quadratojugal.

PLACE FIGURE 8 ABOUT HERE

The medial edge of the posterior surface of the shaft possesses a pillar-like dorsoventrally aligned quadrate ridge that, at the mid-height of the shaft, forms the medial border to a concave region on the shaft's posterior surface. The quadrate ridge is also obvious as a pillar-like thickening when the quadrate is viewed medially: in this view it forms the posterior border to a prominent depression – the medial fossa (Hendrickx et al. 2015) – that occupies the anterior face of the shaft medial to the pterygoid process. Quadrate ridges are present in theropods of many lineages (Hendrickx et al. 2015): within Tyrannosauroidae they are present in both *Proceratosaurus* (Rauhut et al. 2010) and Tyrannosauridae (Brusatte et al. 2012).

The anterodorsally projecting pterygoid process has its ventral margin well dorsal to the condyles (Fig 8c). This is also the case in some allosauroids (Madsen 1976), *Zuolong* (Choniere et al. 2010), *Tanycolagreus* (Carpenter et al. 2003), *Proceratosaurus* (Rauhut et al. 2010) and tyrannosaurids (Molnar 1991; Currie 2003; Brusatte et al. 2012). A large foramen is present on the medial surface of the process, close to its junction with the medial edge of the shaft.

The ventral condyles are bulbous and similar in size; they are short anteroposteriorly and the long axes of both are oriented at about 45° to the mediolateral axis of the quadrate's shaft (Fig 8d). The medial condyle is bulbous and convex ventrally such that it extends further ventrally than the lateral condyle; a similar degree of ventral convexity to the medial condyle is seen in

some allosauroids (Madsen 1976), *Tanycolagreus* (Carpenter et al. 2003) and at least some tyrannosaurids (Brusatte et al. 2012). A proportionally wide channel – it is similar in width to the medial condyle at 4 mm – separates the condyles. Some tyrannosauroids (*Dilong* and Tyrannosauridae) possess a pneumatic foramen or recess dorsal to the condyles on the anterior surface of the quadrate shaft (Brusatte et al. 2012; Hendrickx et al. 2015). No such structure is present in *E. lengi*.

Overall, the quadrate morphology of *E. lengi* is typical for a tyrannosauroid and it is similar to that of both *Tanycolagreus* and tyrannosaurids. The enlarged quadrate fenestra indicates that *E. lengi* is closer to tyrannosaurids than *Proceratosaurus* and similar taxa. If the depression on the medial surface of the pterygoid process is indicative of quadratic pneumaticity, *E. lengi* is more like tyrannosaurids than like *Tanycolagreus*, *Guanlong* or *Proceratosaurus*, since quadrate pneumaticity is absent in those taxa (Carpenter et al. 2003; Rauhut et al. 2010; Brusatte et al. 2012).

## Dentary

Both dentaries are known for *E. lengi*. The left dentary is better preserved (Hutt et al. 2001, fig. 3D) but is incomplete posteriorly, its preserved portion consisting of that part anterior to the 9<sup>th</sup> alveolus. It terminates with a jagged break. The right dentary is less well preserved and is distorted, being strongly bent anterolaterally (Fig. 9g–h). It confirms several features described for the left dentary and is preserved in two pieces, with the 37 mm long anterodorsal tip being separate from the rest of the bone. The anterodorsal tip is duller in color than the rest of the bone and presumably experienced weathering prior to collection. Its dorsoventral height is only measureable at its anterior end where it is 46 mm.

The broken posterior ends of both dentaries reveal the presence of at least two internal cavities, both taller than wide. The more ventral cavity is smaller (9 × 6 mm) than the more dorsal one. It is not possible to determine how far dorsally the more dorsal cavity extends. The bone wall forming the ventral margin of the dentary, ventral to the ventral cavity, is thicker (5 mm) than the medial and lateral walls (both c. 3 mm). The approximate mediolateral width of the dentary at its broken posterior end is 14 mm.

Seven alveoli are preserved on the left dentary, the three anterior-most alveoli appearing sub-circular in outline while the more posterior ones are sub-rectangular. There is space at the posterior end for an eighth and possibly a ninth, but their margins are obscured. As discussed below, interdental plates are present in *E. lengi* (contra Hutt et al. 2001) and are inset relative to

the rest of the medial surface (Fig. 9b, f). A narrow shelf *c.* 1 mm wide, located 26-30 mm dorsal to the ventral edge of the dentary, demarcates the flat medial surface from the interdental plates.

Anterodorsally, an unusual notch is present both laterally and medially around the first alveolus (Fig. 9a–b, d–e). This was not described by Hutt et al. (2001) but a dotted line in fig. 3D indicates that the notch was regarded as a result of damage to the dentary's tip. However, though some of the 'notched' bone surrounding the first alveolus is obscured or damaged, some of it is complete, well preserved and intact, and an identical notch is present on the right dentary. The notch thus appears to have been a natural feature. Anteroventrally, the junction between the anterior margin and ventral edge of the dentary forms a smooth convex arc and thus differs from the condition in tyrannosaurids where a distinct angle is present between the anterior and ventral surfaces (Currie 2003; Holtz 2004). A distinct angle is also present in *Bagaraatan* (Osmólska 1996).

The left dentary's labial side has large foramina and at least four arcuate furrows (Fig 9a). The largest foramen (*c.* 7 × 3 mm) is anteriorly located, and just posteroventral to the notched edge of the first alveolus. Two smaller foramina (each *c.* 1 × 1 mm) are located approximately ventral to this large one and a line of at least six are spaced along the dentary posterodorsal to the largest one. These latter foramina are shallower than the large foramen and arranged in a line that extends subparallel to the dentary's alveolar margin. All are *c.* 8 mm ventral to the labial alveolar margin and appear to represent the more dorsally located section of the alveolar row: in tyrannosauroids generally, the more posterior foramina are located farther ventrally on the dentary's surface (Brochu, 2003; Currie 2003; Xu et al. 2004, 2006; Brusatte et al. 2009, 2011; Rauhut et al. 2010). On the right dentary, a row of foramina subparallel to the alveolar margin also appears to be present, though only two of the foramina are clearly preserved. In *Guanlong*, *Proceratosaurus* and *Sinotyrannus*, some of the dentary foramina are located within a groove that parallels the dentary's dorsal margin (Xu et al. 2006; Ji et al. 2009; Rauhut et al. 2010), but no such structure is present in *E. lengi*. The pattern of foramina at the anterior tip of the right dentary is similar and better preserved than that on the left dentary, with two large foramina (5 × 3 mm and 3 × 2 mm respectively) present posterior to the largest one (6 × 4 mm). These additional foramina are only preserved as ambiguous concavities on the left dentary. The right dentary also preserves a prominent anteroventral foramen (4 × 2 mm) that is preserved in the same position as that occupied by a pair of foramina on the left dentary.

On the labial side of the dentary, extending across the surface ventral to the alveoli 2-5, are five anterodorsally curving, shallow furrows that terminate posteriorly at a single small concavity

(*c.* 8 × 4 mm), located ventral to the junction between alveoli 5 and 6. This concavity may house a foramen. The furrows consist of a ventral horizontal portion and a raised, anterodorsally curving portion. The raised portion is inclined at a shallow angle in the most anterior furrow and a high angle in the most posterior one. The furrows positioned between these two are inclined at intermediate angles. The furrows are far less obvious on the right side, though fracturing of the bone's surface and strong flexion to the right have obscured its original detailed structure. Curved furrows of this sort have not been reported in any other theropod to our knowledge and they are hence regarded as an autapomorphy of *E. lengi*.

PLACE FIGURE 9 ABOUT HERE

The dentary's medial surface is largely flat, though slightly convex in its ventral third or so. Anteriorly it lacks a distinct symphyseal area and there is no suggestion of any kind of medial inflection. However, the anteromedial edge of the dentary does form a low ridge, parallel and posterior to which is a shallow groove. The ridge continues dorsally to form a bony projection anteromedial to the first alveolus. The Meckelian groove is straight and shallow, merges smoothly into the medial surface of the bone, and is located some distance dorsal to the dentary's ventral edge, lying about half-way up the medial surface (Fig 9b). It does not extend to the dentary's anterior end. A very similar condition is present in *Dryptosaurus*, and indeed a 'centred' position of the Meckelian groove on the medial surface of the dentary appears to be typical for tyrannosauroids (Brusatte et al. 2011). A shallow medial groove on the ventral 26-30 mm of the dentary is deepest (*c.* 7 mm) at its posterior-most end and becomes shallow anteriorly, eventually merging imperceptibly with the rest of the dentary's medial surface.

Hutt et al. (2001, p. 232) were unsure as to the presence of interdental plates in *E. lengi* but several of the statements made about interdental plate morphology are incorrect. Hutt et al. (2001) wrote that "the interdental [sic] plates ... cannot be reliably distinguished from the bone on the dentary's labial [sic] surface" (p. 232). In the latter statement, the word 'labial' should read 'lingual'. It was further stated "In *Eotyrannus* the plates may, therefore, be fully fused or, as is the case with *Deinonychus*, reference to these structures as interdental plates may be a question of semantics" (p. 232). Interdental plates can, in fact, be distinguished from the rest of the medial surface, and the interdental plate themselves are not fused at all. They appear similar in form and proportions to those of allosauroids, tyrannosaurids and other groups (e.g. Madsen 1976; Currie 2003). Four interdental plates – the most anterior ones – can be distinguished on the left dentary



(Fig 9b). Another four are probably present but cannot be identified unambiguously. The most anterior interdental plate is incomplete, with only 6 mm of its length being visible. It is not adjacent to the first alveolus but rather to the anterior half of the second. Whether an interdental plate was associated with the first alveolus is unknown. Neither dentary preserves evidence of a plate in this location but this may be due to loss or damage.

Five interdental plates are visible on the right dentary (Fig 9f). As on the left dentary the first plate is smallest in terms of both length and height (breakage creates the impression that two interdental plates are present here). The more posterior interdental plates on both dentaries are all similar in morphology, consisting of an approximately square-shaped body capped by a triangular apex. The tip of the triangle forms the dorsal projection of the alveolar septum. The medial surfaces of the plates have a distinctive wrinkled surface texture distinct from that of the rest of the dentary and similar to the texture present on the maxillary interdental plates.

## Surangular

The near-complete right surangular, 123 mm long, went unmentioned by Hutt et al. (2001). It consists of a shallow, subrectangular, laterally compressed body that, at its dorsal end, has overhanging shelves on both its medial and lateral sides. The cotylar region and retroarticular processes are intact (Fig. 10d–f). In overall form it is similar to the surangulars of *Guanlong*, *Dilong*, *Proceratosaurus* and *Alioramus* (Xu et al. 2006; Rauhut et al. 2010; Brusatte et al. 2012) and less deep than the surangulars of *Bistahieversor* and non-alioramine tyrannosaurids (Molnar 1991; Currie 2003; Carr and Williamson 2010).

The cotyle appears deep and U-shaped in lateral view but, viewed dorsally, it is broad and shallow. A subtriangular eminence forms its posterior border. A shallow, anteroventrally inclined fossa is present on the lateral surface of this posterior eminence, but there is no obvious lateral concavity continuous with the cotyle as there is in tyrannosaurids (Carr 1999; Currie 2003). The process anterior to the cotyle is continuous anteriorly with a prominent dorsolateral ridge – sometimes termed the surangular shelf – that projects laterally from the bone's surface. This ridge is similar to the one present in *Dryptosaurus* and tyrannosaurids but its lateral edge does not curve ventrally as is the case in *Daspletosaurus*, *Tarbosaurus* and *Tyrannosaurus* (Brochu 2003; Currie 2003; Hurum and Sabath 2003). A far less prominent ridge is present in *Guanlong*, *Dilong* and *Proceratosaurus* (Xu et al. 2004, 2006; Rauhut et al. 2010): that of *Proceratosaurus* is positioned close to the dorsal edge of the bone and is thus apparently more dorsally positioned that is typical for tyrannosauroids. In *Dryptosaurus* and tyrannosaurids the extreme posterior end

of the ridge overhangs an enlarged posterior surangular foramen (Currie 2003; Brochu 2003; Holtz 2004; Carr et al. 2005), and no such structure is present in *E. lengi*. *Guanlong*, *Dilong* and *Proceratosaurus* also lack posterior surangular foramina (Xu et al. 2004, 2006; Rauhut et al. 2010).

PLACE FIGURE 10 ABOUT HERE

Medial to the ridge, the dorsal surface of the surangular forms the posterior part of the adductor muscle channel (Currie 2003) which extends to the preserved anterior margin. The part of the bone ventral to the surangular shelf forms a mediolaterally compressed, blade-like region, the ventral edge of which is bluntly rounded and **not thin**. The anterior and anteroventral parts of the bone are absent.

A large, dorsally projecting process forms the anterior border of the mandibular cotyle, but the shape of the process cannot be determined because of damage at the apex. This process is continuous with a low transverse ridge that extends across the dorsal surface of a subtriangular medial process. The latter is continuous posteriorly with the retroarticular process and anteriorly with the posteromedial part of the surangular shelf. An extremely similar morphology is present in tyrannosaurids (Lambe 1917). A short retroarticular process is present posterior to the cotylar region. In contrast to the tyrannosaurid condition, the dorsal surface of the retroarticular process is not separated from the posterior cotylar prominence by a concave area.

# **Unidentified partial mandibular bone**

What appears to be the anterior end of an unidentified mandibular bone – possibly an articular – is well preserved (though only as fragments that had to be glued together), despite its delicate form: it is *c.* 1 mm thick except along its dorsal margin where a dorsomedial groove and accompanying medial shelf increase the mediolateral thickness of the bone to *c.* 6–8 mm. The bulk of this bone fragment is composed of a thin, vertical lamina, the ventral edge of which sweeps anterodorsally to meet the subhorizontal dorsal margin (**Fig. 10a–c**). The presumed anterior tip is missing, as is some of the ventral margin. Dorsomedially, a longitudinal shelf overhangs the rest of the medial surface and forms the medial border of a shallow gutter that extends to the presumed anterior tip.



What appears to be the lateral surface is convex and is deepest at a point just posterior to the termination of the shallow anterior gutter. A low dorsal peak is present here and is flush with the lateral surface. Immediately posterior to this convexity, a laterally directed concave area is present: it is bordered anteriorly and anteroventrally by a low rim. A subhorizontally oriented, anterodorsally located channel extends approximately in parallel with the bone's dorsal margin (Fig 10b). At the posterior end of this channel, an oval foramen perforates the body of the bone: a delicate lamina extends dorsoventrally across part of this foramen. While the channel is inset medially into the bone, the lamina is clearly continuous with the bone's lateral surface.

## Dentition


Approximately 17 teeth are known for *E. lengi*, some of which are preserved within their premaxillary, maxillary or dentary alveoli. The premaxillary teeth are typical for a tyrannosauroid while the maxillary and dentary teeth are of typical theropod morphology. The total preserved length of each tooth was measured and the TCH (total crown height) was recorded if it was possible to distinguish the crown from the root. Given the ambiguous nature of the crown-root junction, the latter measurements are often approximate. Where possible the FABL (fore-aft basal length) was also measured and the denticle size difference index (DSDI) was calculated following Rauhut and Werner (1995). All tooth measurements are given in Table 2.

PLACE TABLE 2 ABOUT HERE

PLACE FIGURE 11 ABOUT HERE

## Premaxillary teeth

The premaxillary teeth of *E. lengi* are U-shaped in cross-section, as is typical for tyrannosauroids (Holtz 2004; Xu et al. 2004). At least three isolated *E. lengi* premaxillary teeth occur in the assemblage: they are easy to identify because of their cross-sectional shape and because their serrated carinae are restricted to the flat lingual surface (Fig. 11a–c). A tooth that seems to be from the left premaxilla was figured in oblique lingual view by Hutt et al. (2001, fig. 8). A change in the color and texture of the tooth indicates the position of the crown-root junction and suggests that c. 18 mm of the tooth was exposed as the crown. The crown is strongly convex labially while the lingual side is flat and bears an apicobasally elongate depression 4 mm long near the apex (Fig 11c). This is presumably a wear facet. The preserved part of the root possesses a roughened external texture looks appears to represent bioerosion of some kind. The second

929  ilable premaxillary tooth is near-complete, attached to the right premaxilla and only exposed  
930 in lingual view: this reveals an oval depression 1.5 mm long near the tip of the lingual surface  
931 that resembles its counterpart on the first premaxillary tooth. The third specimen, however, lacks  
932 any such lingual depression or facet.

### 934 **Dentary teeth**

935 Four emergent tooth crowns are preserved within the left dentary, but only one of them (the  
936 7<sup>th</sup>) protrudes dorsal to the alveolar margins. The crown tips preserved in the 1<sup>st</sup>, 3<sup>rd</sup> and 5<sup>th</sup> alveoli  
937 must have only recently emerged and the remains of a crown preserved anterodorsally to the 5<sup>th</sup>  
938 crown tip indicate that the newly emergent crown was in the process of displacing an older tooth.  
939 The location of the remnant of the older tooth relative to the emergent crown tip implies that  
940 replacement teeth emerged from behind their predecessors. The carinae of all the dentary teeth  
941 (with one exception) face mesially and distally. However, the tiny replacement tooth in the first  
942 alveolus, though broken and incomplete (consisting only of the base of *c.* 2 mm of the base of the  
943 crown), is preserved with its longest axis directed labiolingually (Fig 9d). The tooth is lenticular  
944 in cross-section and what appear to be unserrated carinae are preserved both lingually and  
945 labially. This suggests that the first dentary tooth differed strongly in shape from the other dentary  
946 teeth, and that this might be linked to the unusual morphology of the first alveolus. Unfortunately,  
947 it is possible that the tooth is not in situ, given its broken condition and non-central placement  
948 within the alveolus. Furthermore, no tooth is preserved in the first alveolus of the right dentary,  
949 making it impossible to confirm that the morphology of the first left dentary tooth is pristine.

### 951 **Remaining lateral teeth**

952 At least 14 lateral teeth are known for *E. lengi*, including isolated crowns, isolated partial  
953 roots, isolated crowns with roots, and teeth still embedded in the left maxilla and dentary. An  
954 intact tooth crown representing an emergent tooth that has not fully descended is present in the  
955 first alveolus of the maxilla and a broken tooth crown is present in the third alveolus, the latter  
956 being 9 mm long mesiodistally and 5 mm wide labiolingually. The crowns have a lenticular  
957 cross-section and broadly resemble those of allosauroids while incomplete roots are  
958 mediolaterally compressed and subrectangular in cross-section. All denticles terminate in  
959 squared-off ends, do not exhibit any apical hooking, are slightly inflated apico-basally and  
960 slightly waisted, and are continuous across the crown apex and without apical hooking (Fig. 11d–  
961 e). The interdenticle pits are U-shaped. The distal denticles of *E. lengi* are notably taller (in terms

of their height perpendicular to the tooth's long axis) than the mesial denticles, with a height to basal width ratio of  $> 1.5$  for unworn denticles (Sweetman 2004). At its base, the mesial carina appears prominent relative to the crown's mesial margin.

Hutt et al. (2001, p. 230) reported a DSDI of 1.5 for *E. lengi*, and noted that this was high compared to tyrannosaurids but Sweetman (2004) noted that this value should be considered unreliable as it was based on a partially erupted maxillary tooth in which denticle density could only be measured at the tooth tip. Remeasurement provided DSDIs of 1.03, 1.06, 1.25 and 1.31, with a mean of 1.16 (Sweetman 2004). Similar DSDIs (1.21, 1.36 and 1.06, mean = 1.21) were calculated in the present study.

### **The axial skeleton of *E. lengi***

The vertebral formula of *E. lengi* is unknown but the number of vertebrae present in each segment of the vertebral column can be estimated based on the condition in other coelurosaurs. Tyrannosaurids and other typical non-avian tetanurans possess 10 cervical, 13 dorsal, 5 sacral, and more than 35 caudal vertebrae (Makovicky 1995; Holtz 2004; Holtz et al. 2004). These numbers are assumed for *E. lengi*. Hutt et al. (2001, p. 232) assumed that *E. lengi* possessed 14 dorsal vertebrae because of an adherence to the convention used by Madsen (1976) for *Allosaurus*. Madsen (1976), in turn, followed Osborn (1906, 1917) whose identification of nine cervical vertebrae for *Tyrannosaurus rex* was in error: though, to be fair, he noted how difficult it was to distinguish the last cervical from the first dorsal (Osborn 1917, p. 765). It was subsequently argued by Makovicky (1995) that the eleventh presacral should be identified as the first dorsal since this is the first presacral to possess a hypapophysis. Brochu (2003) argued that any distinction made between cervical and dorsal vertebrae in tyrannosaurids is arbitrary, and subsequently referred to both simply as presacrals. It is of course unknown whether it would be possible to identify the cervical-dorsal junction in *E. lengi*. In order to facilitate description, the traditional distinction between these segments of the column is maintained here.

### **Cervical vertebrae: neural arches**

No complete cervical vertebrae are preserved for *E. lengi* but two near-complete, isolated neural arches and two isolated centra are present (for measurements, see Tables 3–4). The axial neural arch is embedded within a block that also includes a cervical centrum and the proximal

ends of some probable metacarpals. A second neural arch is preserved on the same block as another cervical centrum and several probable cervical rib shaft fragments.

The axial neural arch (Fig. 12a–d) is identified as such because of its flaring postzygapophyses and strong similarity to the axial centrum of *Deinonychus* (Ostrom 1969, fig. 28D) and *Xiongguanlong* (Li et al. 2009, fig. 2c). The prezygapophyses are short, subtriangular prongs that extend 10 mm anterior to the neural spine. Neither preserves a complete articular facet **preserved**. A broad, subcircular space separates the prezygapophyses in dorsal view. The neural spine is **low and subrectangular**, and extends along the entire length of the neural arch. Though somewhat distorted, it is complete apically excepting its posterodorsal portion and lacks the spine table present in *Xiongguanlong* and tyrannosaurids (Brochu 2003; Li et al. 2009). This lack of a transversely flared neural spine apex is surprising in view of its prevalence in other tyrannosauroids and coelurosaurs (Makovicky 1995; Brochu 2003; Li et al. 2009); it most likely indicates that the neural spine apex is missing. A small concavity (**c. 1 mm IN** dorsoventral height) on the anterior face of the neural spine might be a ligament fossa. The prezygapophyses and postzygapophyses are at about the same horizontal level and are connected by a horizontal shelf that projects 11 (left side) and 13 (right side) mm lateral to the neural spine. None of the structures ventral to this shelf are preserved. The postzygapophyses flare posterolaterally and a low, mound-like, partly eroded epiphysis is present on the right side (Fig 12d); the left epiphysis is missing entirely due to erosion. The epiphysis terminates at the posterior edge of the postzygapophyseal facet but may originally have been more extensive. Distinct postzygapophyseal facets are not preserved but appear to have been located in the typical position. There is no indication of a preserved axial intercentrum **is preserved**.

PLACE FIGURE 12 ABOUT HERE

The second neural arch preserves all of its processes, though all are incomplete and many areas are damaged or obscured by irremovable matrix (Fig. 12e–g). In dorsal view the zygapophyses diverge laterally from the mid-line, creating an X-like shape (Fig 12f). The right prezygapophysis preserves a flat, dorsomedially directed articular facet. It is not possible to examine the space between the prezygapophyses, and the existence of interspinous ligament fossae remains uncertain. A displaced rod-like bone, possibly a cervical rib shaft, is preserved between the prezygapophyses and is described below. The broken neural spine is restricted to the posterior half of the neural arch. It extends posteriorly as far as the preserved posterior-most tips

of the postzygapophyses. The latter are incomplete distally and there is no clear indication of epipophyses. On the left side the prezygapophysis is connected to the postzygapophysis by a near-horizontal shelf of bone, and the dorsal-most points of both the prezygapophysis and postzygapophysis are approximately at the same horizontal level. The postzygapophyses have their long axes directed posterodorsally; their precise orientation of their facets cannot be determined but they were evidently directed ventrally. On the left side, a partially visible centropostzygapophyseal lamina joins the underside of the postzygapophysis to the posterolateral part of the centrum.

PLACE TABLE 3 ABOUT HERE

### **Cervical centra and cervical ribs**

A cervical centrum is preserved on the same block as the axial neural arch and may represent the axial centrum (Fig. 12h–k). Its anterior articular surface is flat, and broader than it is deep. Both parapophyses are preserved; the right parapophysis bears a lateral concavity, though it is not possible to determine whether this is natural or the result of damage. Posterodorsal to the right parapophysis is a deep oval pneumatic foramen. If this centrum is indeed the axial one, then *E. lengi* shares with *Dilong* (Xu et al. 2004) and *Xiongguanlong* (Li et al. 2009) the primitive condition of possessing a single axial foramen on each side, rather than the two foramina per side present in tyrannosaurids (Makovicky 1995; Brochu 2003). What might be the serrated neurocentral suture is visible on the centrum's right side. The posterior articular surface is damaged but the curved form of the posterolateral rim of the centrum suggests that the articular surface was concave. The ventral surface of the centrum is flat but the junctions between the ventral and lateral surface are smoothly convex. There is no ventral keel or concavity. The posterior part of the centrum is narrower than the anterior articular surface.

A second, less well preserved cervical centrum is preserved adjacent to the second neural arch. Most of its surfaces are damaged, but we describe here the better preserved left side (Fig 12l). It is deeper and shorter than the other cervical centrum, and the parapophysis is in an anteroventral position with a deep oval pneumatic foramen located posterodorsal to it. The bone around the edges of the foramen slopes into this depression. As in the other cervical centrum, the junction between the lateral and ventral surfaces is smoothly convex. What is preserved of the articular surfaces indicates amphicoely or weak opisthocoely: the former condition is typical for

tyrannosauroids (Li et al. 2009) while the latter is known in *Juratyran* (Benson 2008) and some tyrannosaurids (Holtz 2004).

A rod-like bone fragment 55 mm long, preserved on the side of the block opposite to the one that bears the centrum, may be a cervical rib shaft. It cannot be determined which end is the proximal one, but the broken end reveals a subtriangular cross-section. A similar rod-like bone fragment *c.* 40 mm long is preserved in association with the neural arch, lying diagonally between the prezygapophyses. This element appears circular in cross-section. The fact that two such rod-like elements are both located adjacent to cervical elements provides circumstantial support for their identification as cervical rib shafts.

PLACE TABLE 4 ABOUT HERE

# **Dorsal vertebrae**

The presence of dorsal vertebrae in the holotype of *E. lengi* was mentioned by Hutt et al. (2001, p. 228) and several dorsal centra were alluded to in the description (p. 232). Five of these centra seem to be *E. lengi* dorsals but others are more problematic: two may not be dorsal vertebrae. All specimens have separated from their neural arches at the neurocentral sutures, but an isolated fragment of neural arch is also preserved. For measurements see Tab 5. Pneumatic foramina are absent on all preserved dorsals.

A large centrum that possibly represents the 3<sup>rd</sup>, 4<sup>th</sup> or 5<sup>th</sup> dorsal (on account of its proportional similarity to vertebrae of these positions in other coelurosaurs: Makovicky 1995; Brochu 2003) is hourglass-shaped in dorsal view and ventrally concave in lateral view, with the deepest part of the concavity being 10 mm dorsal to the rims of the articular ends (Fig 13a–f). A faintly developed ventral keel is present, and the lateral side of the dorsal surface of the centrum (lateral to the neural canal) is concave. A neurovascular foramen *c.* 1.5 mm long is present on the left side. One articular surface, presumably the posterior one, is smaller than the other. The presumed anterior articular surface is flat, though near the left dorsolateral margin it forms an anterolaterally sloping surface which is surrounded posteriorly and laterally by a raised bony rim. The left parapophysis was presumably located here. The posterior articular face is concave, and the bony rim that surrounds it is more prominent ventrally, laterally and dorsally than that surrounding the presumed anterior surface. The neural canal (*c.* 7 mm wide) is shallow for most of its length but becomes deep anteriorly. On the left side, the dorsal part of the centrum that borders the neural canal preserves a flat area for articulation with the neural arch.



The ventral half of another, less complete dorsal centrum is medially constricted at mid-length when viewed dorsally or ventrally. There is no trace of a ventral keel, unlike in tyrannosaurids and most other tetanurans where a ventral keel is present (Rauhut 2003b). One articular surface extends further ventrally than the other: in the dorsal vertebrae of tyrannosauroids and other tetanurans, it may be either the anterior or the posterior articular surface that extends furthest ventrally (Harris 1998; Brochu 2003; Brusatte et al. 2012), rendering it impossible to decide with certainty which end the ventrally descending one represents. The preserved height of this posterior surface is 32 mm at most, but when complete the surface was probably *c.* 50 mm tall. The opposite articular face was probably *c.* 45 mm wide when complete. The incompleteness of the articular faces makes it difficult to determine their original shape but they seem to have been flat.

An additional, robust centrum possesses concave lateral surfaces and a flatter ventral surface than the two preceding elements (Fig. 13g–l). The neural canal and adjacent structures are not preserved. Bony rims surround both articular surfaces with the one surrounding the posterior surface extending farther ventrally. The anterior articular surface is flat while the posterior one is slightly concave and slopes anterodorsally. On the basis of how it compares with the other dorsal vertebrae known for *E. lengi*, this vertebra was presumably posterior to the 4<sup>th</sup> or 5<sup>th</sup> position and may belong to the middle part of the dorsal series.

A somewhat distorted dorsal centrum is 52 mm long on one side and 58 mm long on the other (Fig. 13m–r). It is not possible to determine which end is which: one articular surface is flat and the other is concave and the latter is arbitrarily identified as ‘anterior’. This centrum is probably the one described by Hutt et al. (2001, p. 232) as representing dorsal 14 and being 52 mm long. The centrum is elongate and deeply concave ventrally. Both sides exhibit oval concavities that are located slightly closer to the neurocentral sutures than to the ventral surface and occupy much of the length of the centrum between the edge of the articular faces. The concavities are asymmetrical, partly due to distortion of the centrum: one is 34 × 15 mm and the other 27 × 17 mm. There are no indications of pneumaticity within the concavities. Lateral concavities of this sort, albeit not as well defined, have been illustrated for some allosauroids (Madsen 1976; Currie and Zhao 1994). The bony rims around the articular faces flare laterally and ventrally. The ventral surface of the centrum is convex with no midline keel.

Several additional dorsal vertebrae are preserved in the assemblage, mostly represented by distorted and/or incomplete centra. It is not possible to determine their positions within the sequence, or even to be confident that they definitely belong to *E. lengi*. A probable fragment of a

dorsal neural arch is also present. It is robust with a maximum length of 57 mm and a maximum breadth of 47 mm. Its incompleteness makes interpretation difficult and no part of the element is bilaterally symmetrical. The most likely identification is that it is from the right posterolateral part of the neural arch, in which case a process projecting from it would represent an incomplete transverse process. A low ridge with a length of 37 mm runs along what may be the ventrolateral part of the specimen. The large size of this fragment indicates that it belonged to a dorsal vertebra but it is not possible to be more specific.

A poorly preserved, highly pyritised core of what appears to be the centrum of a camellate dorsal vertebra reveals little detail but does display an hourglass-like shape in ventral or dorsal view. The orientation of the element cannot be determined (it is missing all external bone texture and is embedded in matrix on most sides), but one articular end measures 40 mm dorsoventrally and *c.* 35 mm mediolaterally. The opposite articular end is also *c.* 35 mm wide but its depth cannot be measured. The preserved part of the vertebra represents either the dorsal or the ventral part of the centrum (rather than its middle) and consequently the centrum may have been even narrower closer to its middle. The ‘waisted’ proportions of this centrum appear typical for a tetanuran. There is no way of determining its position within the vertebral sequence. A second probable centrum ‘core’ is enclosed in matrix. Its approximate dimensions are 50 × 50 mm, but it cannot be determined whether it belongs to *E. lengi* or the associated dryosaurid.

PLACE FIGURE 13 ABOUT HERE

The relatively long dorsal centra of *E. lengi* are unlike those of tyrannosaurids. Measurements of the *Daspletosaurus torosus* holotype NMC 8506 given by Russell (1970) show this specimen to have dorsal centrum length : height ratios ranging from 0.62 to 0.83, with a mean (*n* = 7) of 0.70. *E. lengi* has much higher ratios ranging from 1.19 to 1.86, with a mean (*n* = 5) of 1.44. The dorsal vertebrae of *Dilong* were described as “relatively long” (Xu et al. 2004, p. 681) and this also appears to have been the case for *Guanlong* (Xu et al. 2006, fig. 1). In *Juratyran*, length : height ratios range from 1.03 to 1.38, with a mean (*n* = 3) of 1.16 (Benson 2008). Relatively elongate dorsal centra thus appear to be a typical (presumably plesiomorphic) feature of non-tyrannosaurid tyrannosauroids.

PLACE TABLE 5 ABOUT HERE

PLACE TABLE 6 ABOUT HERE



# Sacral vertebra

A single sacral centrum is known for *E. lengi* (Fig. 13s–x) and was described by Hutt et al. (2001, p. 232), who suggested that it was the last sacral. It is here regarded as the first due to reinterpretation of the heavily scarred articular face of the centrum as the posterior one (for measurements, see Table 6). As with the better preserved dorsal vertebrae, it is mostly complete ventral to the neurocentral suture; the neural arch is absent. It is shallow and broad compared to the dorsal centra and has a wide, deep neural canal.

The anterior articular face is broad, slightly concave and shallow dorsoventrally. Large, rugose, concave facets for reception of the sacral ribs and transverse processes are present dorsolateral to the articular face. That on the left is more complete and has a width of 28 mm and a length of 25 mm. An oblique groove divides the left facet into two halves, possibly demarcating the attachment area for the sacral rib from that of the transverse process.

Approximately halfway along the length of the centrum, the ventral halves of large, dorsally positioned oval foramina are present (Fig. 13s, v). That on the left side is better preserved and has a complete ventral bony rim. It is 11 mm long and 5 mm tall as preserved. The right foramen is less well preserved and has incomplete margins but appears to have had similar dimensions. Both foramina are set within larger lateral concavities and communicate medially with the neural canal. These foramina are in the same position as the large sacral nerve foramina illustrated by Welles (1984) for *Dilophosaurus* and similar foramina are present at mid-centrum, at the neurocentral suture, in *Juratyran* (Benson 2008). However, openings interpreted as pneumatic foramina occur in precisely the same location in tyrannosaurids (Brochu 2003, p. 89). In *E. lengi*, the connection of the foramina to the neural canal indicates that they are spinal nerve foramina. The neural canal is shallowest anteriorly, deepening posteriorly and also widening to 30 mm. Posteriorly, two lateral subcircular pits are present on its floor, each  $c. 10 \times 10$  mm (Fig 13w). These structures are rarely described or illustrated but the pits seen in *E. lengi* appear typical for theropods and perhaps for saurischians as a whole. Osmólska et al. (1972) described (but did not illustrate) “a pair of large and deep pits for the spinal ganglions in the anterior portion of each vertebra” in the 2<sup>nd</sup> and 3<sup>rd</sup> sacral vertebrae of *Gallimimus bullatus* (p. 122) and apparently homologous structures were figured in a titanosauriform sauropod by Carpenter and Tidwell (2005, fig. 3.7G).

The posterior articular face of the centrum is broader and deeper than the anterior surface. The posterior face is flat, but bears a series of radiating grooves and ridges that create a star-burst

pattern (Fig 13x) that is typical of unfused sacral centra (e.g. Madsen 1976, plates 25-27). The posterior articular surface is deeper than the anterior one, the posterior end descending further ventrally. The ventral surface is concave in lateral view. A low keel is present along the ventral midline and is most pronounced over the anteriormost 30 mm of the centrum.

# **Caudal vertebrae**

Five poorly preserved, incomplete caudal vertebrae are tentatively identified as belonging to the distal part of *E. lengi*'s caudal skeleton: this cannot be confirmed, however, since they provide little information and do not possess any features that are typical for coelurosaurs (such as long prezygapophyses that overlap the centrum of the adjacent vertebra) (for measurements, see Table 6). Three of these vertebrae are represented only by partial centra preserving parts of their articular surfaces. Where known, the ventral surfaces of the centra are convex and lack midline keels or other structures. The additional two distal caudals – both of which preserve a partial neural arch – are incomplete proximally. One has a proximal centrum width of 15 mm but flares outwards distally such that the concave distal articular face would have been at least 25 mm wide at mid-height. Camellate bone texture is visible on the floor of the neural canal. A neural spine was probably absent, suggesting that this vertebra was distal to c30. The incomplete right postzygapophysis extends 3 mm distal to the articular face, is positioned close to the midline, and curves distomedially, indicating that the prezygapophyses in this region of the tail must have been very close together. At most, the postzygapophysis is 12 mm dorsal to the centrum, whereas the neural arch at the proximal end of the centrum is only *c.* 5 mm dorsal to the centrum. A shallow concavity separates the base of the postzygapophysis from the centrum. The lateral surfaces of the centrum are convex but bear low proximodistally oriented ridges. The ventral surface is flattened and chevrons facets are absent.

A second, smaller distal caudal vertebra is even simpler in structure. The postzygapophyses were clearly short and close to the midline and a neural spine seems to have been absent. Again, poorly developed ridges are present on the laterodorsal region of the centrum and are parallel to the centrum's long axis. The centrum flares laterally at its distal end. The maximum width of the centrum at its broken proximal end is 16 mm. The postzygapophyses of both of these vertebrae are unusually short when compared with those of the distal caudal vertebrae of other tyrannosauroids (Brochu 2003; Carr et al. 2005) but are comparable in approximate proportions to those present in some other coelurosaurs, including compsognathids and *Bagaraatan* (Ostrom 1978; Osmólska 1996; Currie and Chen 2001).

# **Dorsal ribs**

Though the presence of ribs associated with the *E. lengi* holotype was not mentioned by Hutt et al. (2001), several rib shaft fragments and dorsal ends are preserved (Fig 14). None are preserved in articulation or association with vertebrae, meaning that the precise positions of the fragments cannot be determined, nor can it be determined which side of the body the ribs belong to. Given the presence of a dryosaurid in the assemblage, it is possible that at least some of these bones do not belong to *E. lengi*. Only the more informative specimens are described here. Ribs are described as imagined in articulation, with directional terms corresponding to those that would apply to a complete ribcage.

The dorsal 41 mm of a rib preserves a near-complete capitulum and tuberculum but only the dorsal ‘neck’ of the shaft (Fig 14b). It is preserved in close association with three rib shaft fragments. From the lateral edge of the tuberculum to the medial tip of the capitulum it is 44 mm long, and from their apparent closeness it would seem that this rib was from the anterior part of the ribcage, probably representing one of the first five dorsal ribs. What appears to be a pneumatic recess is present at the dorsal end of the shaft (this pneumatic structure confirms the rib’s identity as that of *E. lengi*), but is partially concealed by a shelf that overhangs it from the lateral side. The preserved part of the shaft is sub-oval in cross-section.

PLACE FIGURE 14 ABOUT HERE

A rib fragment 80 mm long, preserving the bases of both the capitulum and tuberculum, adheres to a block and is exposed in anterior view (Fig 14a). The capitulum is compressed, being 16 mm deep but just 6 mm wide. The tuberculum is also compressed: in cross-section it is 3 mm wide at its medial end but *c.* 12 mm wide laterally. Its lateral edge is distally continuous with the intercostal ridge. The anteromedial edge of the rib shaft is thickened and anteriorly convex but the shaft becomes concave toward its lateral margin. **It would appear** that the anterior surface of the shaft was concave for all or most of its length, forming a distinct costal groove. Anterolaterally, the intercostal ridge forms the border of this concavity (and the boundary between the anterior and lateral surfaces of the shaft) and the ridge would also presumably have extended for the entire length of the shaft. The shaft is thus U-shaped in cross-section. The lateral surface of the rib is convex and meets the posterior surface at a prominent angle.

The longest rib fragment preserved in the *E. lengi* assemblage has a preserved length of 115 mm and represents the ventral end of a shaft (Fig 14c). The dorsal end of this fragment is oval in cross-section but the ventral part is rounded with a blunt termination capped with unfinished bone. The dorsal part of the medial surface is compressed into a keel-like edge that extends *c.* 50 mm ventrally. The ventral 50 mm of the shaft is narrower mediolaterally (*c.* 13 mm) than the dorsal section (*c.* 25 mm). On either the anterior or posterior surface (it is not possible to determine which is which) a lateral flange-like extension projects from the shaft. A similar structure has not been reported elsewhere in Theropoda, suggesting either that this rib does not belong to *E. lengi* or that *E. lengi* was unique among theropods in this respect.

### **Pectoral girdle and forelimb skeleton**

The morphology of the *E. lengi* forelimb was well characterised by Hutt et al. (2001). That preliminary study noted the presence in *E. lengi* of a gracile humerus, trochleated carpus and gracile metacarpal I with a strongly asymmetrical distal end, as well as proportionally elongate phalanges in at least two of the manual digits and strongly curved unguals (Hutt et al. 2001). The literature on theropod limb osteology features inconsistencies in the application of directional terms, at times because some authors interpret bones in their imagined life postures (e.g. Johnson and Ostrom 1995; Charig and Milner 1997). Here, bones are described in the conventional fashion, i.e. with the flexor surface of the manus described as ventral even though this surface likely faced medially in life (Gisklick 2001; Senter and Robins 2005). *E. lengi* is assumed to have possessed three or four metacarpals on the basis of comparison with other non-tyrannosaurid tyrannosauroids represented by better remains (Xu et al. 2004, 2006).

### **Scapulae**

Both scapulae of *E. lengi* are preserved, though only part of the blade is present in the case of the right scapula. The main new discovery made regarding the morphology of the scapula since Hutt et al. (2001) is the morphology of the bone's dorsal termination.

The left scapula is almost complete (Fig 15e) and preserved in partial articulation with the left coracoid. It is composed of a mediolaterally compressed, strap-like blade *c.* 280 mm long. Both the anterior and posterior margins of the blade are expanded, with the expansion along the anterior edge beginning further dorsally than is the case on the posterior side. In lateral view, the anterior expansion has a small, anterodorsally projecting bump, while the posterior expansion has an arcuate, uninterrupted posterior edge. The anteroventral margins of the scapula are not

preserved so it cannot be determined if acromion region was squared-off as is the case in tyrannosaurids and some other theropods. The anterior and posterior borders of the blade are subparallel and the medial surface of the blade is concave. At approximate mid-length the blade is c. 32 mm wide. The blade has a mediolateral thickness of c. 5 mm. At its ventral end the scapula expands to form a large acromion process. Here the bone is c. 85 mm long anteroposteriorly.

The dorsal tip of the blade is preserved within one of the blocks and can only be viewed in cross-section. It fits on to the rest of the blade and probably added 20 mm or so to the blade's length. With a maximum width of c. 50 mm this fragment (which was unknown to Hutt et al. 2001) shows that the tip of the scapula was wider than the shaft, and it would appear that this expansion was abrupt. The scapula's surface is not sufficiently well preserved to reveal the locations of muscle attachment sites.

PLACE FIGURE 15 ABOUT HERE

The right scapula is represented only by two fragments of the blade, one of which appears to belong to the dorsal end and the other to a more ventral part of the bone (Fig 15f). The more dorsal part is subrectangular, being 70 mm long and c. 40 mm wide. The cross-section of this fragment is lenticular and c. 8 mm thick. The second part of the right scapula has a maximum preserved length of 130 mm, and one end is wider than the other (36 mm vs 30 mm). The longer end appears to be the more dorsal one. At its probable dorsal end, the blade fragment is strongly compressed in cross-section, being at most 7 mm thick, whereas its ventral end is thicker (15 mm). The inferred lateral surface of the blade fragment is convex while the inferred medial surface is flat.

The slender-bladed scapula with its broad acromion and dorsally expanded tip resembles those of tyrannosaurids (Holtz 2004). However, several of the features present in *E. lengi* have a wide distribution within coelurosaurs, including an expanded dorsal tip, subparallel anterior and posterior edges and broad acromion, and tyrannosaurids tend to have a scapula that is narrow ventrally and wider in its dorsal part. The scapula of *Dilong* lacks subparallel edges and is expanded at its dorsal end (Xu et al. 2004). *Guanlong* lacks a dorsal expansion of the scapular blade, and its blade widens only slightly towards its dorsal end (Xu et al. 2006). Ornithomimosaur and maniraptorans lack an expanded scapular tip and are thus also unlike *E. lengi* (Rauhut 2003b).

# Coracoid

The left coracoid (Fig. 15a–d) remains partially articulated with the base of the left scapula. It is mostly complete and preserves an intact glenoid cavity and margin posteroventral to the glenoid (Fig 15c): most of the rest of the other margins are damaged, however. The coracoid appears to have been typical for tetanurans in being semicircular overall with a posteriorly directed glenoid and a short posteroventral process which is separated from the coracoid body by a shallow posterior notch. The preserved height of the coracoid is 85 mm and its length is 70 mm. The body is deeply concave medially and strongly convex ventrolaterally. A prominent coracoid tubercle projects *c.* 8 mm from the lateral coracoid surface (Fig. 15a-b); it is robust, subtriangular in lateral view but with a flattened apex. As discussed by Hutt et al. (2001, p. 233) there is no indication of a coracoid foramen. This is not unprecedented for a coelurosaur as *Bambiraptor feinbergi* was also reported to lack this feature (Burnham et al. 2000). However, damage to the bone surface in *E. lengi* renders this inconclusive: it is possible that a coracoid foramen was present originally but that it is now obscured by damage. Dorsal to the coracoid tubercle, and adjacent to the coracoid's dorsal edge, there is an elongate, oval concavity (Fig 15b).

The glenoid fossa is slightly concave and, as in tyrannosaurids (Brochu 2003, p. 94), the coracoid probably formed the ventral half of the fossa. The fossa is wide (26 mm) and at least 27 mm tall. The adjacent region of the coracoid body is also thick, being 15 mm wide just ventral to the glenoid. The posteroventral process is incomplete posteriorly; much of the process is positioned posterior to the glenoid if the bone is imagined in life position (with the glenoid directed somewhat dorsally). When complete, the process probably extended for a further 20 mm or so. In *Dilong*, the coracoid's posteroventral margin lacks an embayment (Xu et al. 2004, fig. 1i).

The ventral part of the medial surface of the bone is flat. The anterior and ventral margins are only 1-3 mm thick and thus far thinner than the posterior margin. The anterior margin is damaged and the bone has been deflected away from the original union with the acromion process of the scapula. What might be part of the anterior region of the coracoid is still attached the scapula but does not provide any useful information.

# Humerus

Both humeri of *E. lengi* are known (Fig 16) and a preliminary description of the right humerus was provided by Hutt et al. (2001, p. 233). The right humerus is almost complete though



preserved in two pieces and lacking part of the proximal end, parts of the shaft and deltopectoral crest, and some of the distal condyles. With a total length of 240 mm, the humerus is gracile and long-shafted with an anteriorly curving distal end and prominent subtriangular deltopectoral crest. Because the left element is less complete, most observations presented here are based on the right element.

The long axes of both the proximal and distal ends are parallel. In this respect *E. lengi* more recalls *Dryptosaurus* (Brusatte et al. 2011) and tyrannosaurids (Brochu 2003) than *Dilong* or *Guanlong*: in the latter two, the distal end of the humerus is deflected such that it is angled medially relative to the humeral long axis (Xu et al. 2004, 2006). The rounded proximal head is wide and subcylindrical and without the inflated, hemispherical morphology present in tyrannosaurids (Brochu 2003). *E. lengi* is more similar in its humeral head morphology to the plesiomorphic tyrannosauroid condition of *Dilong* or *Guanlong* in this respect (Xu et al. 2004, 2006). The head is tallest and most bulbous medially and is connected laterally to a lower convexity that recalls the “greater tubercle” of Madsen and Welles (2000) (Fig. 16a, d). The latter feature is unexpected since there does not appear to be a similar structure in *Dilong* or Tyrannosauridae (Brochu 2003; Xu et al. 2004), raising the possibility that this is an autapomorphy of *E. lengi*. The condition in both *Tanycolagreus* and *Guanlong* is unclear due to damage (Carpenter et al. 2005a; Xu et al. 2006).

At its medial border the proximal end protrudes anteromedially to produce an internal tuberosity, though this is incomplete. Brochu (2003, p. 97) noted that *E. lengi* appeared superficially similar in internal tuberosity morphology to tyrannosaurids but wondered if this was due to damage. On the posterior surface of the humerus, the head and greater tubercle appear notably convex and posteriorly prominent relative to the humeral shaft but there is no distinct furrow or other structure that demarcates them from the rest of the bone.

PLACE FIGURE 16 ABOUT HERE

Viewed laterally, the deltopectoral crest is subtriangular with a distally located apex and a 90° angle between its distal margin and the anterior face of the humeral shaft (Fig. 16c, e). The crest’s distal margin grades smoothly into the shaft, its edge describing a shallow arc. The crest’s anterior edge is rugose and serrated, though this mostly appears to be the result of erosion. None of this apical, anteriormost area overhangs the shaft or is wider than the crest at mid-height. The crest’s base is wide relative to the apex, such that the crest is subtriangular in cross-section. The



crest's lateral surface is rugose but muscle scars cannot be identified. Extending distally along the humeral shaft for approximately 80 mm, the deltopectoral crest is one-third the length of the humerus, similar in extent to the crests of *Dryptosaurus* (Brusatte et al. 2011) and tyrannosaurids (Brochu 2003). In *Dilong* and *Guanlong* the crest is 40-50% of humerus length (Brusatte et al. 2011).

The proximal part of the anterior surface of the humeral shaft is concave, being bordered on its medial side by a raised rim that extends proximally to reach the internal tuberosity. The humeral shaft is cylindrical and measures 30 mm in width and 25 mm perpendicular to this at its broken point of breakage. Hutt et al. (2001, p. 233) described the presence of four internal compartments: a large posterior one (15 × 10 mm) and three smaller anterior ones (between 2 and 6 mm in width). The shaft is broken just distal to the deltopectoral crest and the apparent internal demarcation into a "large, hollow" part of the shaft and a "region consisting of several smaller cavities" seems to relate to the presence of greater bone thickness in the anterior part of the shaft associated with the presence of the deltopectoral crest (at the point where the shaft becomes demarcated from the distal end of the crest, a cross sectional view results in the appearance of there being distinct cavities inside the deltopectoral crest and shaft, the separation between then being formed by thick bone at the distal end of the crest). The left humerus is also broken across the shaft, though in this case at a level some 60 mm distal to the deltopectoral crest. Though the shaft is crushed and damaged, it is internally hollow with no indication of distinct compartments. The internal structure suggested to be diagnostic for *E. lengi* by Hutt et al. (2001, p. 229) is therefore not significant.

Across its distal condyles the humerus is 48 mm wide. The distal condyles are located more on the anterior surface of the humerus than on the distal end. They are damaged with most of the bone surface missing but it does not appear from their proportions that either was particularly bulbous. The medial condyle is slightly larger than the lateral condyle and connected to it by a shelf of bone, proximal and ventral to which are concavities. Proximomedial to the medial condyle is a prominent entepicondyle (Fig 16b). Similar structures are known in alvarezsaurids (Novas 1996, 1997), oviraptorosaurs (Osmólska et al. 2004), therizinosauroids (Barsbold 1976; Perle 1981; Clark et al. 2004; Kirkland et al. 2005) and dromaeosaurids (Ostrom 1969; Brinkman et al. 1998). The massive entepicondyle of alvarezsaurids is bulbous, subconical and slightly curved medioproximally (Novas 1996, 1997), unlike the more block-like, medially projecting structure of *E. lengi*. In oviraptorosaurs the entepicondyle has been described as projecting anteriorly (Osmólska et al. 2004, p. 175). This is unlike the condition in *E. lengi* in which the

structure is directed medially. The hypertrophied entepicondyle of therizinosaurs is unlike that of *E. lengi* in being clearly demarcated at its distal edge from the ulnar condyle but is similar to the entepicondyle of *E. lengi* in approximate proportions. Similar large entepicondyles are not present in other tyrannosauroids including *Tanycolagreus*, *Dilong* or members of Tyrannosauridae (Russell 1970; Brochu 2003; Carpenter et al. 2003; Xu et al. 2004), nor are they typical outside of Coelurosauria (e.g. Madsen 1976); in these taxa the same region of the humerus form a subtle medial convexity, a structure that might be termed an entepicondyle being absent. The form of the *E. lengi* entepicondyle is thus here regarded as **autapomorphic**. Proximal to the entepicondyle, the medial margin of the shaft is concave when the humerus is viewed anteriorly. There is no suggestion of an ectepicondyle. The lateral side of the distal end of the humerus is flattened with a sharp ridge marking the anterior extent of the flattened lateral surface.

# Ulna

The incomplete shaft of a presumed right ulna was described by Hutt et al. (2001, p. 233). The preserved length of the element is 90 mm long and its lateral and laterodorsal surfaces are obscured by matrix. Both the proximal and the distal ends are broken. At one end the element is subrectangular in cross-section (Fig. 17f), being 25 mm wide and 22 mm deep, while at the other is subovoid, being 30 mm tall and 16 mm wide at mid-height and wider dorsally than ventrally. The resulting “inverted tear-drop” shape seems to be unique and is regarded as a potential autapomorphy of *E. lengi*: the same condition is present in the oviraptorosaur *Avimimus* (Vickers-Rich et al. 2002) but is assumed to be convergent. In tyrannosaurids **the ulna is subrectangular distally but subovoid proximally**, so the ends of the element are identified accordingly. Viewed in profile, one edge of the element is slightly concave while the other is slightly convex and marked with a longitudinal keel. The concave edge is assumed to be the dorsal one and the convex edge the ventral one. It is less easy to determine whether the element is from the left or right side. One of its sides is convex while the other is flat; the convex side seems more likely to be the lateral one, in which case the element is from the animal’s left (Fig. 17e–f). The description given by Hutt et al. (2001, p. 233) does not match the element and should be ignored.

PLACE FIGURE 17 ABOUT HERE

# Radius

Hutt et al. (2001, p. 233) noted that a fragmentary radius may be present among the *E. lengi* material. This element is preserved on the same block as the putative second and third metacarpals, the axial neural arch and a cervical centrum. The element is 74 mm long and is broken both proximally and distally (Fig. 17a–c). It consists of a robust, subcylindrical shaft that flares out to one side at one of its ends. A shallow subtriangular concavity is present on the side of this flaring region. This concavity recalls the lateral radial facet that receives the proximal coronoid process of the ulna. The opposite end resembles the ulna in having a teardrop-like cross-section, which is 32 mm deep and 16 mm wide. The end with the flaring region is tentatively identified as the proximal end. It is not possible to determine whether this incomplete element belongs to the left or right side.

# Distal carpal I

A well-preserved, complete distal carpal is known for *E. lengi* and is regarded here as a left distal carpal I (Fig. 18a–f). Hutt et al. (2001, p. 233) described this bone briefly and suggested that it was a radiale due to its similarity to the bone of *Deinonychus antirrhopus* described as a radiale by Ostrom (1969, pp. 98-99) as a radiale but now known to be a distal carpal I (Chure 2001). The distal carpal of *E. lengi* is complex; due to its discovery in isolation (that is, its being unconnected to any adjacent element), our identification of its several surfaces is based on a perceived homology with distal carpal I in those other non-maniraptoran tetanurans for which this element has been adequately figured and described, namely *Allosaurus* (Chure 2001), *Coelurus* (Carpenter et al. 2005b), *Tanycolagreus* (Carpenter et al. 2005a) and *Guanlong* (Xu et al. 2006). The element in *E. lengi* is especially similar to that of *Guanlong*. In both proximal and distal distal view, the element is slighter wider than tall, the articular surface covering virtually the whole of the bone and with a transverse groove or step dividing the surface into equal dorsal and ventral facets. On the distal surface, these two facets have different orientations: the dorsal facet faces distolaterally while the ventral facet is directed distomedially. In all other views, the carpal is subrectangular.

The dorsal surface is incomplete along its distomedial margin, the bone being broken and eroded along the remainder of the medial margin as well. The surface is otherwise concave and surrounded by a raised margin that is thickest and most prominent distolaterally. This thick margin merges with a rounded ridge that extends ventrally along the bone's lateral edge. Mid-way along the distal edge, a projecting peak is present, the result being a subtriangular margin.

The proximal margin of the dorsal surface is simply convex. The concave part of the dorsal surface is rugose and marked with numerous foramina, small furrows and a wrinkled bone texture.

The ventral surface of the carpal is also mostly concave, this concave region flanked on all sides by tall, thick margins. The surface is curved along the transverse axis, the proximal rim of the surface being more convex than the distal rim, the result being a **rather** crescentic outline. **Again**, the bone surface is marked with foramina and has a rugose texture.

PLACE FIGURE 18 ABOUT HERE

How this carpal articulated with metacarpal I cannot be tested because the proximal end of metacarpal I is damaged. The presence on the distal surface of two facets – one directed distomedially and the other distolaterally – indicates that metacarpals I and II articulated with the carpal. The mc I facet presumably articulated with much of the base of mc I while the mc II facet seems to have articulated with the proximal surface of mc II.

If the interpretation proposed here is correct, *E. lengi* lacked fusion between distal carpals I and II on its probable left side at least (carpal fusion is known to be sometimes asymmetrical in coelurosaurs: see Zanno 2006). The subadult status of the *E. lengi* holotype also raises the possibility that distal carpal II might have fused to carpal I at a later ontogenetic stage in *E. lengi*, forming a semilunate. While tyrannosaurids have what can be regarded as a “reduced” carpal skeleton, consisting only of flattened disc-like carpalia that lack trochleated surfaces (Carpenter and Smith 2001), Holtz (1994) argued that this arose through simplification in the course of evolution from taxa with trochleated complex carpalia.

## Metacarpals

Three probable metacarpals are known for *E. lengi*: the left **mc I** (briefly described by Hutt et al. 2001, p. 233), and two bones interpreted here (see also Hutt et al. 2001, p. 233) as the proximal ends of mc II and III. Both are preserved on a block between the axial neural arch and the cervical centrum; both are incomplete distally and would have been much **larger** when complete.

The left mc I is well preserved, 56 mm long and with an asymmetrical distal end (Fig. 18g–j). The proximal articular surface is **near-complete and only slightly eroded**, lacking the corner of the ulnar side and a small area of bone from the radial side. It is subtriangular with the

longest axis (25 mm wide) being the mediolateral one: this is shorter than the dorsoventral height. The apex of the subtriangular articular surface is laterodorsally positioned. This is approximately similar to cross-sectional shape of the left metacarpal I of *Deinonychus antirrhopus* (Ostrom 1969, fig. 63), except that the ventrolateral projection seen in that taxon is absent in *E. lengi*. The proximal end of metacarpal I of *E. lengi* exhibits a slightly concave 18 mm long facet for reception of metacarpal II on its lateral side. The dorsomedial surface of metacarpal I is also slightly concave, while the ventral surface is flat. The two distal condyles are markedly asymmetrical with the bulbous lateral condyle extending 10 mm further distally than the medial condyle (Fig. 18g–h). The medial condyle is strongly convex distally but is flat on its medial surface and lacks a collateral ligament fossa. It has a maximum dorsoventral height of 18 mm. A shallow U-shaped notch separates it from the lateral condyle which is 20 mm tall dorsoventrally and with a wider convex distal surface. An oval collateral ligament fossa is present on the lateral side of the lateral condyle and is *c.* 7 mm long proximodistally and *c.* 4 mm deep. The strong asymmetry of the metacarpal's condyles shows that the pollex of *E. lengi* must have been strongly divergent. Mc I in *E. lengi* is highly similar to that of *Deinonychus*, the main difference being that the medial condyle is more distally prominent in *E. lengi*. *Tanycolagreus*, *Dilong* and *Guanlong* are also similar with regard to the form of mc I (Xu et al. 2004, 2006; Carpenter et al. 2005a), though in *Guanlong* this bone has a more robust shaft. In tyrannosaurids, the shaft is even more robust; furthermore, the distal articular end is less differentiated from the shaft, the condyles are less prominent and the intercondylar groove is shallower (Russell 1970; Carpenter and Smith 2001; Brochu 2003; Holtz 2004). Compared with non-coelurosaurs, the *E. lengi* mc I is longer and more gracile than mc I of *Allosaurus* and *Acrocanthosaurus* (Madsen 1976; Currie and Carpenter 2000; Chure 2001), and it is also gracile relative to that the compsognathid *Sinosauropteryx* (Currie and Chen 2001). It would appear that early tyrannosauroids uniformly possessed a gracile mc I.

A bone that may be left mc II has a preserved length of 76 mm and includes the proximal articular end and part of the shaft. The proximal articular surface is broad (34 mm) and flat. Only one side of the bone is exposed and this surface is probably the ventral one because it is flat: the opposite side (visible only in cross-section) is convex. At its broken distal end, the shaft is sub-oval with the longest axis being the dorsoventral one: this is 18 mm tall. The shaft is 6 mm wide mediolaterally; its probable lateral side is flat while the probable medial side is shallowly convex. The cross-sectional shape of the metacarpal shaft indicates that the broad proximal end was oriented mediolaterally. Such a large difference between proximal breadth and shaft width is seen

in non-coelurosaurian theropods including allosauroids (Gilmore 1920; Madsen 1976; Currie and Carpenter 2000) but appears less typical of coelurosaurs, in most of which the proximal end of mc II is similar in width to the shaft. This is also true in compsognathids and *Scipionyx* (Currie and Chen 2001; Dal Sasso and Maganuco 2011). However, *Nqwebasaurus* and therizinosauroids possess a proximally broad mc II (Barsbold 1976; Russell and Dong 1994; de Klerk et al. 2000; Clark et al. 2004) and this also appears to be the case in tyrannosaurids (Lambe 1917; Russell 1970; Carpenter and Smith 2001; Brochu 2003; Holtz 2004).

Preserved adjacent to the probable proximal end of mc II is a longer, more robust element 74 mm long. It is also expanded at its proximal end with a preserved mediolateral width of 56 mm. In contrast to the putative mc II, the longest axis of the sub-oval cross-section of the broken shaft is parallel to that of the proximal expansion. This suggests that the expanded end may have been oriented dorsoventrally within the metacarpus, rather than mediolaterally. It is tentatively identified as mc III. If this element was oriented with its longest axis in cross-section arranged mediolaterally, the mc III of *E. lengi* would have been unusually broad compared to that of other tetanurans. The exposed surface of the bone is therefore probably medial. A prominent medial tubercle is located approximately 16 mm ventral to the dorsal edge and adjacent to the proximal articular surface. The bone dorsal to the tubercle is medially flat, whereas that ventral to the tubercle forms a concavity. When the metacarpus was articulated, the proximal end of mc II presumably fitted against one of these surfaces, and the tubercle may have helped prevent it from being displaced ventrally or dorsally.

What appears to represent a more distal part of the same bone (based its similar width) adheres to the shaft of a manual phalanx and is 45 mm long. In cross section it is hollow with bone walls c. 2 mm thick, and is taller (15 mm) than broad (10 mm). It is impossible to establish which end of the shaft is the proximal one. One end is more subcircular in cross-section than the other.

# **Manual phalanges**

Several manual phalanges of *E. lengi* are present, representing elements from both hands (Fig 19). None are articulated, so their positions within the manus are inferred with varying degrees of certainty (Fig 19e'). The identifications proposed here are based on the proportions of the phalanges relative to those of other taxa and to one another, and to the manner in which they sometimes articulate. Phalanges were provisionally identified as belonging to the left or right depending on the proportions of the distal condyles and shapes of the articular surfaces.



PLACE FIGURE 19 ABOUT HERE

A complete, relatively robust phalanx 60 mm long is tentatively identified as the left I-1 (Fig. 19a–f) on the basis of its good level of articulation it achieves with the left metacarpal I. When this phalanx and metacarpal I are articulated, the phalanx is directed medially relative to the long axis of the manus. However, the fact that this possible I-1 is only slightly longer than mc I renders this identification suspicious: it either indicates that *E. lengi* had an unusually proportioned pollex relative to other non-tyrannosaurid tyrannosauroids – in these taxa I-1 is much longer than mc 1 (Xu et al. 2004, 2006) – or the phalanx actually belongs to another digit. The proximal articular surface of this phalanx (25 mm wide, 22 mm tall) is biconcave with a weakly developed, vertically oriented central ridge. Bony rims surround the articular surface with the dorsolateral section of the rim exhibiting a shallow concavity. The shaft is deepest adjacent to the proximal articular surface. The proximal part of the ventral surface of the shaft is excavated by a shallow concavity at its proximal end and low convexities – probably weakly developed, paired flexor processes – flank this concavity proximomedially and proximolaterally. Distally, the left condyle is taller than the right condyle (20 mm vs 19 mm). This minor difference suggests that the phalanx is from the left manus. The distal end is 20 mm wide. The deep collateral ligament fossae are oval and are located high on the sides of the condyles; the fossa on the left side is slightly larger than that on the right. The larger of the two preserved unguals articulates well with this phalanx.

A relatively short, robust phalanx, 62 mm long, is identified as the right II-1 (though an identification as II-2 is also plausible) (Fig. 19g–l). The height and breadth of the proximal articular surface are similar (27 mm and 26 mm, respectively) and this surface is surrounded by a symmetrical bony rim. The collateral ligament fossae are asymmetrical, that on the left being deep and that on the right shallow. Similarly, the left distal articular condyle extends further distally than the right. This phalanx articulates perfectly with the one identified as the right II-2. The proximal end of an incomplete phalanx has a preserved length of 29 mm, and can be identified as belonging to the left II-1 because it is essentially identical to the proximal end of the phalanx just described. The articular surface of the incomplete element (24 mm wide, 27 mm tall) is biconcave with a convex dividing ridge. On the right side of the articular surface, the rim forms a prominent ‘shoulder’. The ventral surface has a shallow transverse concavity flanked by two low convexities.



A long, gracile manual phalanx (total length 85 mm) is preserved attached to the blade of the scapula (Fig. 19m–o). This is probably the phalanx suggested to be II-2 by Hutt et al. (2001, p. 233) and is extremely similar to the manual phalanx II-2 of *Deinonychus* (Ostrom 1969, fig. 63). The proximal articular surface is biconcave and 20 mm tall. The surface is *c.* 13 mm wide at its dorsal end but broadens ventrally to *c.* 18 mm. Flaring rims are present on the lateral and medial sides. The articular rim on the right side is uniformly convex; that on the left possesses two successive convexities, the dorsal convexity being more prominent than the ventral one. The two halves of the articular surface are only weakly separated by a vertical ridge. The phalangeal shaft is straight, and is taller than broad such that the cross section is a mediolaterally compressed oval. Viewed laterally or medially, the shaft is tallest adjacent to the proximal articular surface. The dorsal and ventral margins converge as they begin to pass distally, but are subparallel at the shaft's mid-length. The shaft then expands distally to form the prominent distal articular condyles. These are long (that on the left having a total ventral length of 25 mm) and strongly convex ventrally. They are separated by a deep intercondylar groove but, due to damage, it cannot be determined how far this extends dorsally. Unlike in some of the other manual phalanges, the ventral surface of the proximal end is flat. It cannot be determined with certainty whether this phalanx is from the left or right manus.

Hutt et al. (2001, p. 233) described a manual phalanx 70 mm long and suggested that it belonged to either digit II or III. In view of its length, this specimen is probably III-3 (Fig. 19u–z). It is robust with a broad proximal end and prominent distal condyles. The biconcave proximal articular surface is 26 mm tall and 28 mm broad. The flaring rim on the right side of the articular surface exhibits a ventral convexity not present on the left. The ventral surface is flat with, again, low convexities flanking its proximal region. Both ligament fossae are elliptical, with that on the left being more dorsally located. The left fossa (10 mm long and *c.* 4 mm tall) is also deeper than the right fossa (which cannot be measured unambiguously but is less than 6 mm long). This difference, combined with the ventrally convex rim on the specimen's right side, suggests that it is from the left manus.

An additional phalanx, 60 mm long, is intermediate in robustness between those identified as II-1 and II-2 (Fig. 19p–t). The distal condyles are essentially missing, although their ventralmost portions are preserved. These show that the condyles were small, each with a poorly developed trochlea, and that the intercondylar groove was shallow. Across the distal end the specimen is 15 mm wide. The proximal articular surface is subtriangular and (in contrast to some of the other phalanges) wider than tall (25 mm versus 23 mm). Unlike in all other *E. lengi* manual phalanges,

the proximal surface it is not biconcave. An undivided proximal articular surface is seen elsewhere in phalanx III-1 of certain allosauroids (Gilmore 1920, p. 62; Currie and Carpenter 2000, p. 230). Given that a longer, more robust phalanx described above is inferred to be phalanx III-3 this is unlikely but not impossible. There does not seem to be a way of determining whether this phalanx is from the left or right manus.

Some additional non-ungual phalanges are preserved but their positions are difficult to infer. The distal 40 mm of a phalanx, comprising the articular condyles and a fragmentary part of the shaft, cannot be identified with confidence: it is extremely similar to the distal end of the manual phalanx identified as the right II-1 or II-2 but may belong to the foot. The right condyle has a height of 16 mm and a width of *c.* 8 mm, and appears to extend further distally (by *c.* 3 mm) than does the left; the left condyle is damaged, with some of the ventral surface missing. The right collateral ligament fossa is circular (4 mm high and 4 mm long) and deep. The right condyle flares laterally in one direction, which is presumably ventral.

Two manual unguals are known for *E. lengi*, and both were briefly described by Hutt et al. (2001, pp. 233-234). The first of the two is large, with a preserved length along its proximodistal axis of 85 mm and a length along its curved dorsal margin of 103 mm (Fig. 19a'–b'). The distal tip is missing and conceivably added another 10-15 mm to this curve. The proximal articular surface is deep (26 mm), narrow (15 mm) and surrounded by a bony rim. The flexor tubercle is well developed, bulbous and most prominently convex on the ventral surface of the ungual's base. The tubercle is not continuous with the articular facet. Distally, the tubercle is not distinct from the curved portion of the ungual but grades into it along the ungual's ventral margin. Where the tubercle is most pronounced, the ungual has a maximum dorsoventral depth of 42 mm. The ventral surface of the rest of the ungual is convex and does not form a keel or ridge, though the part of the ventral edge just distal to the flexor tubercle is somewhat mediolaterally compressed and keel-like. The ungual's dorsal margin is **continuous** convex. The sides are flattened but become **more dorsoventrally convex toward** the distal tip. The claw grooves are symmetrically positioned but that on the left is deeper and more prominent than that on the right. It is approximately 3 mm deep at its proximal end but shallows to 1 mm at the ungual's tip. Near the ungual tip, the bone ventral to the groove forms a lamina that overlaps the ventral margin of the groove. Hutt et al. (2001, p. 233) identified this ungual as from the pollex, but there seems to be no way of knowing whether it is from the left or right.

The second manual ungual is very slightly smaller (Fig. 19c'–d') and was regarded by Hutt et al. (2001, p. 233) as belonging to digit II. Its proximal end is cracked and somewhat crushed. As

with the pollex ungual, there does not seem to be a way of determining whether it belonged to the left or right manus. Its ‘straight line’ preserved length is 84 mm while the length along its dorsal curve is 97 mm. Again, 10-15 mm of the distal tip is missing. Overall it is highly similar to the larger ungual but is somewhat straighter, has a less bulbous flexor tubercle, and has a more prominent lateral groove. Along the ventral surface of the ungual, the margin distal to the flexor tubercle slopes gradually away from the tubercle, rather in the more steeply angled fashion present on the ungual inferred to belong to the pollex. A similar degree of variation in ventral topology is present between unguals I and II in *Guanlong* (Xu et al. 2006). The proximal articular surface is tall (26 mm), narrow (14 mm) and approximately symmetrical. This surface is weakly biconcave with a poorly developed vertical ridge separating the two halves. A proximodorsal lip surrounds the articular surface and, in contrast to the larger ungual, there is a demarcation between the convex dorsal surface of the ungual and the rim. In some maniraptorans, the manual unguals of digit II and III possess a proximodorsal lip while the pollex ungual lacks it (Senter et al. 2004); *E. lengi* is somewhat maniraptoran-like in this respect. Where the flexor tubercle is most prominent, the maximum dorsoventral depth of the ungual is 38 mm. Half-way along its length it is 22 mm deep and the distal tip is 7 mm deep. The left and right claw grooves are at the same dorsoventral level but the groove on the right side is less prominent. The right claw groove is 4 mm deep proximally. It becomes narrower toward the ungual’s tip where its depth is *c.* 1.5 mm deep. Again, the bone ventral to the grooves possesses dorsal laminae that overlap the ventral margins of the grooves.

*E. lengi* clearly had a gracile manus similar to that of *Guanlong*, *Dilong*, *Tanycolagreus* and maniraptorans like *Deinonychus* (Ostrom 1969; Gishlick 2001; Xu et al. 2004; Carpenter et al. 2005a) (Fig 19e'). However, several of the phalanges – if correctly identified – are more robust than their equivalents in these taxa, and in this respect are intermediate between a maniraptoran– or *Dilong*–like manus and a tyrannosaurid-type manus. This is clear from the proportions of the phalanx identified as the left I-1. This element is superficially like the I-1 of *Allosaurus* and tyrannosaurids in shape and proportions (Madsen 1976; Brochu 2003), albeit shorter, and substantially less gracile than that of *Dilong*, *Tanycolagreus* and *Deinonychus* (Ostrom 1969; Gishlick 2001; Xu et al. 2004; Carpenter et al. 2005a); it is probably proportionally shorter than that of *Guanlong* as well (Xu et al. 2006). The elongate left II-2 possesses a proximal articular surface almost identical to that seen in *Deinonychus* (Ostrom 1969, fig. 63). However, the proximovertrally ‘squared-off’ projection, ventral to the proximal dividing ridge, differs from the condition in *Deinonychus* (Ostrom 1969). The proximal surface of II-2 also differs from that of

*Guanlong* in that the dorsal part of the proximal articular surface in *Guanlong* is concave on both its lateral and medial sides, the result being an articular facet that is almost twice as wide ventrally as it is dorsally (Xu et al. 2006, supp info, fig, 2j). A more *E. lengi*-like morphology appears to be present in *Tanycolagreus* (Carpenter et al. 2005a). The phalanx suggested to be a right II-1 also resembles the equivalent bone in *Deinonychus*: the proximal articular surface is relatively broad, the phalangeal shaft is deep proximally but shallow adjacent to the distal condyles, and the condyles are only slightly asymmetrical. The same features characterize II-1 in allosauroids (Madsen 1976; Currie and Carpenter 2000), but in allosauroids the phalanx is more robust.

If the phalanx suggested to be a III-3 is correctly identified, *E. lengi* had a proportionally shorter, more robust digit III than *Deinonychus* and other maniraptorans (Ostrom 1969; Osmólska et al. 2004), *Dilong* (Xu et al. 2004) *Tanycolagreus* (Carpenter et al. 2005a) and probably *Guanlong* (Xu et al. 2006), and was instead more like allosauroids in the form of this digit (Madsen 1976; Currie and Carpenter 2000). The distal end of III-3 would almost certainly have articulated with an ungual and there is no indication that the third manual digit was undergoing reduction.

The two manual unguals appear less strongly curved than those of many maniraptorans (Ostrom 1969; Osmólska et al. 2004) but this might be because their distal tips are missing. The subtle development of a proximodorsal lip in *E. lengi* is interesting: this structure is typical of maniraptorans and does not generally appear elsewhere in non-maniraptoran Coelurosauria, including in Tyrannosauridae and apparently *Guanlong* and *Dilong* (Lambe 1917; Carpenter and Smith 2001; Brochu 2003; Holtz 2004; Xu et al. 2004, 2006). However, this structure might be present in the pollex ungual of *Tanycolagreus* (Carpenter et al. 2005a), though we note that Carpenter et al. (2005a) specifically stated otherwise. The presence of a dorsoproximal lip and concavity is therefore considered a possible autapomorphy for *E. lengi*.

## Ilium

A segment of left ilium representing the region dorsal and posterodorsal to the acetabulum as well as part of the pubic peduncle is known for *E. lengi* and was referred to in passing by Hutt et al. (2001, pp. 228, 236). The segment is preserved as two pieces, the larger of which is embedded within a block of plaster. Placed together, the two form an irregularly shaped sheet of bone 137 mm long which is deeper anteriorly (122 mm) than posteriorly. The presence of a prominent, vertically oriented median ridge shows that the exposed side is the lateral one (Fig 20).

Anteroventral to the section preserving the median ridge, a descending, mediolaterally narrow strip of bone appears to represent part of the pubic peduncle: it is too narrow to be a partial ischial peduncle (Brusatte and Benson 2013) and provides further confirmation the the preserved section is from the animal's left side. What seems to be the true dorsal margin of the ilium is preserved in the posterior part of the fragment, where it forms a narrow ridge between 2 and 4 mm wide. It has a straight dorsal margin. However, this section of preserved margin is so short that it cannot be considered representative of the dorsal margin in entirety: when complete, the ilium's dorsal margin may have been either dorsally arched – as it is in *Stokesosaurus*, *Juratyran* and Tyrannosauridae (Benson 2008; Brusatte and Benson 2013) – or dorsally straighter, as it is in *Aviatyrannis* and *Guanlong* (Rauhut 2003a; Xu et al. 2006). The more ventral parts of the blade are thicker than the dorsal margin (9 mm ventral to the posterior end and 12 mm anteroventrally). The flat form of the preserved dorsal part of the ilium may indicate that the ilia were not dorsomedially inclined and hence not in contact across the dorsal midline.

PLACE FIGURE 20 ABOUT HERE

A robust median ridge projects from the body of the blade. The ridge is not perpendicular to the segment's dorsal margin but, rather, inclined posterodorsally at an angle of about 20° relative to the vertical (Fig. 20a, c). This posterodorsal inclination has previously been considered autapomorphic of *Juratyran* (Benson 2008) and is distinct from the vertical attitude of the median ridge seen in *Aviatyrannis*, *Guanlong* and tyrannosaurids (Rauhut 2003a; Xu et al. 2006; Benson 2008). Outside of Tyrannosauroida, the ridge is also posterodorsally inclined in *Siamotyrannus* and *Iliosuchus* (Buffetaut et al. 1996). The ridge merges into the body of the blade and terminates more than 30 mm ventral to the bone's dorsal margin, leaving a region of flat, featureless bone is present between the dorsal end of the ridge and the bone's dorsal margin. In most other tyrannosauroids, the ridge extends further dorsally, terminating close to the bone's dorsal margin. *Juratyran* is an exception and exhibits the same condition as *Eotyrannus* (Benson 2008; Brusatte and Benson 2008). *Juratyran* possesses two additional distinctive (autapomorphic) features of the ilium: a narrow preacetabular notch and an iliac body with a strongly arched, semioval outline (Benson 2008). It remains unknown whether these were also present in *Eotyrannus*.

Ventrally, the median ridge protrudes beyond the preserved margin of the bone as a blunt-tipped, finger-like process. In ventral view, the ridge forms a robust triangle, 25 mm across and

25 mm tall. The broken ventral end, irregular bone texture across the ventral margin of the whole segment, and lack of a supra-acetacular shelf show that the segment does not preserve the acetabular border but instead represents a region somewhat dorsal to it.

The two ilium fragments were discovered in close association with the tibia. A thin, plate-like bone still embedded in the same block as the tibia likely represents more of the iliac blade. Only its cross-section, which is 120 mm long (probably representing part of the dorsoventral height of the iliac blade) and 3-6 mm thick mediolaterally, is visible.

# **Tibia**

Virtually the whole length of the left tibia is known, though it is broken into fragments that were not preserved in close association. A proximal section c. 360 mm long was preserved on the same block as metatarsal IV and the left humerus (Figs 10-11) (Fig 21). A distal section, c. 210 mm long, was not discovered in close association with the proximal section but the two fit together at various points of contact and their shafts are similar in width and cross-sectional shape. Placed together, they form a tibia c. 570 mm long (Fig 22d). Much of the tibial shaft is fractured and mediolaterally compressed.

PLACE FIGURE 21 ABOUT HERE

The proximal articular surface is c. 70 mm long anteroposteriorly, 35 mm wide and with a cnemial crest that curves laterally, as is typical for coelurosaurs (Fig 21d). The cnemial crest is simple, convex proximally, poorly developed, and with no trace of an accessory ridge on its lateral side. It grades distally into the anterior margin of the shaft and does not project with a squared-off profile as do the cnemial crests of *Tanycolagreus* (Carpenter et al. 2005a), *Juratyrant* (Benson 2008), tyrannosaurids (Brochu 2003) and numerous other theropods. Notably, the cnemial crest in *Guanlong* does not appear squared-off but is a subtriangular projection that grades distally into the shaft (Xu et al. 2006). In *Eotyrannus*, the apex of the crest is eroded; nevertheless, this lack of a prominent squared-off profile does appear natural. The lateral surface of the shaft laterodistal to the cnemial crest is concave due to post-mortem compaction. Neither proximal condyle is prominent along the posterior edge of the proximal surface and the intercondylar groove is shallow and poorly defined; this might also be due to erosion and damage. There is no indication of an anterolateral projection on the lateral condyle. The posteromedial edge of the proximal end is higher than the lateral edge, so the articular surface



faces somewhat laterally in this region. Overall, the proximal articular surface is morphologically simpler than is typical for theropods, most of which exhibit a prominent cnemial crest that curves laterally to a marked degree, well defined proximal articular condyles, and a distinct posterior intercondylar groove. It is assumed that the cnemial crest and articular condylars were all more prominent and more sharply defined in their original condition.

The tibial shaft tapers along its length, that part distal to the fibular crest being notably narrower (50 mm thick) than the proximal region between the articular surface and fibular crest (where the shaft is 80 mm thick). The fibular crest is a D-shaped flange, 80 mm long, that begins 90 mm distal to the margin of the proximal end: it is thus distinctly separate from the proximal articular surface. The fibular crest is similar in size and position to that of other coelurosaurs (Ostrom 1969; Carpenter et al. 2005a) and is similar to that of *Juratyran* (Benson 2008). The crest is robust with the approximate shape of a broad V in cross-section. A large foramen (*c.* 7 mm long distoproximally and 3 mm in width) is located adjacent and posterior to the distal 20 mm of the crest (Fig 21a). The tibial foramen is located adjacent to the distal part of the crest as it is in *Juratyran* (Benson 2008). Distally, the shaft becomes less compressed mediolaterally, taking on a circular cross-section. At about mid-length the shaft is 50 mm long anteroposteriorly and at most 33 mm wide, but at its major break it is *c.* 36 × 36 mm. Internally, the bone is composed of tubular, shell-like layers that decrease in thickness toward the middle of the bone (it is likely that the boundaries between these layers correspond to histological features, like lines of arrested growth. We hope to see histological analysis carried out on *E. lengi* in future). This is apparently typical for theropod long bones.

The distal portion of the tibia preserves a subcircular section of shaft and the anteroposteriorly flattened distal-most region with its facets for the astragalus and calcaneum (Fig. 22a–c). This segment (preserved separately from the rest of the tibia) is peculiar and was suggested by Hutt et al. (2001) to be the incomplete radius of an additional theropod taxon. However, the proximal end of the shaft is almost identical in proportions to the distal end of the other section; the two are identical in colour and style of preservation, and fit together well.

PLACE FIGURE 22 ABOUT HERE

The anterior surface of the distal end consists of three structures, described here in order of their position relative to the medial and lateral edges, with the structure close to the medial edge being described first. The distomedial section of the surface is occupied by a large flat facet, the



lateral and medial edges of which are slightly convex, meaning that the facet as a whole projects somewhat relative to the remainder of the anterior face of the bone's distal end. Occupying the middle of the distal surface, adjacent to this facet on its lateral side, is a poorly defined concavity shaped somewhat like an inverted U. It does not extend as far proximally as the facet. Finally, the distolateral part of the bone possesses a distinct projecting 'shoulder' along its lateral edge that merges into the shaft proximally. Distal to this projection, it appears as if the distolateral corner of the bone has been broken away. This appear likely based on the shape of the distal tibia present in other coelurosaurs (Rauhut and Xu 2005; Benson 2008). Raised rims form the proximal and medial borders to this broken section; the raised medial border separates it from the midline concavity. Proximal to the distolateral shoulder-like structure, a distoproximally aligned channel runs parallel to the shaft's lateral border (Fig. 22a, c). We are not aware of any similar channel being reported for any other theropod taxon and thus regard this character as an autapomorphy of *E. lengi*.

An extremely similar distal tibial configuration was illustrated for the coelurosaur *Tugulusaurus faciles* (Rauhut and Xu 2005), the only obvious difference being the lack of the distolateral extremity of the bone in *E. lengi*. On its posterior surface, the distal end of the *E. lengi* tibia is mostly taken up by a concave area that is bordered laterally by a thick, distoproximally aligned ridge. The distal end has a maximum width of 64 mm.

# **Fibula**

The incomplete shaft of the left fibula of *E. lengi* is preserved within the same block of matrix as the proximal part of the left tibia. Though the fibula's distal end is preserved subparallel to the tibial shaft, the proximal end is beneath the tibia's posterior surface. Hutt et al. (2001, p. 236) described the fibula **was** an "elongate, slender element in which the proximal third is expanded craniocaudally". 134 mm of the bone is preserved within the block and much of it is concealed by matrix. The preserved proximal end terminates well short of the original proximal end and, contra Hutt et al. (2001, p. 236), has the same cross-sectional dimensions as the preserved distal end (Fig 21e). At both ends, the shaft has an anteroposterior length of 15 mm and a maximum width of 7 mm. It is mediolaterally compressed and slightly concave medially. This fibular cross-sectional shape is typical for tetanurans (Osmólska et al. 1972; Madsen 1976; Osmólska 1996; Charig and Milner 1997; Carpenter et al. 2005a), though the fibula of *Deinonychus* is described as being nearly circular in cross-section (Ostrom 1969) and that of tyrannosaurids has been described as D-shaped in cross-section (Brochu 2003, p. 115). A further 35 mm of the left fibula

is separate from the block and preserved adjacent to the shaft of the tibia. This fragment does not include the true distal end of the fibula and is similar in cross-sectional dimensions and shape to the rest of the fibular shaft, being mediolaterally compressed, convex on its lateral side and slightly concave on its medial side. These fragments are extremely gracile relative to the tibial shaft and suggest proportions of the fibula similar to those known for other early tyrannosauroids (Carpenter et al. 2005a; Xu et al. 2004, 2006). It is assumed that the shaft tapered continually from its broad proximal end towards its narrower distal part but this cannot be confirmed: a distinct condition, where the fibula narrows markedly distal to the insertion point of the m. iliofibularis tendon, is present in *Bagaraatan* and maniraptorans but not in other theropods (Rauhut 2003b). It is also assumed – based on the condition in other non-tyrannosaurid tyrannosauroids (Carpenter et al. 2005a; Xu et al. 2006) – that the fibula reached the proximal tarsals.

# **Metatarsals**

Sections of metatarsals II, III and IV are known for *E. lengi* (Fig 23) and show that it had a gracile metatarsus, as expected for a tyrannosauroid. The proximal ends of mt II and IV show that *E. lengi* was not arctometatarsalian, in contrast to *Appalachiosaurus* and Tyrannosauridae but like *Guanlong* and *Dilong* (Holtz 2004; Xu et al. 2004, 2006; Carr et al. 2005). The distal ends of the metatarsals are not ginglymoid, as they are in some maniraptoran taxa (Ostrom 1969; Norell and Makovicky 1997; Rauhut 2003b) and the deep and prominent collateral ligament fossae are typical for tetanurans.

PLACE FIGURE 23 ABOUT HERE

The right mt II of *E. lengi* was figured and described by Hutt et al. (2001, p. 236, fig. 4A) and the distal end of left mt II is known as well (consisting only of the condylar region and the distalmost part of the shaft). The more complete right mt II is elongate and gracile with a total length of 253 mm (Fig. 23a–d). The shaft is broken in several places and the proximal 100 mm is slightly artificially rotated so that the anterior surface faces somewhat laterally. The shaft is straight and the distal end is not deflected medially. Viewed anteriorly or posteriorly, the lateral and medial margins of the shaft are subparallel. With the exception of the lateral articular facet for mt III, most surfaces of the shaft are convex, though the proximal and distal parts of the anterior surface of the shaft are flattened. The proximal articular surface of the metatarsal is

semicircular with a convex medial surface and flat lateral surface (Fig 23e). This morphology is typical for tetanurans (Gilmore 1920, fig. 51; Ostrom 1969, fig. 70; Currie and Zhao 1994, fig. 26C; Currie and Carpenter 2000, fig. 14A) and differs from the more complex shape present in arctometarsalian tyrannosauroids (Brochu 2003, fig. 103; Carr et al. 2005, fig. 19F). The anteroposterior length of the proximal articular surface (44 mm) exceeds that of the shaft (*c.* 25 mm) so it is accurate to describe the proximal end as expanded relative to the shaft. The proximal articular end has a maximum width of 23 mm. The flat lateral facet for the articulation of mt III extends distally for approximately 70 mm from the proximal articular end. More distally, the lateral surface of the shaft becomes convex, although the presence of a low distoproximal ridge extends along the anterolateral surface and indicates distal continuation of this surface. Because of the slight distortion of the proximal part of the shaft, in life the facet for mt III was probably directed laterally rather than anterolaterally as preserved.

No distinct facet for mt I could be detected. If mt I was present it was – based on the relative position of the mt I facet in other tyrannosauroids (Brochu 2003; Carpenter et al. 2005a) – presumably located approximately 100 mm proximal to the distal articular end of the bone. The scar for the insertion of *M. gastrocnemius*, often mistaken for the mt I facet (Tarsitano 1983; Carrano and Hutchinson 2002), could not be detected either.

The distal end is wider than the shaft because the bone surrounding the collateral ligament fossae flares medially and laterally, giving the posterior surface of the distal end a width of 40 mm. The distal end appears to form a single condyle when viewed anteriorly but is in fact bilobed, comprising a bulbous, more prominent lateral condyle (20 mm wide) that is separated from a smaller medial condyle (*c.* 9 mm wide) by a shallow intercondylar canal 13 mm wide. The medial condyle is only complete in the left element and is a prominent subrectangular eminence with an anteromedial inclination. A similar distal metatarsal II morphology is seen in allosauroids (Madsen 1976, plate 54; Currie and Zhao 1994, fig. 27), *Appalachiosaurus* (Carr et al. 2005, fig. 19) and tyrannosaurids (Brochu 2003, fig. 103). Both condyles are restricted to the posterior part of the distal surface of the bone and the lateral condyle extends 11 mm further distally than the medial condyle. Both collateral ligament fossae are well defined and deep, with the lateral one being larger (*c.* 11 × 13 mm) and more distally located than the medial fossa (*c.* 9 × 11 mm).

The incomplete left mt II has a preserved length of 45 mm and is 40 mm wide across the condyles. Breakage of the subcircular shaft shows that the bone was hollow as far distally as the condyles. The bone walls are 3-5 mm thick. As in the right mt II, the lateral ligament fossa (*c.* 10 × 13 mm) is larger and deeper than the medial fossa (*c.* 7 × 5 mm).

The distal end of what is almost certainly the left mt III of *E. lengi* is known but this fragment consists only of the distal 116 mm (Fig. 23g–k). It was not mentioned by Hutt et al. (2001). Even allowing for crushing at the preserved proximal end, the shaft is compressed anteroposteriorly and subrectangular in cross-section. The inferred anterior surface of the shaft is smoothly convex while the inferred posterior surface is flat. The distal articular end is broader than the shaft, being 30 mm wide across the posterior surface. Viewed medially or laterally, the distal end is symmetrical. However, a shallow extensor fossa just proximal to the articular end on one side identifies the surface concerned as the anterior one, a deduction supported by the fact that this inferred anterior surface is narrower (26 mm) than the inferred posterior surface. As expected for an mt III, the distal end is block-like, convex on all sides, and not differentiated into separate condyles. However, one side of the distal end is anteroposteriorly deeper than the other (33 mm vs c. 29 mm), suggesting that it is the medial side. Accordingly, the specimen is here identified as belonging to the left pes. Both collateral ligament fossae are prominent and subcircular; the right and left fossae have dimensions of 12 × 12 mm 15 × 15 mm, respectively. The distal end of what appears to be the right mt III, consisting of the distal condyle and the adjacent part of the shaft, is preserved within matrix and only visible from one side. The shaft is subrectangular in cross-section, having a width of 24 mm wide and a maximum anteroposterior length of 20 mm. One side, possibly the posterior one, is flat, while the medial and lateral surfaces are convex. The visible collateral ligament fossa is large and circular, measuring 14 × 14 mm. These dimensions are similar to those of the ligament fossae of the left mt III.

A near-complete left mt IV, broken into two pieces, is known for *E. lengi* and was stated by Hutt et al. (2001, p. 236) to be 260 mm long. Again, this element is long and gracile (Fig. 23l–p). Most of the bone is embedded within a block and only its posterior surface is visible. The proximal 96 mm is free of matrix and largely complete. When the two pieces are united the total length is more like 280 mm, but this is probably exaggerated by breakage and distortion. The metatarsal was discovered immediately beneath the tibia. The proximal end is complex (Fig. 23m–p). Although the posterior face of the metatarsal shaft is flat, it is overhung by the proximal articular surface, especially medially. Proximally, the articular surface is 38 mm wide across the posterior face of the bone, the bone narrowing in width to c. 20 mm distally. A ridge demarcates the proximal 50 mm of the posterior surface of the shaft from the convex lateral side. This convexity is continuous on to the anterior surface. A similar ridge also demarcates the proximal part of the posterior surface from the medial surface. Anteromedial to this ridge, the proximal end of the bone is convex, passing into a deep concavity that would have been directed

anteromedially. This concavity extends 30 mm distally down the shaft, is c. 20 mm wide proximally, and is for reception of the proximal end of mt III. No similar well-developed medial facet for mt III seems to be present in the majority of theropods but one has been figured for *Sinraptor dongi* (Currie and Zhao 1994, fig. 26A). In arctometatarsalian tyrannosauroids like *Appalachiosaurus* (Carr et al. 2005, fig. 19D) and tyrannosaurids (Brochu 2003, fig. 103) the facet is shorter anteroposteriorly, shaped more like a ‘U’ in proximal view, and located further toward the posterior surface of the shaft. The proximal end of mt IV is also blockier and more robust in these taxa.

Few details of the distal end can be discerned but, in contrast to tyrannosaurids, the distal end is not laterally deflected relative to the shaft’s long axis. The distal articular surface is 35 mm wide and bilobed, with the two halves of the condyle restricted to the posterior surface of the distal end and separated by a 9 mm wide intercondylar groove. Accurate measurements of the two halves of the condyle cannot be made but the medial part appears to have been distally bulbous and c. 35 mm long anteroposteriorly. Any collateral ligament fossae are obscured by immoveable matrix.

# **Pedal phalanges**

Six pedal **unguals**, one of which is an ungual, are known for *E. lengi* (Fig 24). Essentially, they appear typical for a tetanuran that is intermediate in size and proportions between small and giant taxa.

A pedal phalanx 85 mm long is preserved on the same block as the blade of the left scapula (Fig. 24g–j), but **it’s the left** side of the phalanx cannot be examined and much of the left condyle is absent. The proximal articular surface, likewise, cannot be examined but the shaft adjacent to the articular surface is 34 mm tall. The shaft is shallowest just proximal to the distal condyles, where it is only 16 mm deep. The proximoventral part of the shaft is flattened and low ridges mark the boundaries between the ventral surface and the sides of the shaft. A deep concavity lies proximal to the distal condyles. Both condyles of this phalanx are deeper and more extensive dorsally and ventrally than the condyles of other preserved pedal phalanges: in turn, the right condyle on this phalanx is more prominent than the left. The right condyle is 27 mm tall and extends c. 6 mm dorsal to the adjacent part of the shaft. The intercondylar groove is shallow but extends as far dorsoproximally as do the articular surfaces of both condyles. The ventral part of the right condyle extends to the right but this may be the result of deformation. The right collateral ligament fossa is rounded and taller than it is long (8 × 6 mm). The large size of this

phalanx suggests that it is II-1. If the “right-ward” inclination of the right distal condyle is a genuine feature, this phalanx is probably from the right pes.

PLACE FIGURE 24 ABOUT HERE

The largest preserved phalanx of *E. lengi* is 94 mm long (Fig. 24a–f) and was suggested by Hutt et al. (2001, p. 236) to be phalanx III-1. This bone has been broken at mid-length, somewhat distorted dorsoventrally, and lengthened by matrix that has infilled the break. Hutt et al. (2001, p. 236) estimated the original length of the phalanx to be 87 mm. Its proximal articular surface is concave, subcircular, measures 37 mm wide and 35 mm tall, and has a rugose articular surface and bony rim. It is not biconcave, supporting its identification as the most proximal phalanx of its digit. In lateral view, the shaft is deepest (34 mm) proximally and shallowest (17 mm) just proximal to the distal condyles. The proximal part of the ventral part of the shaft is flattened and flanked by two low convexities, both of which are more prominent on this phalanx than on any others. They mark the boundaries between the sides of the phalangeal shaft and its ventral surface. A deep extensor fossa is present on the dorsal side of the shaft. Ventrally, the part of the shaft adjacent to the condyles is flat. The condyles themselves are poorly expressed on the dorsal and ventral surfaces and the intercondylar groove is shallow. However, the collateral ligament fossae are large, deep and well rounded, with the left one being more elliptical. The right fossa measures *c.* 10 × 10 mm, and that on the left is 12 mm long and 7 mm tall. The maximum width across the distal condyles is 33 mm. There is no reliable way of determining whether this III-1 belongs to the left or right foot.

The smallest preserved pedal phalanx is 45 mm long (Fig. 24k–p). This bone appears too broad and robust to be a manual phalanx of *E. lengi*, but the possibility remains that it belongs to the associated dryosaurid. This is the ‘small, isolated phalanx’ discussed by Hutt et al. (2001, p. 236), who suggested that it was probably IV-3 or IV-4. Given its length compared to those of the inferred pedal phalanges III-1 and II-1, this could be correct. Because the left distal condyle is deeper than the right condyle, the small phalanx is regarded as belonging to the right foot. The proximal articular surface is broader than it is tall (26 × 23 mm) and biconcave, with two concave areas separated by a low ventrodorsal ridge. The proximodorsal process dorsal to the ridge is well developed, extending further proximally than the lateral and medial bony rims that surround the articular surface. In lateral or medial view, the ventral surface of the shaft is concave, the shaft being only 14 mm tall at its shallowest point but 22 mm deep adjacent to the proximal articular



surface. The shaft is convex dorsally, laterally and medially, though flat to slightly concave on its ventral surface. Viewed dorsally, the shaft narrows slightly to 21 mm at mid-shaft. The distal condyles are not extensive either ventrally or dorsally, and the intercondylar groove is shallow. A shallow extensor fossa is present on the dorsal surface, just proximal to the distal condyles. The right condyle extends slightly further distally than the left. The collateral ligament fossae are rounded and deep, but not as deep as those on the other pedal phalanges. The phalanx is 26 mm wide across the distal condyles.

A pedal ungual (Fig 24q) is preserved on the same block as the left humerus, a pedal phalanx and other fragments. It was suggested by Hutt et al. (2001, p. 236) to pertain to digit IV. The ungual is only exposed in right lateral view, and its maximum length is *c.* 60 mm. The distalmost 20 mm or so appears to be missing. The distal part of the preserved length of the ungual curves to the left, but a vertical break separating this distal part from the rest of the bone suggests that this represents post-mortem distortion. The bone is 26 mm deep proximally, and tapers gradually toward its tip. A shallow concavity near the proximal end of the dorsal surface is present: this is unusual within Tetanurae, but has been reported for *Appalachiosaurus* within Tyrannosauroidea (Carr et al. 2005). No flexor tubercle is present, although some of the bone surface on the proximal part of the ventral surface is striated. A shallow lateral groove is present *c.* 5 mm from the ventral edge of the ungual's lateral surface.

# **Revised diagnosis of *Eotyrannus lengi***

*E. lengi* exhibits several unique morphological features and thus is diagnosable. Reevaluation shows that most of the supposedly distinctive features mentioned in the preliminary description of *E. lengi* are not diagnostic, and the original diagnosis is here critiqued. Hutt et al. (2001, p. 229) provided the following diagnosis of *E. lengi* (individual features are numbered for ease of reference below):

Tyrannosauroid coelurosaurian theropod with [1] serrated carinae on D-shaped premaxillary teeth. [2] Maxillary and dentary teeth with apically complete denticulation; [3] rostral carinae bear denticles for less than half the length of the denticle-bearing part of the caudal carinae. [4] Denticle size difference index of *c.* 1.5. [5] Anterior portion of maxilla laterally flattened with anterior border to the antorbital fossa sharply defined, [6] ventral edge of maxilla straight. [7] Coracoid with prominent mediolaterally-wide, subcircular glenoid directed caudally. [8] Humerus with large internal cavity situated dorsally (anconally) with several smaller cavities situated ventrally. [9] Manus proportionally long (digit II *c.* 95% humerus length) with [10] three well-developed metacarpals. [11] Carpals not reduced to simple elements as in tyrannosaurids.



The new information on *E. lengi* presented here substantially updates our understanding of the morphology of this species (Fig 25), and a huge amount of new information on the morphology and diversity of tyrannosauroids in general has become available since Hutt et al. (2001) was published (e.g. Xu et al., 2004, 2006; Carr et al. 2005; Benson 2008; Averianov et al. 2010; Li et al. 2010; Brusatte et al. 2011). Accordingly, the above diagnosis can now be replaced. On the numbered points made in the diagnosis of Hutt et al. (2001) the following points can now be made:

1. The presence of “serrated carinae on D-shaped premaxillary teeth” is far from unique to *E. lengi*, being present in most other tyrannosauroid taxa (Currie et al. 1990; Holtz 2004). Description of premaxillary teeth of *E. lengi* as D-shaped is misleading since it fails to differentiate the tyrannosauroid condition from that of other theropods: the premaxillary teeth of *E. lengi* and other tyrannosauroids are better described as “U-shaped” in cross section since their sagittal axis is obviously longer than their mediolateral one.
2. Apically complete denticulation is not rare or unusual in Theropoda and is widespread across the group, so much so that it should probably be considered typical within coelurosaurs. Within Tyrannosauroidea, it is certainly not unique to *E. lengi* (Holtz 2004; Brusatte et al. 2012).
3. The condition of having rostral carinae (= mesial carinae) that bear denticles for less than half the length of the denticle-bearing part of the caudal carinae (= distal carinae) probably would be diagnostic for *E. lengi*, were it present. Restudy failed to identify it and *E. lengi* seemed to be much like other tetanurans in the distribution of denticles on its lateral teeth (Currie et al. 1990).
4. The DSDI of *E. lengi* is not *c.* 1.5 but rather 1.16 (with 1.21 reported by Sweetman (2004)). This lower figure is comparable to those obtained for many other tyrannosauroids and thus cannot be regarded as diagnostic for *E. lengi*.
5. Neither the presence of a laterally flattened anterior region on the maxilla nor a pronounced rim to the antorbital fossa are unique to *E. lengi* – both features are widespread in Tetanurae and Tyrannosauroidea (e.g. Currie and Dong 2001; Hwang et al. 2004; Xu et al. 2004; Dal Sasso and Maganuco 2011).
6. The presence of a straight ventral edge on the maxilla is not unique to *E. lengi*, being present in *Dilong* and other coelurosaur taxa. Furthermore, this condition is clearly

plesiomorphic for Coelurosauria and normal for non-tyrannosauroid coelurosaurs (e.g. Hwang et al. 2004; Holtz et al. 2004; Dal Sasso and Maganuco 2011): *E. lengi* thus retains a primitive condition that distinguishes it from tyrannosaurids and their closest relatives.

7. The morphology of the coracoid part of the glenoid in *E. lengi* is not diagnostic, and is similar to that seen in of other tyrannosauroids (Xu et al. 2004) and non-tyrannosauroid tetanurans (e.g. Currie and Zhao 1994).
8. The use of internal cavities within the humerus as part of the diagnosis of *E. lengi* seems unwise as internal structures such as these often cannot be observed across a wide range of taxa. Furthermore, the internal cavities in the humerus of *E. lengi* do not seem to differ from those present in other theropod humeri.
9. *E. lengi* does appear to have a proportionally long manus, with digit II measuring c. 95% the length of the humerus. However, this condition seemingly represents the plesiomorphic state for Tyrannosauroidea: the humeral fragments figured for *Dilong* suggest that its hand was as proportionally elongate as that of *E. lengi* relative to humerus length (Xu et al. 2004). Furthermore, both *Tanycolagreus* and *Guanlong* possesses a manual digit II whose length exceeds 95% of that of the humerus (Carpenter et al. 2005a; Xu et al. 2006).
10. The presence of three **well developed** metacarpals is obviously the plesiomorphic state for Tyrannosauroidea. Actually, the presence of *at least* three metacarpals is primitive, since *Guanlong* possesses four (Xu et al. 2006).
11. Similarly, the presence of a distal carpal with a trochlear articulate surface in *E. lengi* represents the plesiomorphic state for Tyrannosauroidea.

In conclusion, the 11 purportedly diagnostic features proposed for *E. lengi* by Hutt et al. (2001) can all be rejected as potentially diagnostic for *E. lengi* since they are either plesiomorphic for Tyrannosauroidea, shared with at least some other tyrannosauroid taxa, or not truly present in *E. lengi*. It is now clear, however, that *E. lengi* possesses a number of unusual unique characters that allow an emended diagnosis to be formulated.

PLACE FIGURE 25 ABOUT HERE

# **Emended diagnosis**

2145

2146 The following unique suite of features are as yet unknown in other tyrannosauroids or in the  
2147 member of those coelurosaurian lineages close to Tyrannosauroidea and hence are regarded as  
2148 probable autapomorphies of *Eotyrannus lengi*: lateral surface of dentary bearing five shallow  
2149 arcuate furrows that extend anterodorsally from a common origin on the ventral part of the bone;  
2150 large, block-like humeral entepicondyle; distal end of tibia with distoproximally aligned channel,  
2151 demarcated laterally by a low ridge, located close to the lateral border of the shaft.

2152 Five other characters may represent additional autapomorphies of *E. lengi*, but their status  
2153 remains somewhat uncertain. The first of these is the presence of a concave notch and  
2154 accompanying anteromedial tooth-like projection on the anterodorsal part of the dentary is an  
2155 additional possible autapomorphy. This feature is of ambiguous standing as goes its use as a  
2156 potential autapomorphy since poor preservation renders it possible that it has been misinterpreted.  
2157 The second potential autapomorphy is the presence of a sinuous ridge that extends across the base  
2158 of the vomeropterygoid process of the palatine: the bone dorsal to this ridge is inset or embayed  
2159 relative to the ventral part. This character is also difficult to evaluate given our poor knowledge  
2160 as goes palatine anatomy in non-tyrannosaurid tyrannosauroid and more data is needed before it  
2161 can be evaluated further. The third potential autapomorphy also pertains to the palatine and  
2162 concerns the long, straight dorsal margin present between the vomeropterygoid and pterygoid  
2163 processes: this contrasts with the shorter, dorsally concave edge present in other tyrannosauroids  
2164 (Currie 2003; Carr et al. 2005; Xu et al. 2006; Brusatte et al. 2012). Again, however, a lack of  
2165 data from other taxa prevents us from being more confident about use of this configuration as an  
2166 autapomorphy.

2167 The fourth potential autapomorphy is the apparent presence of tear-drop-shaped cross-sections  
2168 to the shafts of the radius and ulna. However, identification of the relevant partial bone shafts as a  
2169 radius and ulna is uncertain, so more information is needed before their cross-sectional geometry  
2170 can be considered diagnostic.

2171 Finally, one other character can be considered a potential autapomorphy since, while not  
2172 unique to *E. lengi* relative to all other theropod taxa, it is unique within Tyrannosauroidea. As  
2173 described here, *E. lengi* possesses a proximodorsal lip and adjacent concavity on at least one of  
2174 its manual unguals. These structures are a familiar feature of oviraptorosaurs and some other  
2175 maniraptorans but are, excepting *E. lengi*, unknown in Tyrannosauroidea (Lambe 1917; Carpenter  
2176 and Smith 2001; Brochu 2003; Holtz 2004; Xu et al. 2004, 2006). As discussed above, what may

be a subtly developed proximodorsal lip and adjacent concavity has been figured for the possible tyrannosauroid *Tanycolagreus* (Carpenter et al. 2005a).

# **Comments on other Wealden Supergroup theropods**

Numerous theropod specimens, most recently reviewed by Naish (2011), have been reported from the Wessex Formation (Fig 26) and the possibility that at least some might represent additional *E. lengi* specimens was kept in mind throughout our research on this dinosaur. Some taxa can be removed from consideration immediately. Baryonychine spinosaurids are represented in the Wessex Formation by teeth and an isolated dorsal vertebra (Buffetaut 2009; Naish 2011) (Fig. 26m–p), elements that differ greatly in morphology from their counterparts in tyrannosauroids. The carcharodontosaurian allosauroid *Neovenator salerii* (Brusatte et al. 2008), known from the excellent holotype and several referred specimens, is osteologically well known and clearly has no close affinity with *E. lengi*. Benson et al. (2009) described an additional large, as yet unnamed Wessex Formation theropod, presently known only from the distal end of the femur, the dorsal end of the left pubis, and the pubic boot and adjacent parts of the pubic shafts (listed together as MIWG 6350). The presence of an extensor groove on the femur and a slit-shaped pubic fenestra shows that MIWG 6350 is a tetanuran, but the additional presence of a proportionally broad pubic boot excludes the specimen from Coelurosauria. It cannot, therefore, be considered referable to *E. lengi*. Numerous smaller, and often very poorly known, theropods have also been recovered from the Wessex Formation. As noted by Hutt et al. (2001), and as explained in full here, it does not seem that any of these can be considered conspecific with *E. lengi*.

The first Wealden theropod to be named was *Calamospondylus oweni* Fox in Anon., 1866, said by Fox (in Anon. 1866) to consist of “five cemented vertebrae with the sacral ribs and portions of the other iliac bones”. The current location of the holotype is unknown, so the only source of information on this specimen is the brief, semi-popular publication in which it was first described (Naish 2002a). However, *C. oweni* is a nomen dubium because its describer (Fox in Anon. 1866) failed to provide diagnostic features for the taxon (Naish 2002a). The small size and possible vertebral pneumaticity of *C. oweni* suggest that it was a coelurosaur but it cannot be directly compared with *E. lengi* in the absence both of the *C. oweni* holotype and of any reported diagnostic features (Naish 2002a).

PLACE FIGURE 26 ABOUT HERE

*Aristosuchus pusillus* (Owen 1876) is based on a sacrum and partial pelvis NHMUK R178 (Fig. 26e–g) that have been suggested to belong to a compsognathid (Naish et al. 2001, 2004). More recently, a tyrannosauroid identification has been considered plausible (Naish 2011) since *A. pusillus* strongly resembles the possible tyrannosauroid *Mirischia asymmetrica*. The latter possesses an anterodorsal concavity on the anterior margin of the ilium and an anterodorsally concave margin on the pubic peduncle (Naish et al. 2004) and hence is tyrannosauroid-like. However, both characters are also present in some non-tyrannosauroids (Rauhut 2003a, b; Dal Sasso and Maganuco 2011). We presently, therefore, interpret these characters as tyrannoraptoran symplesiomorphies, and indeed *Mirischia* was not recovered as a tyrannosauroid in our analysis (see below). Whether *A. pusillus* is a tyrannosauroid or not, the overlapping material known for *A. pusillus* and *E. lengi* (sacral vertebrae) reveals profound differences. The posterior-most sacral vertebrae of *A. pusillus* are fused together, indicating that the holotype was closer to skeletal maturity than was the holotype of *E. lengi*. However, the *A. pusillus* sacrum is *c.* 120 mm long, suggesting a total length of *c.* 2 m, whereas the subadult holotype of *E. lengi* represents an animal *c.* 4.5 m in length. The sacral vertebrae of *A. pusillus* differ from those of *E. lengi* in being ventrally rounded rather than bearing ventral keels.

*Ornithodesmus cluniculus* Seeley, 1887 was named for six fused sacral vertebrae (NHMUK R178) (Fig. 26q–s). It has been given a variety of phylogenetically disparate suggested identities but seems most likely to represent a dromaeosaurid (Norell and Makovicky 1997; Naish 2011). *O. cluniculus* recalls *E. lengi* in possessing lateral foramina on its sacral centra. However, while the openings present in *E. lengi* are likely sacral nerve foramina, those present in *O. cluniculus* are smaller and located lower on the centra, and hence appear to be pneumatic. The sacral fusion present in *O. cluniculus* indicates skeletal maturity. With a sacrum length of 96 mm (suggesting a total length of approximately 1.5 m), this apparent adult would have been a far smaller animal than the subadult holotype of *E. lengi*. In addition, *O. cluniculus* possesses a ventral sulcus that extends continuously along the ventral surfaces of the second to sixth sacral vertebrae (no such structure is present in *E. lengi*) and the ventral surfaces of its sacral centra are flattened (Howse and Milner 1993). In *E. lengi*, no ventral sulcus is present and the ventral surface of the sacral centrum is ventrally keeled.

A partial cervical vertebra from the Wessex Formation (NHMUK R181) was named *Thecocoelurus daviesi* (Seeley 1888) (Fig. 26a–d). Similarities between this specimen and the

cervical vertebrae of both oviraptorosaurs and abelisauroids have been noted but it seems unwise to speculate further on its possible affinities (Naish 2011). A lack of extensive cervical material of *E. lengi* makes detailed comparison with *T. daviesi* difficult. However, the two taxa differ in that the single known cervical vertebra of *T. daviesi* possesses an oval pneumatic fossa on the side of the centrum, a deep interspinous ligament pit, ventrolateral ridges and a ventral sulcus, none of which are present in the known cervical vertebrae of *E. lengi*.

*Calamosaurus foxi* is also based on cervical material, in this case the two articulating vertebrae NHMUK R901 (Lydekker 1889) (Fig. 26h–l). Based on their small size and strong opisthocoely mean that these vertebrae were previously referred to Compsognathidae (Naish et al. 2001) but they are similar in shape and proportion to those of *Dilong* and hence may also be from a small tyrannosauroid (Naish 2011). Because the neurocentral sutures in *C. foxi* are closed (though not fused), despite the fact that each vertebra is only 40 mm long, it seems unlikely that they could represent the same taxon as *E. lengi*. The posterolaterally flaring postzygapophyses in *E. lengi* differ from the shorter, less flaring ones in *C. foxi* and, while the more complete *C. foxi* vertebra possesses a short neural spine, the one cervical neural spine known for *E. lengi* extends for much of the centrum's length. However, these differences could reflect positioning within the cervical series. It is possible that *C. foxi* and *E. lengi* might be synonymous but there is no good evidence to support this.

Several isolated hindlimb and pelvic elements from the Wessex Formation have been referred to *Calamosaurus* and *Aristosuchus* (Lydekker 1891; Galton 1973; Naish 2002; Naish et al. 2001). The tibia NHMUK R186, long known as the “*Calamosaurus* tibia” (Fig. 26t–u) has an unusually prominent medial malleolus that projects medially as a distinct flange (Naish 2011). No such structure is present in *E. lengi* and NHMUK R186 most likely represents a different non-maniraptoran coelurosaur. An additional small tibia (MIWG 5137) (Fig. 26y–b') differs from *E. lengi* in possessing well separated proximal condyles, and also lacks the distinctive distal tibial morphology of *E. lengi*. Two small femora (NHMUK R5194 and MIWG 6214) (Fig. 26w–z) from the Wessex Formation (Galton 1973; Naish 2000) likely belong to non-maniraptoran coelurosaurs but cannot be identified more precisely and do not overlap with any *E. lengi* material. Finally, the partial ischium NHMUK R6426 (Naish 2002) also does not overlap with any *E. lengi* material, does not possess any tyrannosauroid characters, and cannot be identified more precisely than Tetanurae indet. It should be noted that all of these specimens belong to animals substantially smaller than the *E. lengi* holotype.



Most of the small Wessex Formation theropods are too poorly known to allow confident identification but they seemingly include one or more non-maniraptoran coelurosaurs, such as compsognathids or small tyrannosauroids (e.g. *Calamosaurus*, *Aristosuchus*), and maniraptorans (*Ornithodesmus*, isolated teeth described by Sweetman (2004)) (Naish 2011). None of the material reported for these taxa is congeneric with *E. lengi*, meaning that this taxon is currently represented only by its holotype. In addition to the enigmatic smaller theropods, *E. lengi* lived alongside a large, non-coelurosaurian tetanuran (Benson et al. 2009), baryonychine spinosaurids (Charig and Milner 1997; Naish 2011) and the carcharodontosaurian *Neovenator* (Brusatte et al. 2008).

### Phylogenetic analysis

In order to test the phylogenetic affinities of *Eotyrannus*, we incorporated it into a phylogenetic analysis of Theropoda that focuses on non-maniraptoran coelurosaurs and non-coelurosaurian tetanurans (see Appendix 1 and 2 for character list and sources for coding, and Appendix 3 for data matrix). We compiled a data matrix describing the distribution of 1145 phylogenetically informative morphological characters in 83 ingroup neotheropods and 3 non-neotheropod saurischian outgroups. *Eoraptor* was chosen to root the tree. The data matrix was analysed with the Hennig Society version of TNT (Goloboff et al. 2008). The search for islands of shortest length trees was performed with the ‘New Technology’ strategy; the resulting trees were then explored using 1000 Tree Bisection Reconnection branch swapping with the ‘Traditional Search’ strategy. The Bremer Support (BS, Bremer 1988) was calculated performing 1000 ‘Traditional Search’ analyses and saving all trees with a length no more than 10 steps longer than the shortest trees. The analysis recovered 12 shortest trees of 4349 steps each, with a Consistency Index and Retention Index of 0.2752 and 0.5230 respectively, the strict consensus of which is shown in Fig 27. The analysis supports the monophyly of Coelophysoidea (including ‘dilophosaurs’, Tykoski and Rowe 2004, BS = +4), *Averostra* (*sensu* Ezcurra and Novas 2007, BS = +3), Ceratosauria (*sensu* Rauhut 2003b, BS = +2) and Tetanurae (BS = +2). Within Tetanurae, the bizarre *Chilesaurus* (Novas et al. 2015) was recovered as outside a clade that includes all other tetanurans, and *Xuanhanosaurus* and *Zuolong* are recovered within a polytomy also involving Neotetanurae (BS = +2). Megalosauroida (Benson et al. 2010a, BS = +2) is recovered as the sister-taxon to Allosauroida (BS = +3); Rauhut 2003b). Coelurosauria (*sensu* Gauthier 1986, BS = +3) includes Compsognathidae as its earliest-diverging lineage, in addition to Tyrannoraptora

(BS = +2), the latter including Tyrannosauroidae (BS = +2), and the lineage including *Ornitholestes*, *Aorun* and maniraptoriforms.

PLACE FIGURE 27 ABOUT HERE

In the strict consensus of the shortest trees (Fig. 27), Tyrannosauroidae includes a pectinate series of early-diverging lineages leading to Tyrannosauridae. A *Juratyran* + *Stokesosaurus* clade (BS = +2) is found to be outside the clade that contains all remaining tyrannosauroids. Coeluridae, including *Coelurus*, *Tanycolagreus* and *Tugulusaurus*, is recovered as the sister-group of remaining tyrannosauroids. The nodal support values among these early-diverging tyrannosauroids are weak, mainly due to the inclusion of fragmentary taxa like *Stokesosaurus* and *Tugulusaurus*. Among those members of Tyrannosauroidae whose evolution post-dates the divergence of coelurids, Proceratosauridae, including *Dilong*, form the earliest-diverging branch. *Yutyranus* is recovered as sister-taxon to the clade containing *Eotyrannus* and remaining tyrannosauroids (BS = +2). The latter subclade includes *Xiongguanlong* as sister-taxon of the clade that includes *Dryptosaurus* and arctometatarsalian tyrannosauroids (including Tyrannosauridae; BS = +2), in addition to megaraptorans (Benson et al. 2010a; BS = +3). The relationships among megaraptorans are well resolved but weak, mainly due to the inclusion of fragmentary taxa like *Chilantaisaurus*, *Orkoraptor* and *Siats*, the latter recovered as outside the clade that includes all remaining megaraptorans. The enigmatic South American tetanuran *Aniksosaurus* (Martínez and Novas 2006) is recovered as a megaraptoran. *Chilantaisaurus* and *Fukuiraptor* are recovered as successively closer to Megaraptoridae (Novas et al. 2013). The topology among the arctometatarsalian tyrannosauroids places *Appalachiosaurus*, *Bistahieversor* and *Teratophoneus* as outside of Tyrannosauridae (the ‘*Gorgosaurus* + *Tyrannosaurus*’ node in our ingroup; BS = +2).

The analysis found no support for a close relationship between the two European tyrannosauroids, *Eotyrannus* and *Juratyran*, previously discussed by Brusatte et al. (2010) and recovered by Brusatte and Carr (2016). Such disagreement is probably biased by the different taxon sampling between the two analyses (e.g., megaraptorans are not included in the dataset of Brusatte and Carr, 2016). The two European taxa are distinct among theropods in possessing a posterodorsally inclined supracetabular ridge that fails to reach the dorsal margin of the ilium. With regard to the position of *Eotyrannus* specifically, its inclusion within Tyrannosauroidae is supported by the lack of a prominent keel on the ventral surface of the cervical centra (char.

207.0) and the presence on the lateral surface of the ilium of a vertical crest dorsal to the acetabulum (char. 382.1). Within Tyrannosauroidae, *Eotyrannus* is recovered as a member of the “Coeluridae + remaining tyrannosauroids” clade on the basis of a fibular crest on the tibia that does not extend proximally to the level of the proximal end of the bone (char. 909.0), as a member of the “Proceratosauridae + remaining tyrannosauroids” clade on the basis of **ita** nasal pneumatic recesses (char. 47.1), medially fused nasals (char. 874.1), the distinct dorsal expansion on its scapula (char. 896.0) and a medial condyle on the humerus that is larger than the lateral condyle (char. 1164.1), and as a member of the “*Yutyrannus* + remaining tyrannosauroids” clade on the basis of a maxilla that lacks a lateral ridge ventral to the antorbital fossa (char. 24.0) and manual ungual I being longer than its preceding phalanx (char. 309.1). Finally, *Eotyrannus* is recovered as closer to Tyrannosauridae than *Yutyrannus*, *Dilong* and other proceratosaurids because it lacks both a distinct median nasal crest (char. 45.0) and a deep lateral groove on the dentary (char. 178.0), possesses premaxillary teeth where the longest axis is labiolingually arranged (char. 793.1), bears a deep surangular shelf (char. 1570.1), lacks a distinct extensor sulcus on the second metatarsal (char. 481.0) and possesses a transversely compressed fourth metatarsal (char. 560.0). *Eotyrannus* lacks several synapomorphies of tyrannosaurids and tyrannosaurid-like tyrannosauroids, including the absence of nasal participation to the antorbital fossa, paired nasal crests, an enlarged paraquadrate foramen, an acute anterodorsal corner on the dentary (as seen in lateral view), an enlarged posterior surangular foramen, shortened cervical neural arches, and posterior dorsal pleurocoels.

The tyrannosauroid affinities of megaraptorans – first suggested by Novas et al. (2013) and subsequently supported by Porfiri et al. (2015) and discussed by Bell et al. (2015) – are here confirmed using the largest morphological dataset and a wider taxon sample among non-coelurosaurian tetanurans and coelurosaurs than employed in previous analyses. We do not, however, support Porfiri et al.’s (2015) inclusion of *Eotyrannus* within Megaraptora: they described how this position was supported by the presence of (1) strongly opisthocoelous cervical centra and (2) pleurocoels in dorsal vertebrae in this taxon; this is an error, since *Eotyrannus* possesses amphicoelous or weakly opisthocoelous cervical centra and lacks pleurocoels (pneumatic foramina) in its dorsal vertebrae. **The hypothesis that megaraptorans are tyrannosauroids seemingly resolves the identity of controversial Lower Cretaceous specimens from Australia, interpreted as possible tyrannosauroid remains by some (Benson et al. 2010b) but linked to megaraptorans by others (Herne et al. 2010).** Furthermore, our analysis confirms a megaraptoran affinity for both *Chilantaisaurus* and *Siats* (Benson et al. 2010a; Zanno and

Makovicky 2013; Bell et al. 2015). This phylogenetic model indicates that Cretaceous tyrannosauroids were a more successful and diverse clade than previous suggested. Large-bodied ‘mid-Cretaceous’ forms like *Chilantaisaurus* and *Siats* – previously placed among non-coelurosaurian tetanurans – are now interpreted as a ‘second wave’ of tyrannosauroid gigantism that evolved later than the Early Cretaceous taxa *Sinotyrannus* and *Yutyrannus* (Brusatte and Carr 2016), but still prior to the emergence of Tyrannosauridae. Furthermore, the ‘mid-Cretaceous’ megaraptoran radiation fills both stratigraphically and morphologically significant gaps present in tyrannosauroid evolution between the Jurassic-Early Cretaceous early-diverging tyrannosauroids (e.g., proceratosaurids) and the Late Cretaceous tyrannosaurids. It is noteworthy that our results also support the conclusion of Brusatte et al. (2016), who suggested that a grade of mid-Cretaceous, mid-sized, longirostine tyrannosauroids (including *Xiongguanlong*, and, according to our study, megaraptorans too) were ancestral to the advanced large-bodied tyrannosaurids.

PLACE FIGURE 29 ABOUT HERE

By placing our phylogeny on a stratigraphic timescale (Fig 28), we speculatively infer that tyrannosauroids are primitively Eurasian (Bell et al. 2015), with eastern Asia perhaps being more important in their evolution during the Jurassic and Early Cretaceous than Europe or North America, though they also occurred in these regions (Madsen 1974; Foster and Chure 2000; Rauhut 2003a; Benson 2008). Most of the younger and most anatomically modified lineages within Tyrannosauroidea are North American, including the early-diverging megaraptoran *Siats*, indicating invasion of that region after the divergence of *Xiongguanlong* (Fig 30). A novel result of our analysis is that megaraptorans underwent a global radiation during the ‘middle’ Cretaceous, including large-bodied forms in Laurasia (Zanno and Makovicky 2013) and gracile-limbed megaraptorids in Laurasia (Bell et al. 2015). Hardly anything is known about the *Dryptosaurus* + Tyrannosauridae clade prior to the Campanian. An intriguing hypothesis is whether the late radiation of the tyrannosaurid-like forms in Laurasia was delayed by the megaraptoran radiation (see Zanno and Makovicky (2013) for a discussion of early-diverging lineages within the megaraptoran radiation, therein interpreted as carcharodontosaurian allosauroids). Furthermore, while tyrannosauroids are now known from the Middle and Upper Jurassic (Rauhut 2003a; Xu et al. 2006; Benson 2008; Averianov et al. 2010; Rauhut et al. 2010), comparatively few early representatives of the group have been discovered. Close relatives of

both *E. lengi*, and of *Dilong*, likely await discovery in the Upper Jurassic, Berriasian, Valanginian and Hauterivian strata of Eurasia.

## Conclusions

*Eotyrannus lengi* Hutt et al., 2001 is a valid tyrannosauroid taxon from the Barremian Wessex Formation of the Isle of Wight, presently known only from the holotype (IWCMS : 1997.550). Substantial cranial material, cervical, dorsal and sacral vertebrae, the scapulocoracoid and much of the forelimb and hindlimb are known, and allow us to characterise *E. lengi* as a mid-sized, long-handed tyrannosauroid with a tyrannosaurid-like scapulocoracoid and elongate, gracile distal hindlimbs (its femur remains unknown). It was presumably a fast runner, and its long forelimbs and enlarged manual unguals suggest that the forelimbs were important in the capture of prey. Thickened, pneumatic, fused nasals, a premaxilla with a steep anterior border, a tyrannosaurid-like quadrate and premaxillary teeth that are U-shaped in cross-section show that *E. lengi* was tyrannosaurid-like in cranial morphology and perhaps well adapted for powerful biting. Diagnostic characters include the presence of peculiar curving furrows on the lateral surface of the dentary, a large, block-like humeral entepicondyle and a tibia with a distoproximally aligned, laterally positioned channel on the distal end. The femur, pubis and ischium remain unknown and virtually nothing is known of the caudal skeleton

While several theropods have been named from the Wessex Formation, none can be shown to be synonymous with *E. lengi*. The fragmentary nature of the holotypes of most of these taxa renders their affinities uncertain, but *E. lengi* was contemporaneous with baryonychine spinosaurids, carcharodontosaurian allosauroids, probable compsognathids and maniraptorans (Naish et al. 2001; Sweetman 2004; Benson et al. 2009, 2010; Naish 2011). Like the majority of other early-diverging tyrannosauroids (Brusatte et al. 2010), *E. lengi* was a mid-sized predator in a fauna whose dominant large predators were megalosauroids or allosauroids.

PLACE FIGURE 30 ABOUT HERE

Our study confirms Hutt et al.'s (2001) proposal that *E. lengi* is a non-tyrannosaurid tyrannosauroid. Of several Jurassic and Early Cretaceous tyrannosauroids described since Hutt et al.'s (2001) paper was published, *E. lengi* seems to be among those most closely related to Tyrannosauridae. Our phylogenetic analysis recovers a topology broadly consistent with other

analyses of Tyrannosauroidea (e.g. Senter 2007, 2010; Li et al. 2009; Brusatte et al. 2010, 2011; Brusatte and Benson 2013; Loewen et al. 2013; Brusatte and Carr 2016), with Proceratosauridae, *Yutyrannus*, *Eotyrannus* and *Xiongguanlong* being successively closer to the tyrannosauroid clade that includes *Dryptosaurus*, *Appalachiosaurus*, *Bistahieversor* and Tyrannosauridae. We support a tyrannosauroid identity for megaraptorans and suggest that they are an important ‘mid-Cretaceous’ clade that represent a second wave of large-bodied tyrannosauroids, the diversification of which may even have slowed the radiation of the tyrannosaurid lineage. *E. lengi* shares two characters of the ilium with *Juratyran* (posterodorsally inclined vertical ridge, failure of vertical ridge to reach dorsal margin of ilium) (Benson 2008), but we did not consistently recover a consistent strong relationship between these two taxa.

**Acknowledgements** This work results primarily from the first author’s PhD thesis, completed at the University of Portsmouth (UK). Thanks are due to Dave M. Martill for his assistance with that project, Bob Loveridge for help with photography and SEM techniques, and Dave Hughes and Mike Barker (both formerly of SEES, University of Portsmouth) for co-operation and support. Stig Walsh, Steve Sweetman, Tony Butcher, Dean Bullen and Sarah Fielding are thanked for technical assistance and advice; David Loydell and Eric Buffetaut are thanked for comments on an earlier version of this work. For discussion, opinions and identifications of *Eotyrannus* material, we thank Chris Brochu, Jonah Choiniere, Thomas R. Holtz Jr., Mathew Wedel and Peter Makovicky. Steve Brusatte, Roger Benson and Christophe Henrickx are thanked for their helpful advice in interpreting details of the morphology of *Eotyrannus*. We thank our reviewers – Jonah Choiniere and Corwin Sullivan – for numerous corrections, observations and suggestions which substantially improved the quality of the manuscript, and to Steve Brusatte and Peter Makovicky for further comments and advice on the manuscript. For access to specimens we thank Angela Milner and Sandra Chapman (NHM) and Martin Munt, Dan Pemberton and Trevor Price (IWCMS). Steve Hutt (IWCMS) is thanked for his thoughts on theropod anatomy, functional morphology and evolution and for putting so much work into the preparation and interpretation of *Eotyrannus*. The program TNT is made publicly available via the sponsorship of the Willi Hennig Society.

## References



- 2472 Allen P, Wimbledon WA (1991) Correlation of NW European Purbeck-Wealden (non-marine  
2473 Lower Cretaceous) as seen from the English type-areas. *Cretaceous Research* 12:511–526
- 2474 Anon 1866. Another new Wealden reptile. *The Athenaeum* 2014:740
- 2475 Averianov AO, Krasnolutskii SA, Ivantsov SV (2010) A new basal coelurosaur (Dinosauria:  
2476 Theropoda) from the Middle Jurassic of Siberia. *Proceedings of the Zoological Institute*  
2477 RAS 314:42–57
- 2478 Barrett PM, Butler RJ, Twitchett RJ, Hutt S (2011) New material of *Valdosaurus canaliculatus*  
2479 (Ornithischia: Ornithopoda) from the Lower Cretaceous of southern England. *Special*  
2480 *Papers in Palaeontology* 86:131–163
- 2481 Barsbold R (1976) New data on *Therizinosaurus* (Therizinosauridae, Theropoda). *Sovmestnaya*  
2482 *Sovetsko-Mongol'skaya Paleontologicheskaya Ekspiditsiya, Trudy* 3:76–92 [in Russian]
- 2483 Barsbold R, Osmólska H (1999) The skull of *Velociraptor* (Theropoda) from the Late Cretaceous  
2484 of Mongolia. *Acta Palaeontologica Polonica* 44:189–219.
- 2485 Bell PR, Cau A, Fanti F, Smith E (2015) A large-clawed theropod (Dinosauria: Tetanurae) from  
2486 the Lower Cretaceous of Australia and the Gondwanan origin of megaraptorid theropods.  
2487 *Gondwana Res* 36:473–487
- 2488 Benson RBJ, Brusatte SL, Hutt S, Naish D (2009) A new large basal tetanuran (Dinosauria:  
2489 Theropoda) from the Wessex Formation (Barremian) of the Isle of Wight, England. *J*  
2490 *Vertebrate Paleontol* 29:612–615
- 2491 Benson RBJ, Carrano MT, Brusatte SL (2010a) A new clade of archaic large-bodied predatory  
2492 dinosaurs (Theropoda: Allosauroidae) that survived to the latest Mesozoic.  
2493 *Naturwissenschaften* 97:71–78
- 2494 Benson RBJ, Barrett PM, Rich TH, Vickers-Rich P (2010b). A southern tyrant reptile. *Science*  
2495 327:1613
- 2496 Bilbey SA (1999) Taphonomy of the Cleveland-Lloyd Dinosaur Quarry in the Morrison  
2497 Formation, central Utah – a lethal spring-fed pond. In: Gillette, DD (ed) *Vertebrate*  
2498 *Paleontology in Utah. Miscellaneous Publications, Utah Geological Survey (Salt Lake*  
2499 *City), pp. 121–133*
- 2500 Bonaparte JF, Novas, FE, Coria, RA (1990) *Carnotaurus sastrei* Bonaparte, the horned, lightly  
2501 built carnosaur from the middle Cretaceous of Patagonia. *Natural History Museum of Los*  
2502 *Angeles County, Contributions in Science* 416:1–42
- 2503 Bremer K (1988) The limits of amino-acid sequence data in angiosperm phylogenetic  
2504 reconstruction. *Evolution* 42:795–803

- 2505 Brinkman DL, Cifelli RL, Czaplewski NJ (1998) First occurrence of *Deinonychus antirrhopus*  
2506 (Dinosauria: Theropoda) from the Antlers Formation (Lower Cretaceous: Aptian-Albian) of  
2507 Oklahoma. Oklahoma Geological Survey Bulletin 146:1–27
- 2508 Britt BB (1991) Theropods of Dry Mesa Quarry (Morrison Formation, Late Jurassic), Colorado,  
2509 with emphasis on the osteology of *Torvosaurus tanneri*. Brigham Young University  
2510 Geology Studies 37:1–72
- 2511 Brochu CA (1996) Closure of neurocentral sutures during crocodilian ontogeny: implications for  
2512 maturity assessment in fossil archosaurs. J Vertebrate Paleontol 16:49–62
- 2513 Brochu CA (2003) Osteology of *Tyrannosaurus rex*: insights from a nearly complete skeleton and  
2514 high-resolution computed tomographic analysis of the skull. J Vertebrate Paleontol 22,  
2515 Supplement to Number 4, pp. 1–138
- 2516 Brusatte SL, Carr TD (2016) The phylogeny and evolutionary history of tyrannosauroid  
2517 dinosaurs. Sci. Rep. 6, 20252; doi: 10.1038/srep20252
- 2518 Brusatte SL, Averianov A, Sues H-D, Muir A, Butler IB (2016). New tyrannosaur from the mid-  
2519 Cretaceous of Uzbekistan clarifies evolution of giant body sizes and advanced senses in  
2520 tyrant dinosaurs. PNAS: 3447–3452
- 2521 Brusatte SL, Lloyd GT, Wang SC, Norell MA (2014) Gradual assembly of avian body plan  
2522 culminated in rapid rates of evolution across the dinosaur-bird transition. Curr Biol  
2523 24:2386–2392
- 2524 Brusatte SL, Norell MA, Carr TD, Erickson GM, Hutchinson JR, Balanoff AM, Bever GS,  
2525 Choiniere JN, Makovicky PJ, Xu X (2010) Tyrannosaur paleobiology: new research on  
2526 ancient exemplar organisms. Science 329: 1481–1485
- 2527 Brusatte SL, Benson RBJ, Norell MA (2011) The anatomy of *Dryptosaurus aquilunguis*  
2528 (Dinosauria: Theropoda) and a review of its tyrannosauroid affinities. American Museum  
2529 Novitates 3717: 1–53
- 2530 Brusatte SL, Benson RBJ (2013) The systematics of Late Jurassic tyrannosauroid theropods from  
2531 Europe and North America. Acta Palaeontologica Polonica 58: 47–54
- 2532 Brusatte S, Benson RBJ, Hutt S (2008) The osteology of *Neovenator salerii* (Dinosauria:  
2533 Theropoda) from the Wealden Group (Barremian) of the Isle of Wight. Monograph of the  
2534 Palaeontographical Society 162:1–75
- 2535 Brusatte SL, Carr TD, Norell MA (2012) The osteology of *Alioramus*, a gracile and long-snouted  
2536 tyrannosaurid (Dinosauria: Theropoda) from the Late Cretaceous of Mongolia. Bull  
2537 American Museum of Natural History 366: 1–197

- 2538 Buffetaut E, Suteethorn V, Tong H (1996) The earliest known tyrannosaur from the Lower  
2539 Cretaceous of Thailand. *Nature* 381: 689–691
- 2540 Burnham DA, Derstler KL, Currie PJ, Bakker RT, Zhou Z, Ostrom JH (2000) Remarkable new  
2541 birdlike dinosaur (Theropoda: Maniraptora) from the Upper Cretaceous of Montana. The  
2542 University of Kansas Paleontological Contributions 13:1–14
- 2543 Carpenter K, Miles CA, Cloward K (2005a) New small theropod from the Upper Jurassic  
2544 Morrison Formation of Wyoming. In: Carpenter K (ed) *The Carnivorous Dinosaurs*. Indiana  
2545 University Press, Bloomington and Indianapolis, pp. 23–48
- 2546 Carpenter K, Miles CA, Ostrom JH, Cloward K (2005b) Redescription of the small maniraptoran  
2547 theropods *Ornitholestes* and *Coelurus* from the Upper Jurassic Morrison Formation of  
2548 Wyoming. In: Carpenter K (ed) *The Carnivorous Dinosaurs*. Indiana University Press,  
2549 Bloomington and Indianapolis, pp. 49–71
- 2550 Carpenter K, Smith M (2001) Forelimb osteology and biomechanics of *Tyrannosaurus rex*. In:  
2551 Tanke DH, Carpenter K (eds) *Mesozoic Vertebrate Life*. Indiana University Press,  
2552 Bloomington and Indianapolis, pp. 90–116
- 2553 Carpenter K, Tidwell V (2005) Reassessment of the Early Cretaceous sauropod *Astrodon*  
2554 *johnsoni* Leidy 1865 (Titanosauriformes). In: Tidwell V, Carpenter K (eds) *Thunder-*  
2555 *Lizards: The Sauropodomorph Dinosaurs*. Indiana University Press, Bloomington and  
2556 Indianapolis, pp. 78–114
- 2557 Carr TD (1999) Craniofacial ontogeny in Tyrannosauridae (Dinosauria, Coelurosauria). *J Vertebr*  
2558 *Paleontol* 19:497–520
- 2559 Carr TD, Williamson TE (2004) Diversity of late Maastrichtian Tyrannosauridae (Dinosauria:  
2560 Theropoda) from western North America. *Zool J Linn Soc* 142:479–523
- 2561 Carr TD, Williamson TE (2010) *Bistahieversor sealeyi*, gen. et sp. nov. a new tyrannosauroid  
2562 from New Mexico and the origin of deep snouts in Tyrannosauroida. *J Vertebr Paleontol*  
2563 30:1–16
- 2564 Carr TD, Williamson, TE, Schwimmer DR (2005) A new genus and species of tyrannosauroid  
2565 from the Late Cretaceous (middle Campanian) Demopolis Formation of Alabama. *J Vertebr*  
2566 *Paleontol* 25:119–143
- 2567 Carrano MT, Hutchinson, JR (2002) Pelvic and hindlimb musculature of *Tyrannosaurus rex*  
2568 (Dinosauria: Theropoda). *J Morphology* 253:207–228
- 2569 Charig AJ, Milner AC (1997) *Baryonyx walkeri*, a fish-eating dinosaur from the Wealden of  
2570 Surrey. *Bull Nat Hist Mus Geol* 53:11–70

- 2571 Choiniere JN, Clark JM, Forster CA, Xu X (2010) A basal coelurosaur (Dinosauria: Theropoda)
- 2572 from the Late Jurassic (Oxfordian) of the Shishugou Formation in Wucuiwan, People's
- 2573 Republic of China. *J Vertebr Paleontol* 30:1773–1796
- 2574 Chure DJ (2001) The wrist of *Allosaurus* (Saurischia: Theropoda), with observations on the
- 2575 carpus in theropods. In Gauthier J, Gall LF (eds) *New Perspectives on the Origin and Early*
- 2576 *Evolution of Birds: Proceedings of the International Symposium in Honor of John H.*
- 2577 *Ostrom*. Peabody Museum of Natural History, Yale University, New Haven, pp. 283–300
- 2578 Clark JM, Maryńska T, Barsbold R (2004) Therizinosauroidea. In: Weishampel DB, Dodson P,
- 2579 Osmólska H (eds) *The Dinosauria*, Second Edition. University of California Press,
- 2580 Berkeley, pp. 151–164
- 2581 Currie PJ (2003) Cranial anatomy of tyrannosaurid dinosaurs from the Late Cretaceous of
- 2582 Alberta, Canada. *Acta Palaeontologica Polonica* 48:191–226
- 2583 Currie PJ, Carpenter K (2000) A new specimen of *Acrocanthosaurus atokensis* (Theropoda,
- 2584 Dinosauria) from the Lower Cretaceous Antlers Formation (Lower Cretaceous, Aptian) of
- 2585 Oklahoma, USA. *Geodiversitas* 22:207–246
- 2586 Currie PJ, Chen PJ (2001) Anatomy of *Sinosauropteryx prima* from Liaoning, northeastern
- 2587 China. *Can J Earth Sci* 38:1705–1727
- 2588 Currie PJ, Dong Z (2001) New information on *Shanshanosaurus huoyanshanensis*, a juvenile
- 2589 tyrannosaurid (Theropoda, Dinosauria) from the Late Cretaceous of China. *Can J Earth Sci*
- 2590 38:1729–1737
- 2591 Currie PJ, Hurum JH, Sabath K (2003) Skull structure and evolution in tyrannosaurid dinosaurs.
- 2592 *Acta Palaeontologica Polonica* 48:227–234
- 2593 Currie PJ, Rigby JK, Sloan RE (1990) Theropod teeth from the Judith River Formation of
- 2594 southern Alberta, Canada. In: Carpenter K, Currie PJ (eds) *Dinosaur Systematics:*
- 2595 *Approaches and Perspectives*. Cambridge University Press, Cambridge, pp. 107–125
- 2596 Currie PJ, Varricchio DJ (2004) A new dromaeosaurid from the Horseshoe Canyon Formation
- 2597 (Upper Cretaceous) of Alberta, Canada. In: Currie PJ, Koppelhus EB, Shugar MA, Wright
- 2598 JL (eds) *Feathered Dragons. Studies on the Transition from Dinosaurs to Birds*. Indiana
- 2599 University Press, Bloomington and Indianapolis, pp. 112–132
- 2600 Currie PJ, Zhao X (1994) A new carnosaur (Dinosauria, Theropoda) from the Jurassic of
- 2601 Xinjiang, People's Republic of China. *Can J Earth Sci* 30:2037–2081

- 2602 Dal Sasso C, Maganuco S (2011) *Scipionyx samniticus* (Theropoda: Compsognathidae) from the
- 2603 Lower Cretaceous of Italy. *Memorie della Società Italiana di Scienze Naturali e del Museo*
- 2604 *Civico di Storia Naturale di Milano* 37:1–281
- 2605 De Klerk W, Forster CA, Sampson SD, Chinsamy A, Ross CF (2000) A new coelurosaurian
- 2606 dinosaur from the Early Cretaceous of South Africa. *J Vertebr Paleontol* 20:324–332
- 2607 Elzanowski A (1999) A comparison of the jaw skeleton in theropods and birds, with a description
- 2608 of the palate in the Oviraptoridae. *Smithsonian Contributions of Paleobiology* 89:311–323
- 2609 Ezcurra MD, Novas FE (2007) Phylogenetic relationships of the Triassic theropod *Zupaysaurus*
- 2610 *rougieri* from NW Argentina. *Historical Biology* 19:35–72
- 2611 Foster JR, Chure DJ (2000) An ilium of a juvenile *Stokesosaurus* (Dinosauria, Theropoda) from
- 2612 the Morrison Formation (Upper Jurassic: Kimmeridgian), Meade County, South Dakota.
- 2613 *Brigham Young University Geology Studies* 45:5–10
- 2614 Gauthier J (1986) Saurischian monophyly and the origin of birds. *Mem Calif Acad Sci* 8:1–55
- 2615 Gilmore CW (1920) Osteology of the carnivorous Dinosauria in the United States National
- 2616 Museum, with special reference to the genera *Antrodemus* (*Allosaurus*) and *Ceratosaurus*.
- 2617 *Bulletin of the United States National Museum* 110:1–154
- 2618 Gishlick AD (2001) The function of the manus and forelimb of *Deinonychus antirrhopus* and its
- 2619 importance for the origin of avian flight. In: Gauthier J, Gall LF (eds) *New Perspectives on*
- 2620 *the Origin and Early Evolution of Birds: Proceedings of the International Symposium in*
- 2621 *Honor of John H. Ostrom*. Peabody Museum of Natural History, Yale University, New
- 2622 Haven, pp. 301–318
- 2623 Goloboff PA, Farris S, Nixon, KC (2008) TNT, a free program for phylogenetic analysis.
- 2624 *Cladistics* 24:774–786
- 2625 Harris JD (1998) A reanalysis of *Acrocanthosaurus atokensis*, its phylogenetic status, and
- 2626 paleobiogeographic implications, based on a new specimen from Texas. *New Mex Nat Hist*
- 2627 *Sci Bull* 13:1–75
- 2628 Hendrickx C, Araújo R, Mateus O (2015) The non-avian theropod quadrate I: standardized
- 2629 terminology with an overview of the anatomy and function. *PeerJ* 3: e1245; DOI
- 2630 10.7717/peerj.1245
- 2631 Herne MC, Nair JP, Salisbury SW (2010) Comment on “A southern tyrant reptile.” *Science*
- 2632 329:1013
- 2633 Hill AP (1980) Early postmortem damage to the remains of some contemporary east African
- 2634 mammals. In: Behrensmeyer AK, Hill AP (eds) *Fossils in the Making*. Vertebrate

- 2635       Taphonomy and Paleoecology. The University of Chicago Press, Chicago and London, pp.  
2636       131–152
- 2637   Holtz TR (1994) The phylogenetic position of the Tyrannosauridae: implications for theropod  
2638       systematics. *J Palaeontol* 68:1100–1117
- 2639   Holtz TR (2004) Tyrannosauroidae. In: Weishampel DB, Dodson P, Osmólska, H (eds) *The*  
2640       *Dinosauria*, Second Edition. University of California Press, Berkeley, pp. 111–136
- 2641   Holtz TR, Molnar RE, Currie PJ (2004) Basal Tetanurae. In: Weishampel DB, Dodson P,  
2642       Osmólska H (eds) *The Dinosauria*, Second Edition. University of California Press,  
2643       Berkeley, pp. 71–110
- 2644   Howse SCB, Milner AR (1993) *Ornithodesmus* – a maniraptoran theropod dinosaur from the  
2645       Lower Cretaceous of the Isle of Wight, England. *Palaeontology* 36:425–437
- 2646   Hurum JH, Sabath K (2003) Giant theropod dinosaurs from Asia and North America: skulls of  
2647       *Tarbosaurus bataar* and *Tyrannosaurus rex* compared. *Acta Palaeontologica Polonica*  
2648       48:161–190
- 2649   Hutchinson JR (2002) The evolution of hindlimb tendons and muscles on the line to crown-group  
2650       birds. *Comparative Biochemistry and Physiology Part A* 133, 1051–1086
- 2651   Hutt S (2002) Mr Leng’s dinosaur. *The Geological Society of the Isle of Wight Newsletter* 2  
2652       (6):12–14
- 2653   Hutt S, Martill DM, Barker MJ (1996) The first European allosaurid dinosaur (Lower Cretaceous,  
2654       Wealden Group, England). *Neues Jahrb Geol Päl M* 1996:635–644
- 2655   Hutt S, Naish D, Martill DM, Barker MJ, Newbery P (2001) A preliminary account of a new  
2656       tyrannosauroid theropod from the Wessex Formation (Early Cretaceous) of southern  
2657       England. *Cretaceous Res* 22:227–242
- 2658   Hwang SH, Norell MA, Ji Q, Gao K (2004) A large compsognathid from the Early Cretaceous  
2659       Yixian Formation of China. *J Syst Palaeontol* 2:13–30
- 2660   Insole AN, Hutt S (1994) The palaeoecology of the dinosaurs of the Wessex Formation (Wealden  
2661       Group, Early Cretaceous), Isle of Wight, southern England. *Zool J Linn Soc* 112:197–215
- 2662   Johnson RE, Ostrom JH (1995) The forelimb of *Torosaurus* and an analysis of the posture and  
2663       gait of ceratopsian dinosaurs. In: Thomason J (ed) *Functional Morphology in Vertebrate*  
2664       *Paleontology*. Cambridge University Press, Cambridge, pp. 205–218
- 2665   Kirkland JI, Gaston R, Burge D (1993) A large dromaeosaur (Theropoda) from the Lower  
2666       Cretaceous of eastern Utah. *Hunteria* 2 (10):1–16



- 2667 Kirkland JI, Zanno LE, Sampson SD, Clark JM, DeBlieux DD (2005) A primitive  
2668 therizinosauroid dinosaur from the Early Cretaceous of Utah. *Nature* 435:84–87
- 2669 Lambe LM (1917) The Cretaceous theropodous dinosaur *Gorgosaurus*. *Mem Geological Society*  
2670 of Canada 100:1–84
- 2671 Loewen, M.A., Irmis, R.B., Sertich, J.J.W., Currie, P.J., Sampson, S.D. (2013). Tyrant dinosaur  
2672 evolution tracks the rise and fall of Late Cretaceous oceans. *PLoS ONE* 8(11): e79420
- 2673 Madsen JH (1974) A new theropod dinosaur from the Upper Jurassic of Utah. *J Paleontol* 48:27–  
2674 31
- 2675 Madsen JH (1976) *Allosaurus fragilis*: a revised osteology. *Utah Geological and Mineral Survey*  
2676 *Bulletin* 109:1–163
- 2677 Madsen JH, Welles SP (2000) *Ceratosaurus* (Dinosauria, Theropoda) a revised osteology. *Utah*  
2678 *Geological Survey Miscellaneous Publication* 00-2:1–80
- 2679 Makovicky PJ (1995) Phylogenetic Aspects of the Vertebral Morphology of Coelurosauria  
2680 (Dinosauria: Theropoda). Unpublished MSc thesis. University of Copenhagen.
- 2681 Martill DM (2001) Taphonomy and preservation. In: Martill DM, Naish D (eds.) *Dinosaurs of the*  
2682 *Isle of Wight*. The Palaeontological Association, London, pp. 49–59
- 2683 Martill DM, Naish D (2001) The geology of the Isle of Wight. In: Martill DM, Naish D (eds)  
2684 *Dinosaurs of the Isle of Wight*. The Palaeontological Association, London, pp. 25–43
- 2685 Martínez RD, Novas FE (2006) *Aniksosaurus darwini* gen. et sp. nov., a new coelurosaurian  
2686 theropod from the early Late Cretaceous of central Patagonia, Argentina. *Revista del Museo*  
2687 *Argentino de Ciencias Naturales*, n.s. 8(2):243–259.
- 2688 Molnar RE (1991) The cranial morphology of *Tyrannosaurus rex*. *Palaeontographica Abteilung A*  
2689 217, 137–176
- 2690 Naish D (2000) A small, unusual theropod (Dinosauria) femur from the Wealden Group (Lower  
2691 Cretaceous) of the Isle of Wight, England. *Neues Jahrb Geol Pal M* 2000:217–234
- 2692 Naish D (2002) The historical taxonomy of the Lower Cretaceous theropods (Dinosauria)  
2693 *Calamospondylus* and *Aristosuchus* from the Isle of Wight. *Proceedings of the Geologists’*  
2694 *Association* 113:153–163
- 2695 Naish D (2011) Theropod dinosaurs. In: Batten, DJ (ed.) *English Wealden Fossils*. The  
2696 *Palaeontological Association*, London, pp. 526–559
- 2697 Naish D, Hutt S, Martill DM (2001) Saurischian dinosaurs 2: Theropods. In: Martill, DM, Naish  
2698 D (eds) *Dinosaurs of the Isle of Wight*. The Palaeontological Association, London, pp. 242–  
2699 309

- 2700 Naish D, Martill, DM (2007) Dinosaurs of Great Britain and the role of the Geological Society of  
2701 London in their discovery: basal Dinosauria and Saurischia. *Journal of the Geological*  
2702 *Society*, London 164:493–510
- 2703 Naish D, Martill DM, Frey E (2004) Ecology, systematics and biogeographical relationships of  
2704 dinosaurs, including a new theropod, from the Santana Formation (?Albian, Early  
2705 Cretaceous) of Brazil. *Historical Biology* 16:57–70
- 2706 Norell MA Makovicky PJ (1997) Important features of the dromaeosaur skeleton: information  
2707 from a new specimen. *American Museum Novitates* 3215:1–28
- 2708 Novas, FE (1996) Alvarezsauridae, Cretaceous basal birds from Patagonia and Mongolia. *Mem*  
2709 *Queensland Museum* 39:675–702
- 2710 Novas, FE (1997) Anatomy of *Patagonykus puertai* (Theropoda, Avialae, Alvarezsauridae), from  
2711 the Late Cretaceous of Patagonia. *J Vertebrate Paleontol* 17:137–166
- 2712 Novas FA, Agnolín FL, Ezcurra MD, Porfiri J, Canale JI (2013) Evolution of the carnivorous  
2713 dinosaurs during the Cretaceous: The evidence from Patagonia. *Cret Res* 45:174–215
- 2714 Novas, FE, Salgado L, Suárez M, Agnolín FL, Ezcurra MND, Chimento NSR, de la Cruz R, Isasi  
2715 MP, Vargas AO, Rubilar-Rogers D. (2015) An enigmatic plant-eating theropod from the  
2716 Late Jurassic period of Chile. *Nature* 522:331–334
- 2717 Oldham TCB (1976) The plant debris beds of the English Wealden. *Palaeontology* 19:437–502
- 2718 Osborn HF (1906) *Tyrannosaurus*, Upper Cretaceous carnivorous dinosaur (second  
2719 communication). *Bull American Museum of Natural History* 22:281–296
- 2720 Osborn HF (1917) Skeletal adaptations of *Ornitholestes*, *Struthiomimus*, *Tyrannosaurus*. *Bull*  
2721 *American Museum of Natural History* 32:133–150
- 2722 Osmólska H (1996) An unusual theropod dinosaur from the Late Cretaceous Nemegt Formation  
2723 of Mongolia. *Acta Palaeontologica Polonica* 41:1–38
- 2724 Osmólska H, Currie PJ, Barsbold R (2004) Oviraptorosauria. In: Weishampel DB., Dodson P,  
2725 Osmólska H (eds) *The Dinosauria*, Second Edition. University of California Press,  
2726 Berkeley, pp. 165–183
- 2727 Osmólska H, Roniewicz E, Barsbold P (1972) A new dinosaur, *Gallimimus bullatus* n. gen., n. sp.  
2728 (Ornithomimidae) from the Upper Cretaceous of Mongolia. *Palaeontologica Polonica*  
2729 27:103–143
- 2730 Ostrom JH (1969) Osteology of *Deinonychus antirrhopus*, an unusual theropod from the Lower  
2731 Cretaceous of Montana. *Bull Peabody Museum of Natural History* 30:1–165

- 2732 Owen R (1876) Monograph of the fossil Reptilia of the Wealden and Purbeck Formations.  
2733 Supplement 7. Crocodilia (*Poikilopleuron*), Dinosauria (*Chondrosteosaurus*).  
2734 Palaeontographical Society Monograph 30:1–7
- 2735 Perle A (1981) A new segnosaurid from the Upper Cretaceous of Mongolia. Sovmestnaya  
2736 Sovetsko-Mongol'skaya Paleontologicheskaya Ekspiditsiya, Trudy 8:50–59 [in Russian]
- 2737 Peyer K (2006) A reconsideration of *Compsognathus* from the Upper Tithonian of Canjuers,  
2738 southeastern France. J Vertebrate Paleontol 26:879–896
- 2739 Porfiri JD, Novas FE, Calvo JO, Agnolín FL, Ezcurra MD, Cerda IA. (2014) Juvenile specimen  
2740 of *Megaraptor* (Dinosauria, Theropoda) sheds light about tyrannosauroid radiation.  
2741 Cretaceous Research 51: 35–55
- 2742 Radley JD (1994) Stratigraphy, palaeontology and palaeoenvironment of the Wessex Formation  
2743 (Wealden Group, Lower Cretaceous) at Yaverland, Isle of Wight, southern England.  
2744 Proceedings of the Geologists' Association 105:199–208
- 2745 Rauhut OWM (2003a) A tyrannosauroid dinosaur from the Upper Jurassic of Portugal.  
2746 Palaeontology 46:903–910
- 2747 Rauhut OWM (2003b) The interrelationships and evolution of basal theropod dinosaurs. Special  
2748 Papers in Palaeontology 69:1–213
- 2749 Rauhut OWM, Milner AC, Moore-Fay S (2010) Cranial osteology and phylogenetic position of  
2750 the theropod dinosaur *Proceratosaurus bradleyi* (Woodward, 1910) from the Middle  
2751 Jurassic of England. Zool J Linn Soc 158:155–195
- 2752 Rauhut OWM, Xu X (2005) The small theropod dinosaurs *Tugulusaurus* and *Phaedrolosaurus*  
2753 from the Early Cretaceous of Xinjiang, China. J Vertebrate Paleontol 25:107–118
- 2754 Rauhut OWM, Werner C (1995) First record of the family Dromaeosauridae (Dinosauria:  
2755 Theropoda) in the Cretaceous of Gondwana (Wadi Milk Formation, northern Sudan).  
2756 Paläontologische Zeitschrift 69:475–489
- 2757 Rayfield EJ, Norman, DB, Horner CC, Horner JR, Smith PM, Thomason JJ, Upchurch P (2001)  
2758 Cranial design and function in a large theropod dinosaur. Nature 409:1033–1037
- 2759 Russell DA (1970) Tyrannosaurs from the Late Cretaceous of western Canada. National  
2760 Museums of Canada Publication in Palaeontol 1:1–34
- 2761 Russell DA, Dong ZM (1994) The affinities of a new theropod from the Alxa Desert, Inner  
2762 Mongolia, People's Republic of China. Can J Earth Sci 30:2107–2127

- 2763 Sampson SD, Witmer LM, Forster CA, Krause DW, O’Conner, PM, Dodson P, Ravoavy F (1998)
- 2764       Predatory dinosaur remains from Madagascar: implications for the Cretaceous
- 2765       biogeography of Gondwana. *Science* 280:1048–1051
- 2766 Seeley HG (1887) On a sacrum apparently indicating a new type of bird, *Ornithodesmus*
- 2767       *cluniculus* Seeley. *Quarterly J Geological Society, London* 43:206–211
- 2768 Seeley HG (1888) On *Thecospondylus daviesi* (Seeley), with some remarks on the classification
- 2769       of the Dinosauria. *Quarterly J Geological Society, London* 44:79–86
- 2770 Senter P (2007) A new look at the phylogeny of Coelurosauria (Dinosauria: Theropoda). *J*
- 2771       *Systematic Palaeontol* 5:429–463
- 2772 Senter P (2010) Using creation science to demonstrate evolution: application of a creationist
- 2773       method for visualizing gaps in the fossil record to a phylogenetic analysis of coelurosaurian
- 2774       dinosaurs. *J Evolutionary Biology* 23:1732–1743
- 2775 Senter P, Barsbold R, Brtñ BB, Burnham DA (2004) Systematics and evolution of
- 2776       Dromaeosauridae (Dinosauria, Theropoda). *Bulletin of the Gunma Museum of Natural*
- 2777       History 8:1–20
- 2778 Senter P, Robins JH (2005) Range of motion in the forelimb of the theropod dinosaur
- 2779       *Acrocanthosaurus atokensis*, and implications for predatory behaviour. *Journal of Zoology*
- 2780       266:307–318
- 2781 Sereno PC (1999) The evolution of dinosaurs. *Science* 284, 2137–2147
- 2782 Sereno PC, Dutheil DB, Iarochene M, Larsson HCE, Lyon GH, Magwene PM, Sidor CA,
- 2783       Varricchio DJ, Wilson JA (1996) Predatory dinosaurs from the Sahara and Late Cretaceous
- 2784       faunal differentiation. *Science* 272:986–991
- 2785 Sereno PC, Wilson JA, Larsson HCE, Dutheil DB, Sues HD (1994) Early Cretaceous dinosaurs
- 2786       from the Sahara. *Science* 266:267–270
- 2787 Snively E, Henderson DM, Phillips DS (2006) Fused and vaulted nasals of tyrannosaurid
- 2788       dinosaurs: implications for cranial strength and feeding mechanics. *Acta Palaeontologica*
- 2789       Polonica 51: 435–454
- 2790 Stewart DJ (1978) The Sedimentology and Palaeoenvironment of the Wealden Group of the Isle
- 2791       of Wight, Southern England. Unpublished PhD thesis, Portsmouth Polytechnic, pp. 347.
- 2792 Stewart DJ (1981) A field guide to the Wealden Group of the Hastings area and the Isle of Wight.
- 2793       In: Elliot T (ed) *Field Guides to Modern and Ancient Fluvial Systems in Britain and Spain*.
- 2794       International Fluvial Conference, University of Keele, pp. 3.1-3.32.

- 2795 Sues HD (1997) On *Chirostenotes*, a Late Cretaceous oviraptorosaur (Dinosauria: Theropoda)
- 2796 from western North America. J Vertebrate Paleontol 17:698–716
- 2797 Sweetman SC (2004) The first record of velociraptorine dinosaurs (Saurischia, Theropoda) from
- 2798 the Wealden (Early Cretaceous, Barremian) of southern England. Cretaceous Research
- 2799 25:353–364
- 2800 Tarsitano SF (1983) Stance and gait in theropod dinosaurs. Acta Palaeontologica Polonica
- 2801 28:251–264
- 2802 Tykoski RS, Rowe T (2004) Ceratosauria. In: Weishampel DB, Dodson P, Osmólska H (eds) The
- 2803 Dinosauria, Second Edition. University of California Press, Berkeley, pp. 47–70
- 2804 Vickers-Rich P, Chiappe LM, Kurzanov S (2002) The enigmatic birdlike dinosaur *Avimimus*
- 2805 *portentosus*: comments and a pictorial atlas. In: Chiappe LM, Witmer LM (eds) Mesozoic
- 2806 Birds: Above the Heads of Dinosaurs. University of California Press, Berkeley, pp. 65–86
- 2807 Welles SP (1984) *Dilophosaurus wetherilli* (Dinosauria, Theropoda) osteology and comparisons.
- 2808 Palaeontographica Abteilung A 185:85–180
- 2809 Witmer LM (1997) The evolution of the antorbital cavity of archosaurs: a study in soft-tissue
- 2810 reconstruction in the fossil record with an analysis of the function of pneumaticity. J
- 2811 Vertebrate Paleontol 17 (Supplement to No.1), pp. 73.
- 2812 Wright JL, Barrett PM, Lockley MG, Cook E (1998) A review of the Early Cretaceous terrestrial
- 2813 vertebrate track-bearing strata of England and Spain. New Mexico Museum of Natural
- 2814 History and Science Bulletin 14:143–153
- 2815 Xu X, Clark JM, Forster CA, Norell MA, Erickson GM, Eberth DA, Jia C, Zhao Q (2006) A
- 2816 basal tyrannosauroid dinosaur from the Late Jurassic of China. Nature 439:715–718
- 2817 Xu X, Norell, MA, Kuang X, Wang X, Zhao Q, Jia C (2004) Basal tyrannosauroids from China
- 2818 and evidence for protofeathers in tyrannosauroids. Nature 431:680–684
- 2819 Wang K, Zhang K, Ma Q, Xing L, Sullivan C, Hu D, Cheng S, Wang S (2012) A gigantic
- 2820 feathered dinosaur from the Lower Cretaceous of China. Nature 484:92–95
- 2821 Zanno LE (2006) The pectoral girdle and forelimb of the primitive therizinosauroid *Falcarius*
- 2822 *utahensis* (Theropoda, Maniraptora): analyzing evolutionary trends within
- 2823 Therizinosauroida. Journal of Vertebrate Paleontology 26:636–650
- 2824 Zanno LE, Makovicky PJ (2013) Neovenatorid theropods are apex predators in the Late
- 2825 Cretaceous of North America. Nature Comm 4: 2827
- 2826 Zhao XJ, Currie PJ (1994) A large crested theropod from the Jurassic of Xinjiang, People's
- 2827 Republic of China. Can J Earth Sci 30:2027–2036

2828

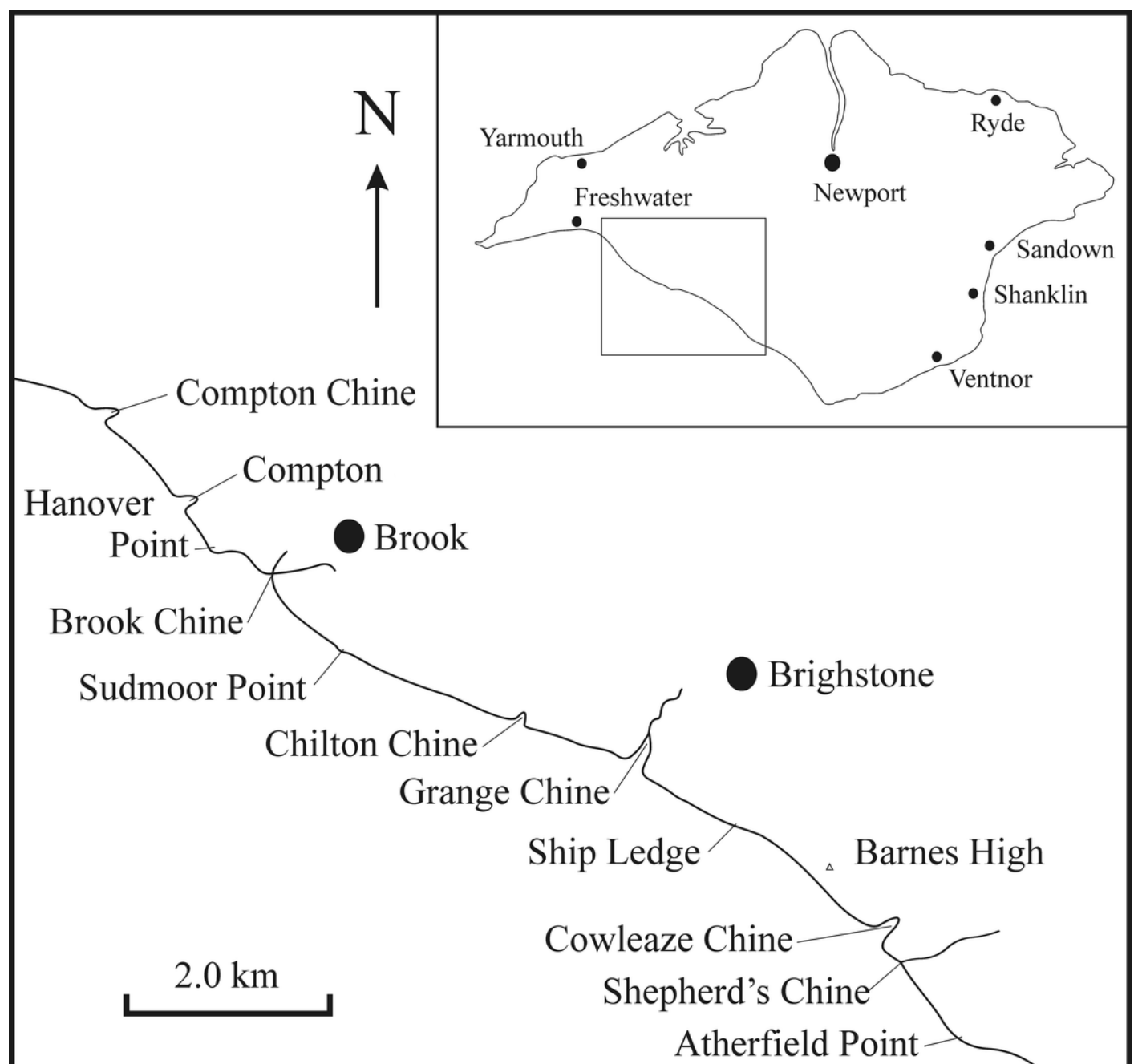
2829



# Figure 1

Fig. 1 Map of the Isle of Wight, with enlarged area showing key dinosaur-bearing sites on south-west coast.

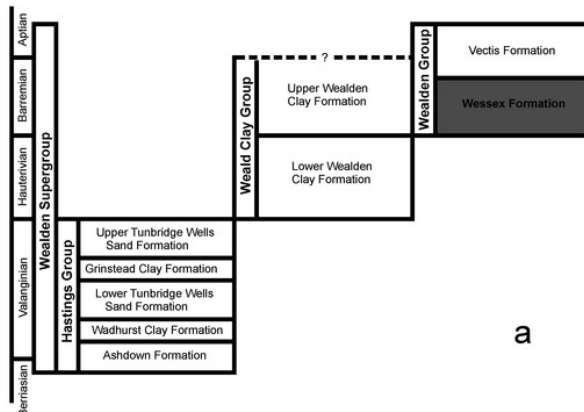
The *Eotyrannus lengi* holotype was discovered at Grange Chine. From Martill and Naish (2001).



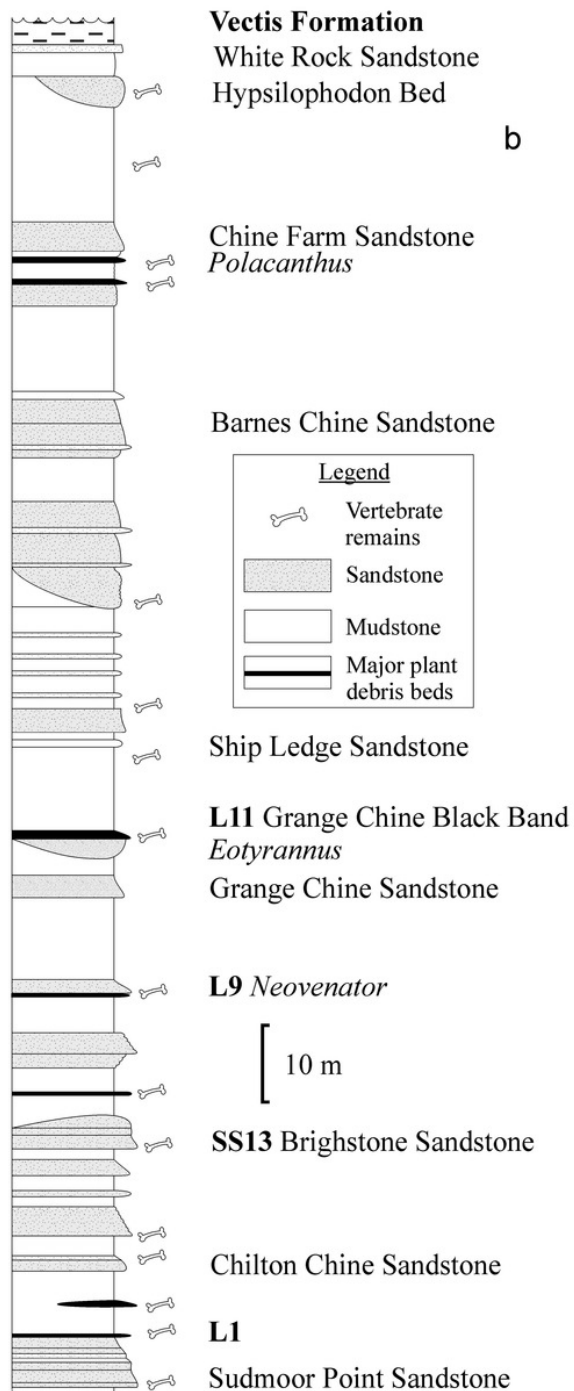
# Figure 2

Fig. 2 Stratigraphic position of the bed that yielded *Eotyrannus lengi*.

**a** schematic relationship of the Wessex Formation to other Wealden Supergroup strata; **b** column showing Wessex Formation exposure between Sudmoor Point and Cowleaze Chine, depicting beds from which *E. lengi* and some other Wessex Formation dinosaurs were recovered. Modified from Sweetman (2004).



a



b

# Figure 3

Fig. 3 Incomplete right premaxilla and partial maxilla of *E. lengi*.

**a** right premaxilla in lateral view; **b** medial view; **c** ventral view; **d** anterior view; **e** dorsal view; **f** anterior portion of left maxilla in lateral view; **g** oblique dorsomedial view; **h** medial view; **i** ventral view; **j** reconstructions of the maxilla as it may have appeared when complete, showing preserved opening representing promaxillary foramen and with maxillary foramen present but not preserved; **k** alternative reconstruction, showing preserved opening representing either maxillary foramen or combined promaxillary-maxillary foramen. *alv* alveoli, *bnpr* base of basal process, *dp* dorsal process, *intpl* interdental plates, *mn* margin of external naris, *maf* margin of antorbital fossa, *nefo* neurovascular foramina, *ps* palatal shelf. Scale bars 30 mm.

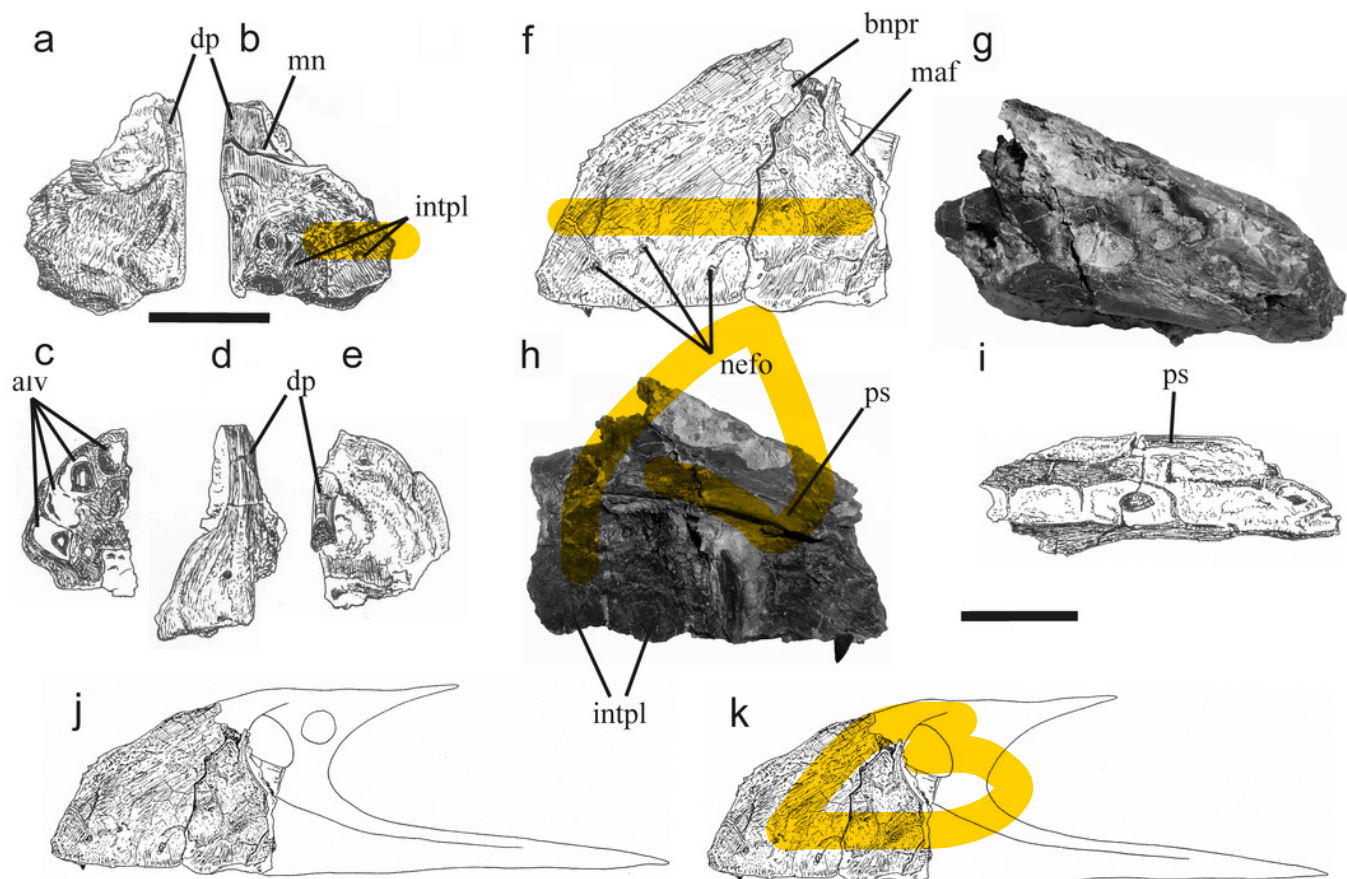


# Figure 4

Fig. 4 Fused nasals of *E. lengi*.

**a** left lateral view; **b** right lateral view; **c** dorsal view; **d** ventral view. *extn* external nostril, *lacproc* lacrimal process, *latdr* laterodorsal ridge, *latrec* lateral recess, *mlri* midline ridge, *mpp* medial premaxillary process, *ndpp* notch for dorsal process of premaxilla, *nefo* neurovascular foramina, *vpp* ventral premaxillary process. *Scale bar* 30 mm.

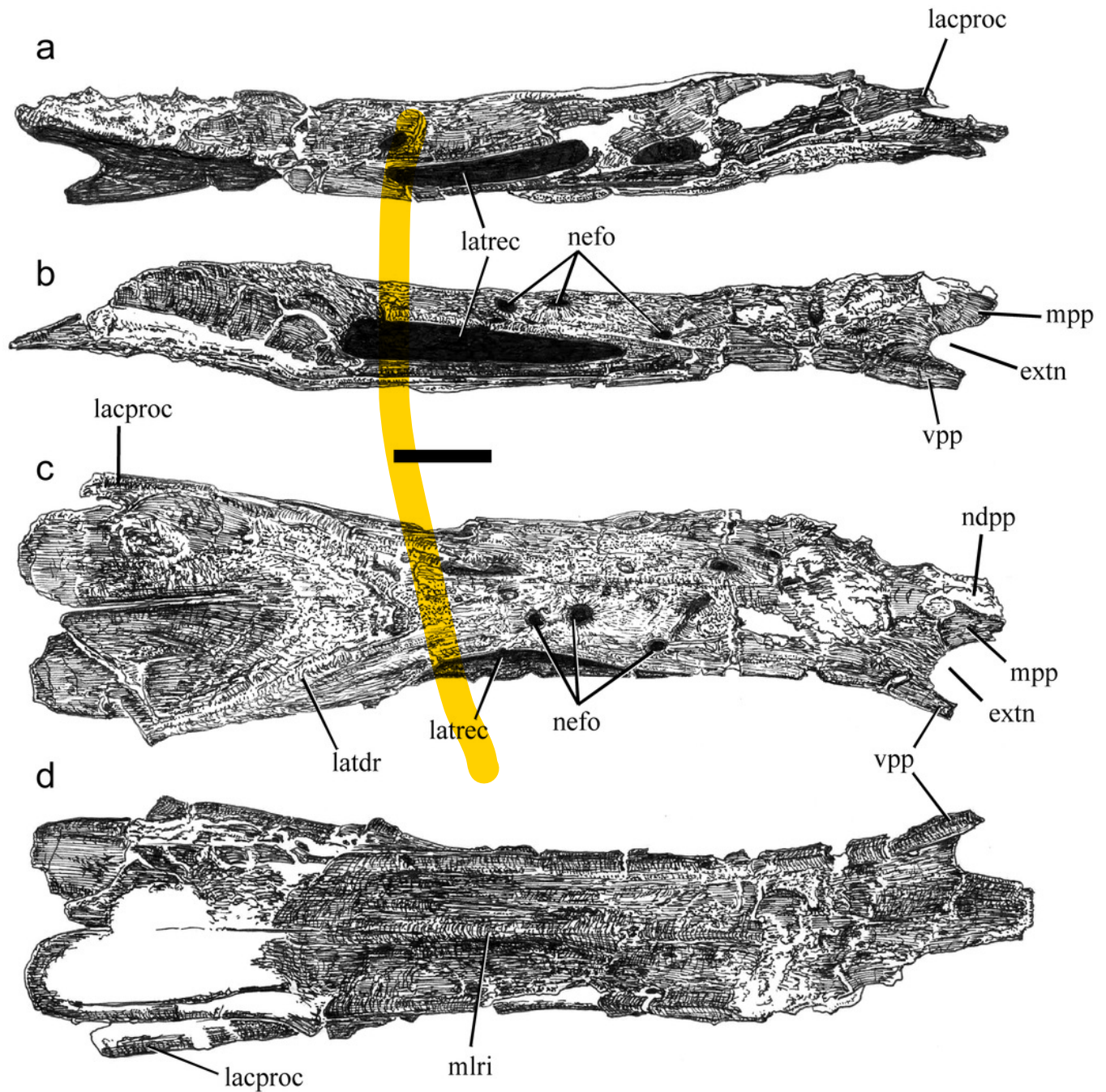




# Figure 5

Fig. 5 Detailed views of specific sections of *E. lengi* fused nasals.

**a** lateral recess and adjacent area on lateral surface of right nasal; **b** anterior end of right nasal in dorsal view, showing region around external naris; **c** posterior part of fused nasals in dorsal view, anterior to left. *lacproc* lacrimal process, *latrec* lateral recess, *mpp* medial premaxillary process, *ndpp* notch for dorsal process of premaxilla, *nefo* neurovascular foramina, *vpp* ventral premaxillary process. Scale bars 30 mm in a and c, 20 mm in b.

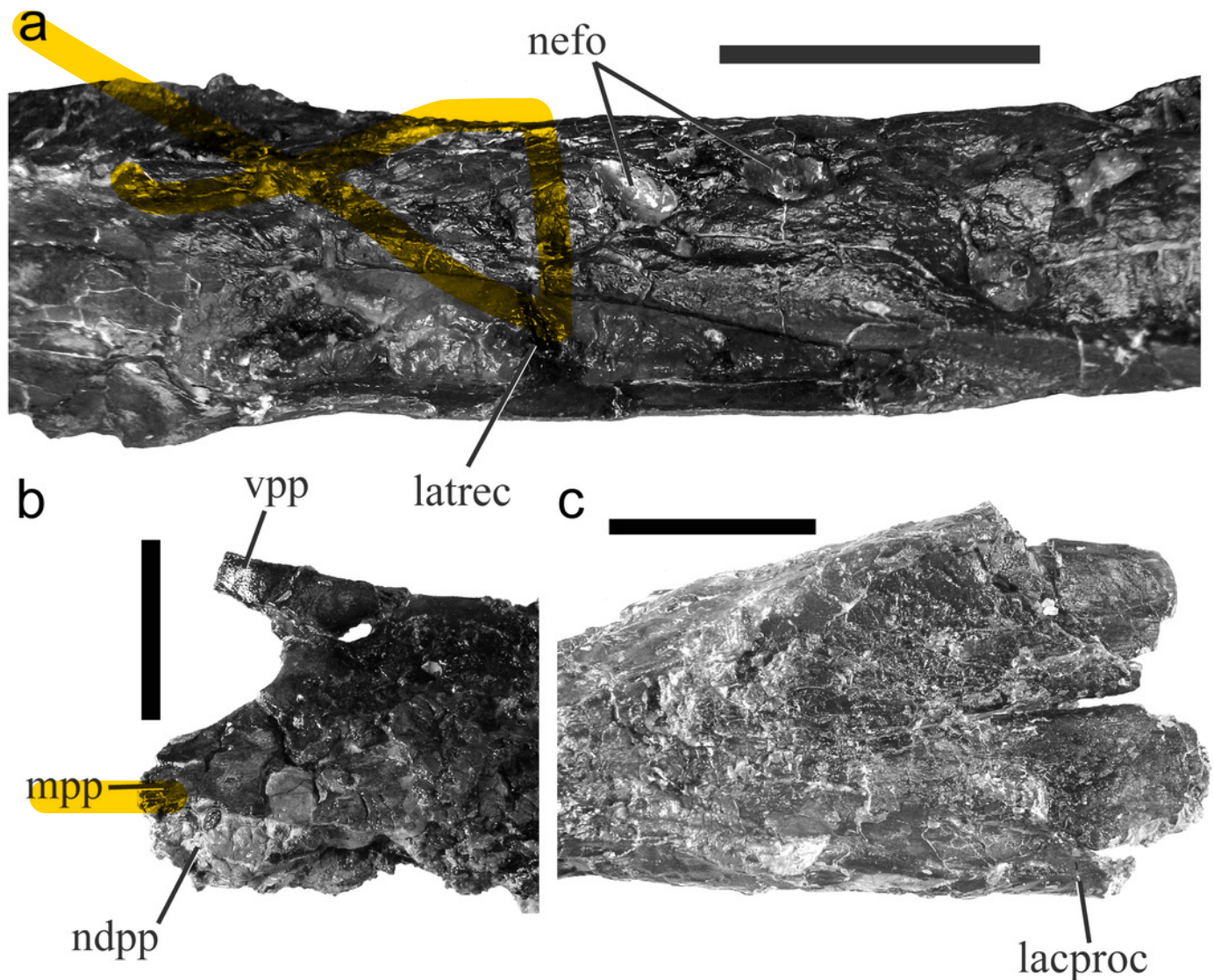


# Figure 6

Fig. 6 Right lacrimal (and possible prefrontal) and partial jugal of *E. lengi*.

**a** dorsal view; **b** lacrimal and partial jugal in lateral view; **c** lacrimal in medial view; **d** oblique posteromedial view; **e** lacrimal shaft in anterior view. *df* dorsoventral furrow, *latf* lateral flange, *medr* medial ridges, *pospr* possible prefrontal, *vgm* ventral groove for posteroventral part of maxilla. Scale bars 30 mm.

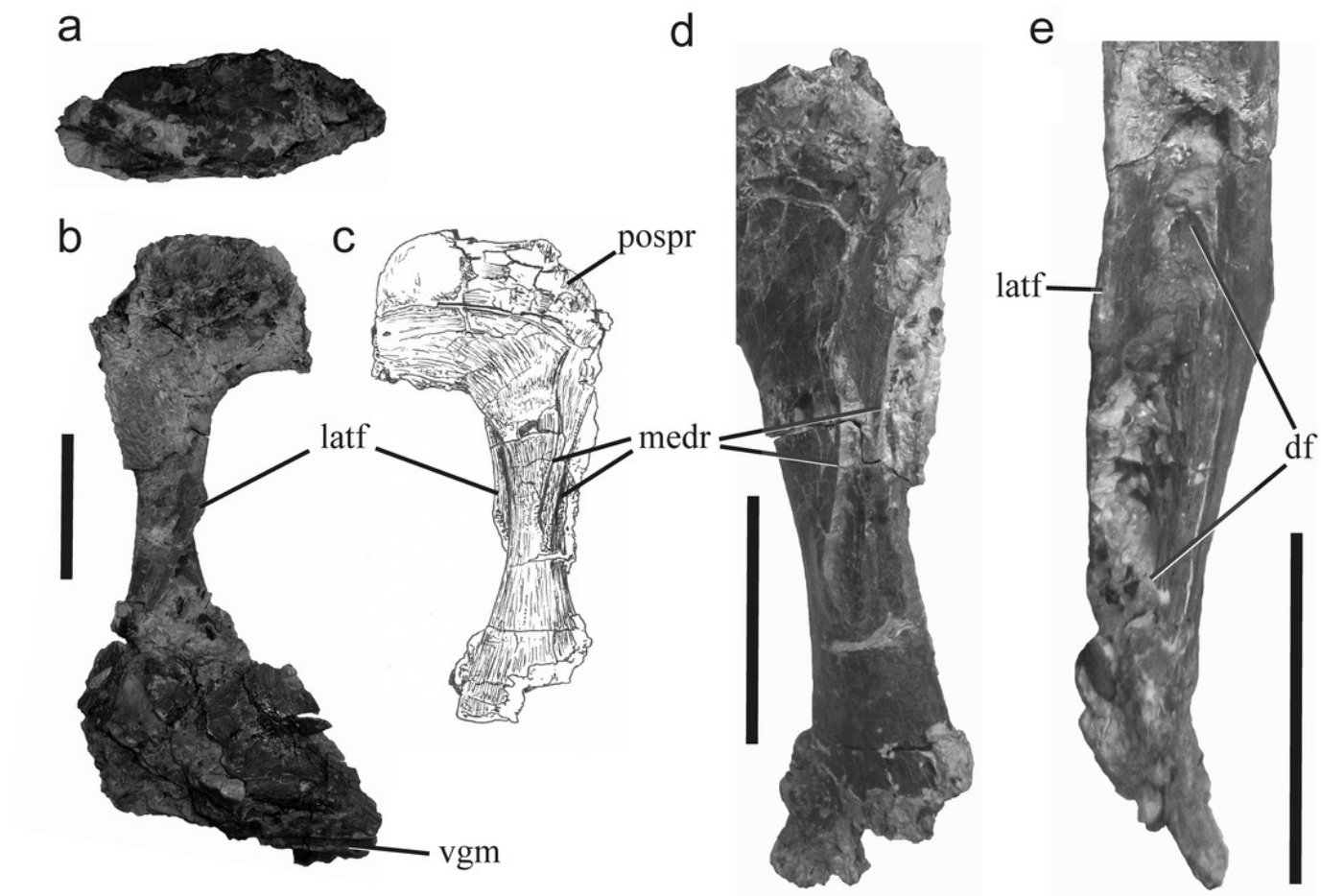


# Figure 7

Fig. 7 Right palatine of *E. lengi*.

**a** as preserved on block of matrix. If interpreted correctly, anterior is at left and palatal midline at bottom of image. **b** interpretative diagram. *bin* border of internal naris, *juar* jugal articulation, *jproc* jugal process, *maxa* maxillary articulation, *ppr* palatine pneumatic recess, *vproc* vomeropterygoid process. *Scale bar* 30 mm.

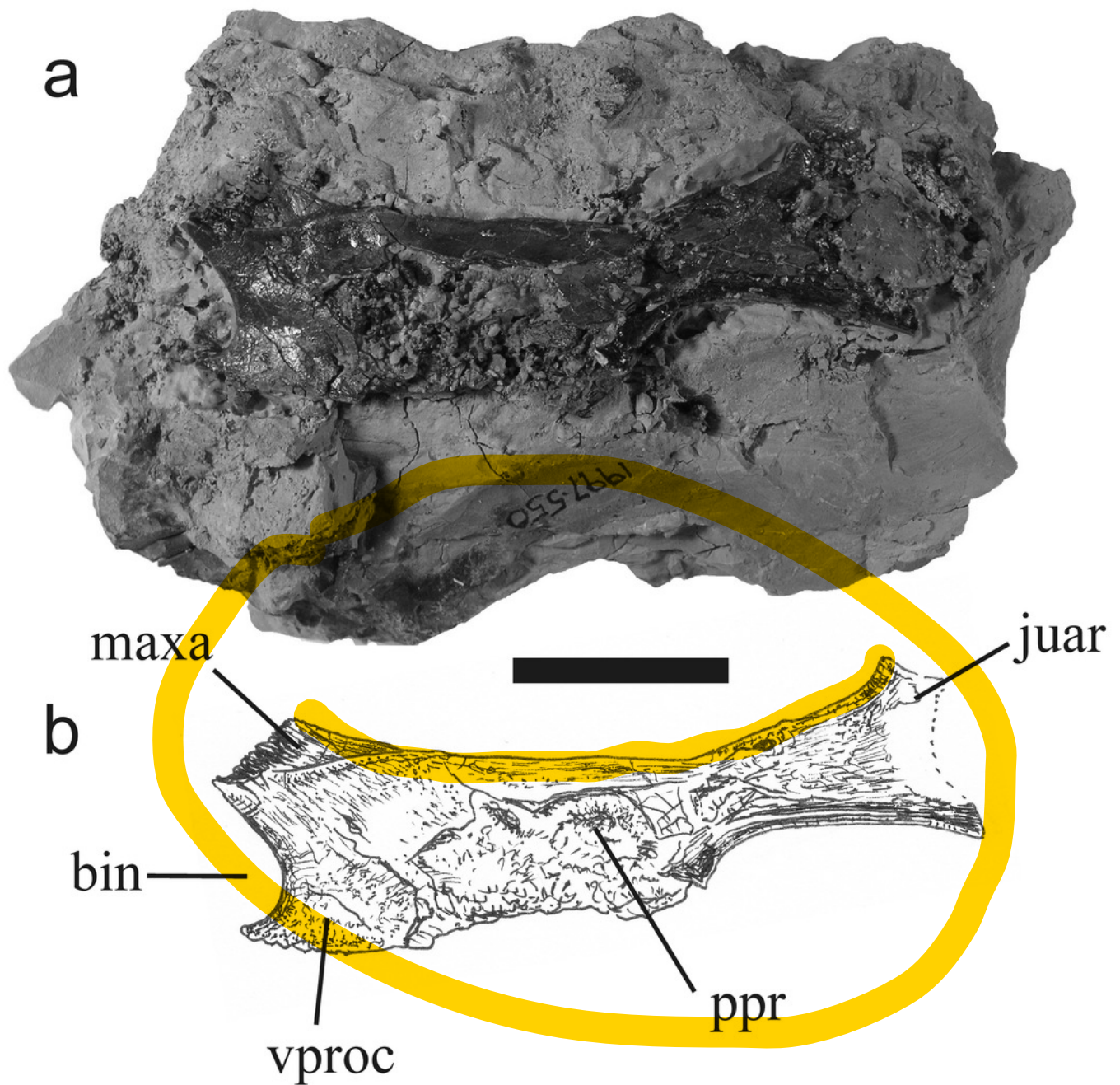


# Figure 8

Fig. 8 Incomplete right quadrate of *E. lengi*.

**a** posterior view; **b** anterior view; **c** medial view; **d** ventral view. *Latc* lateral condyle, *medc* medial condyle, *ptpr* pterygoid process, *qfor* quadrate foramen, *qfos* quadrate fossa, *qjfl* quadratojugal flange. Scale bar 30 mm.

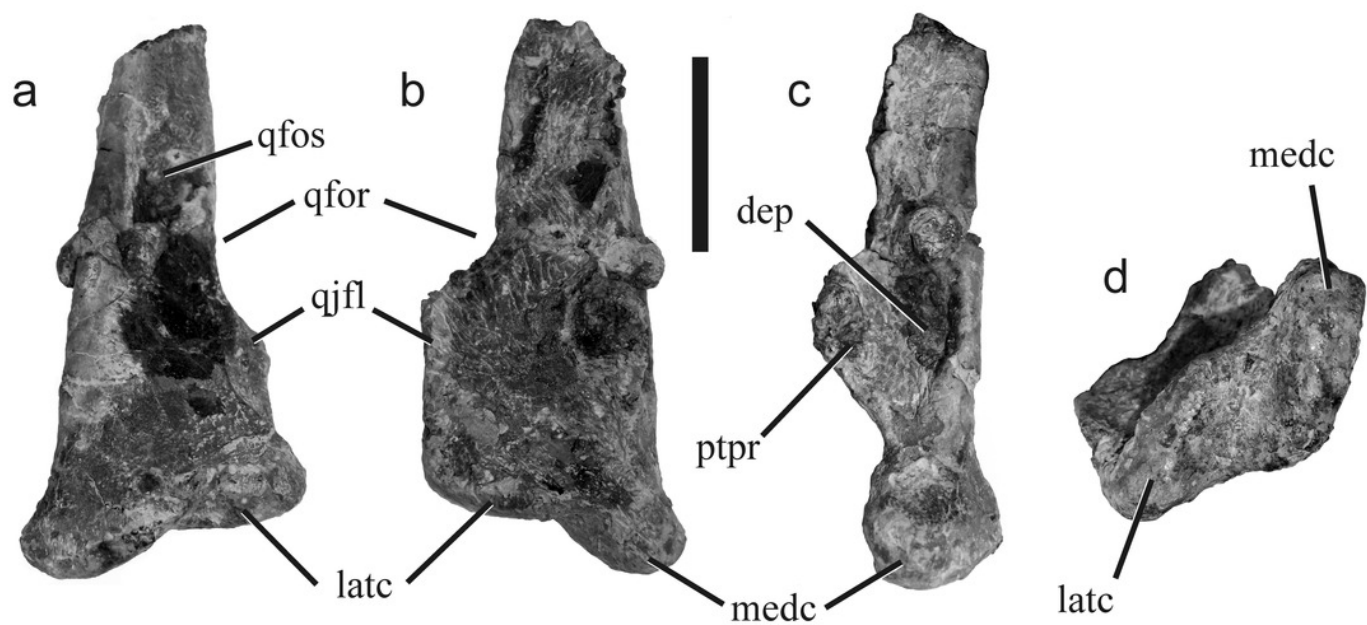




# Figure 9

Fig. 9 Incomplete left and right dentaries of *E. lengi*.

**a** left dentary in lateral view; **b** left dentary in medial view; **c** left dentary in dorsal view; **d** oblique dorsolateral view of anterior end of left dentary; **e** right dentary in lateral view; **f** right dentary in medial view; **g** right dentary in dorsal view; **h** right dentary in ventral view. *intpl* interdental plates, *latf* lateral furrows, *nefo* neurovascular foramina, *rosno* rostral notch. Scale bar 30 mm.

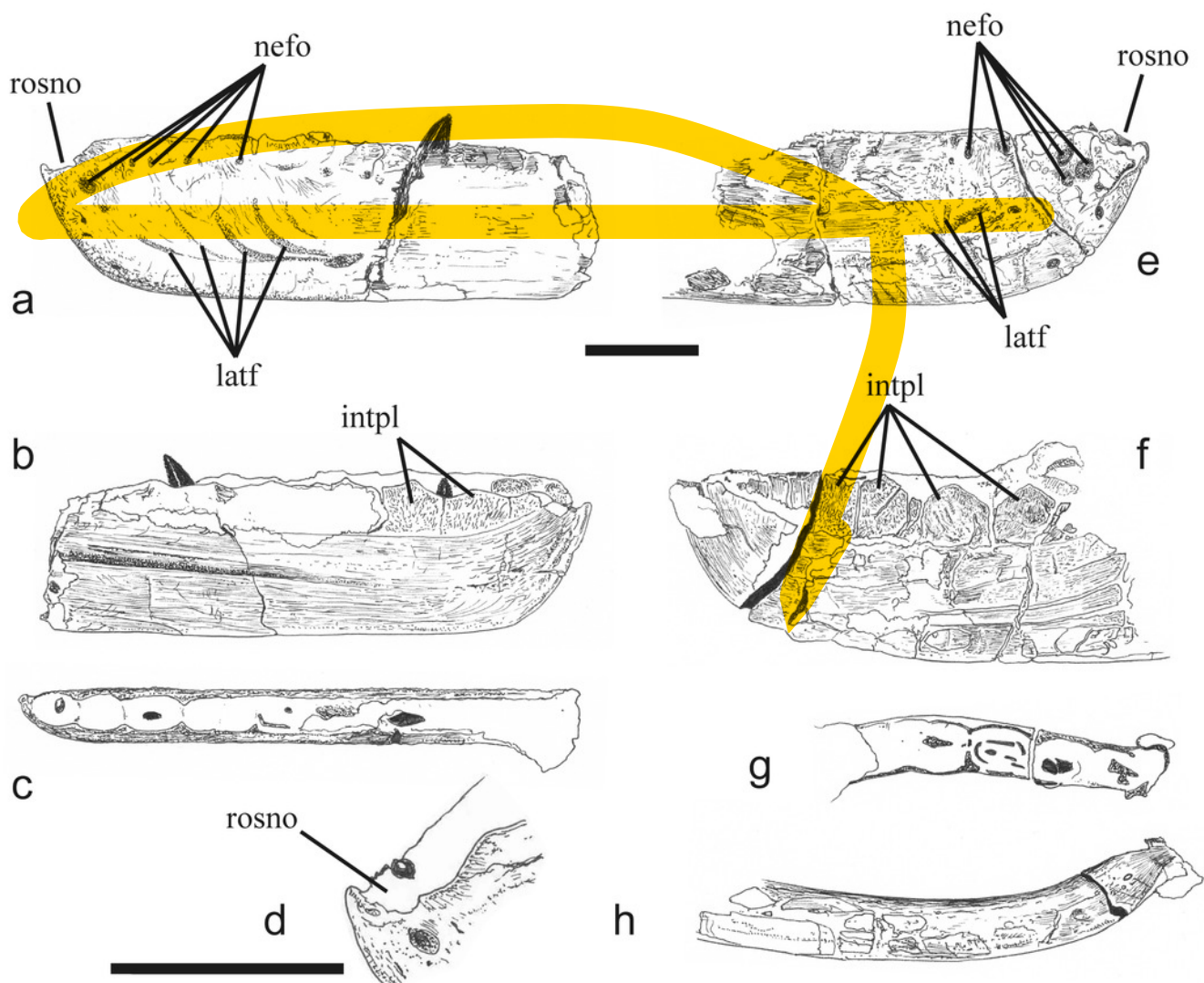




# Figure 10

Fig. 10 Anterior and posterior sections of the surangular of *E. lengi*.

**a** anterior section of left surangular in dorsal view (anterior to right); **b** lateral view; **c** medial view; **d** posterior section of right surangular in medial view; **e** lateral view; **f** dorsal view. *acp* anterior cotylar prominence, *adch* anterodorsal channel, *doch* dorsal channel, *maco* mandibular cotyle, *pcp* posterior cotylar prominence, *retpr* retroarticular process, *smp* subtriangular medial process, *sush* surangular shelf, *trr* transverse ridge. Scale bars 30 mm.

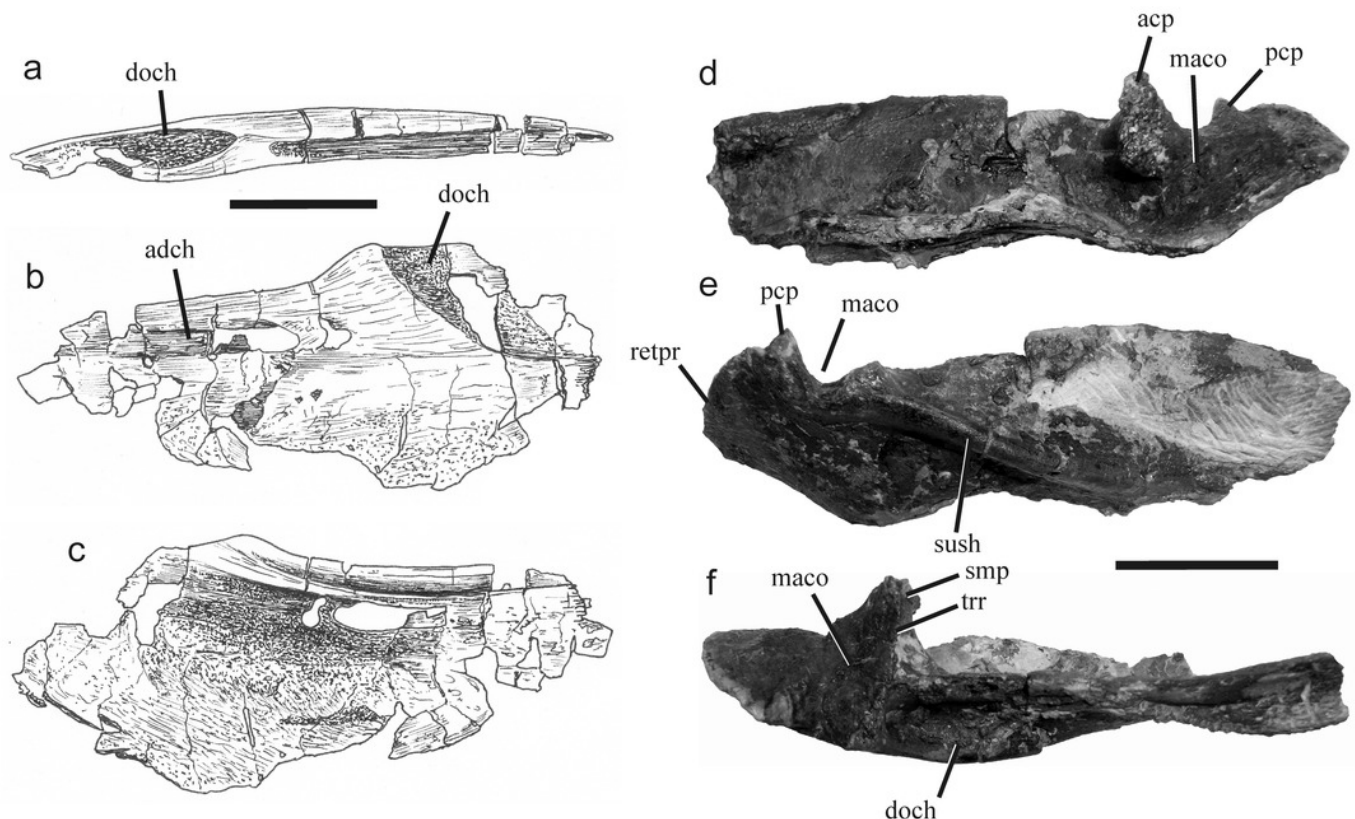


# Figure 11

Fig. 11 Premaxillary and lateral teeth of *E. lengi*.

**a** premaxillary tooth in lingual view; **b** oblique lingual or labial view; **c** tip of premaxillary tooth in lingual view; **d** tip of lateral tooth; **e** distal carina of lateral tooth. *Scale bars* 10 mm in a-b, 1 mm in c and e, 2 mm in d.

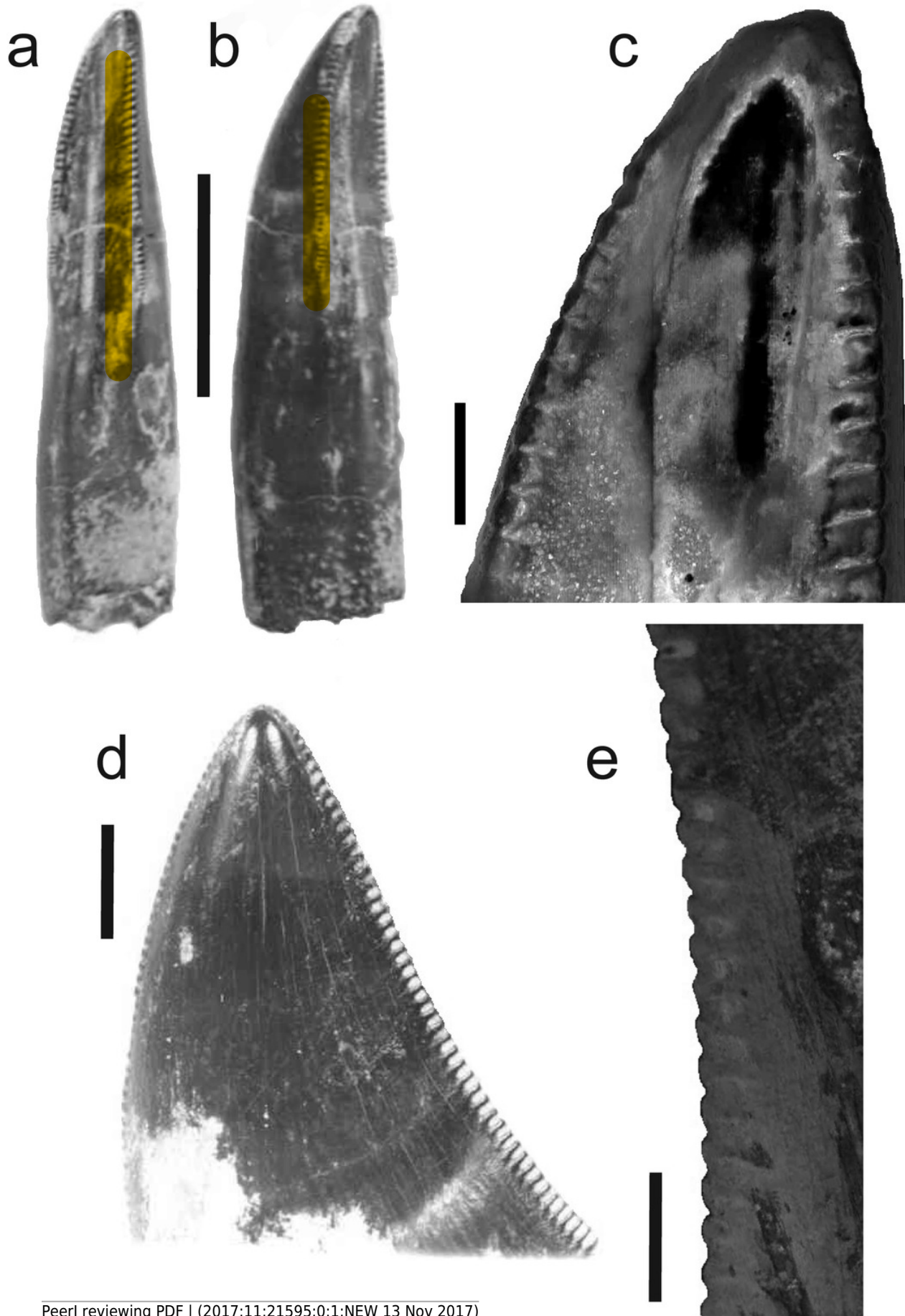


# Figure 12

Fig. 12 Cervical vertebrae of *E. lengi*.

**a** axial neural arch in anterior view; **b** dorsal view; **c** left lateral view; **d** right lateral view; **e** post-axial cervical neural arch in left lateral view; **f** dorsal view; **g** posterior view; **h** possible axial centrum in anterior view; **i** ventral view; **j** left lateral view; **k** right lateral view; **l** isolated cervical centrum in left lateral view. *aas* anterior articular surface, *cri* cervical rib shaft, *epi* epipophysis, *ligfo* ligament fossa, *ncs* neurocentral suture, *ns* neural spine, *par* parapophysis, *pnfo* pneumatic foramen, *poz* postzygapophysis, *prez* prezygapophysis, *prezf* prezygapophyseal facet. Scale bars 30 mm.

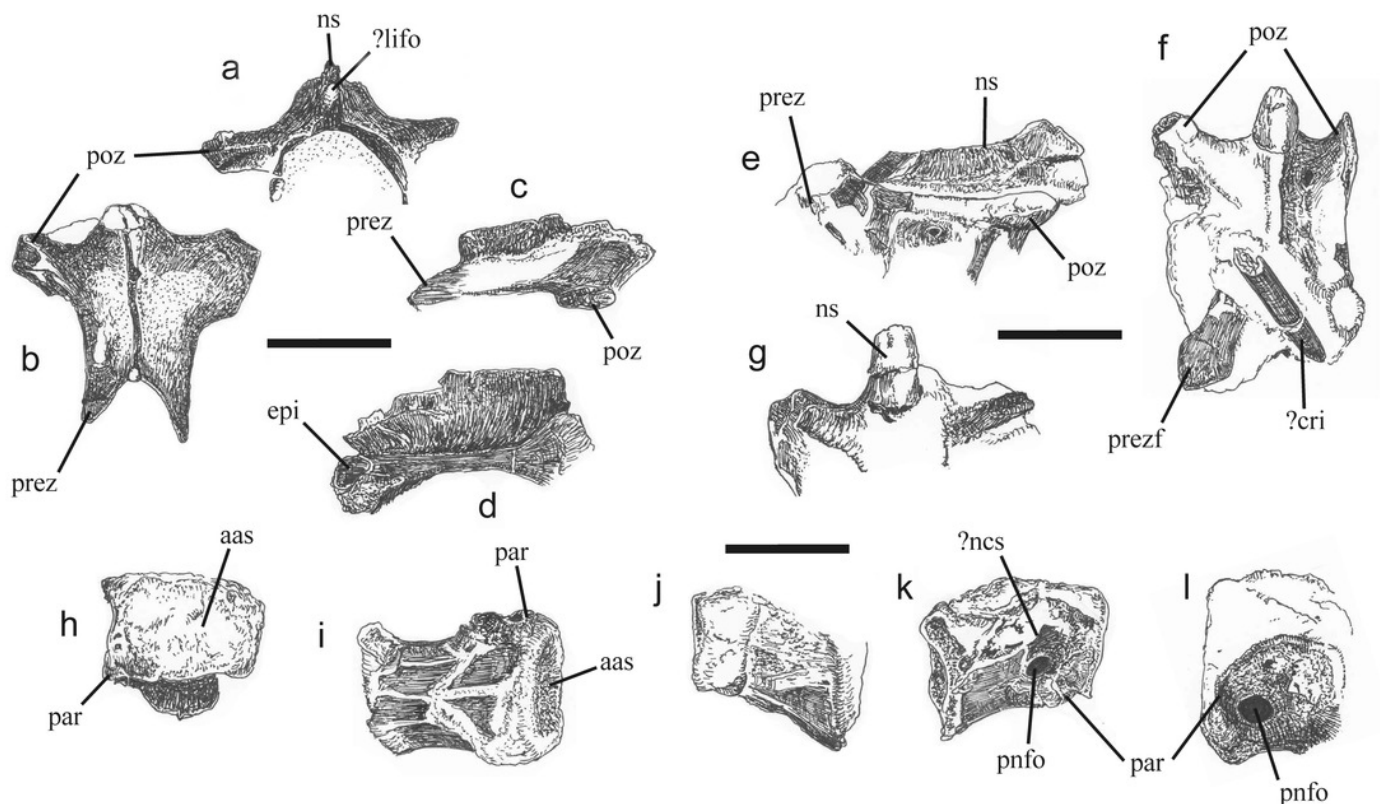


# Figure 13

Fig. 13 Dorsal and sacral vertebrae of *E. lengi*.

**a** dorsal vertebra in anterior view; **b** left lateral view; **c** ventral view; **d** posterior view; **e** right lateral view; **f** dorsal view; **g** additional dorsal vertebra in left lateral view; **h** ventral view; **i** anterior view; **j** right lateral view; **k** dorsal view; **l** posterior view; **m** posterior dorsal vertebrae in presumed anterior view; **n** presumed left lateral view; **o** ventral view; **p** presumed posterior view; **q** presumed right lateral view; **r** dorsal view; **s** sacral vertebra in left lateral view; **t** ventral view; **u** anterior view; **v** right lateral view; **w** dorsal view; **x** posterior view. *latfo* lateral fossa, *lsp* lateral subcircular pit, *nc* neural canal, *odg* oblique dorsal groove, *rag* radiating groove, *rar* radiating ridge. Scale bars 30 mm.

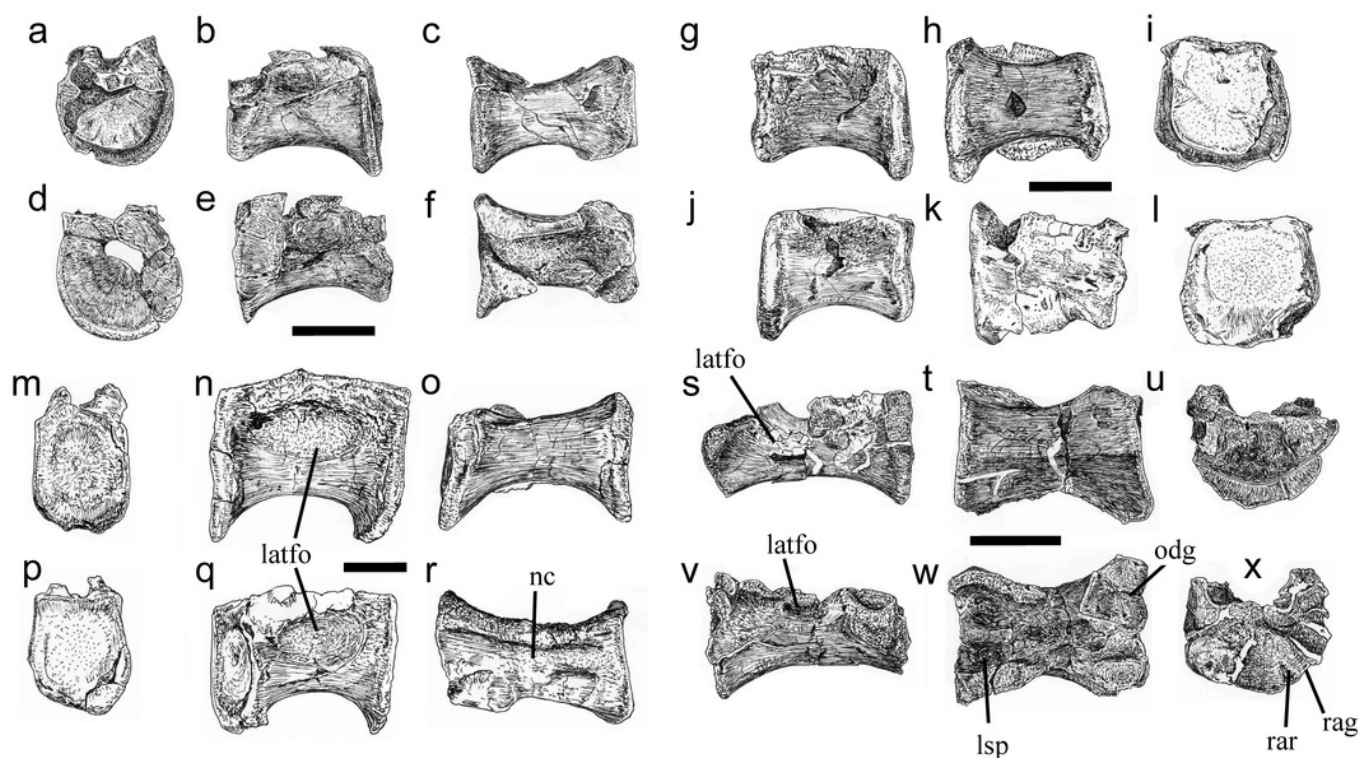


# Figure 14

Fig. 14 The more informative of the several rib fragments known for *E. lengi*.

**a** dorsal rib segment with cross-sections depicted; **b** dorsal rib segment showing pneumatic recess; **c** partial rib shaft with flange-like lateral extension. *cap* capitulum, *cog* costal groove, *intr* intercostal ridge, *pnre* pneumatic recess, *tub* tuberculum. Scale bar 30 mm.

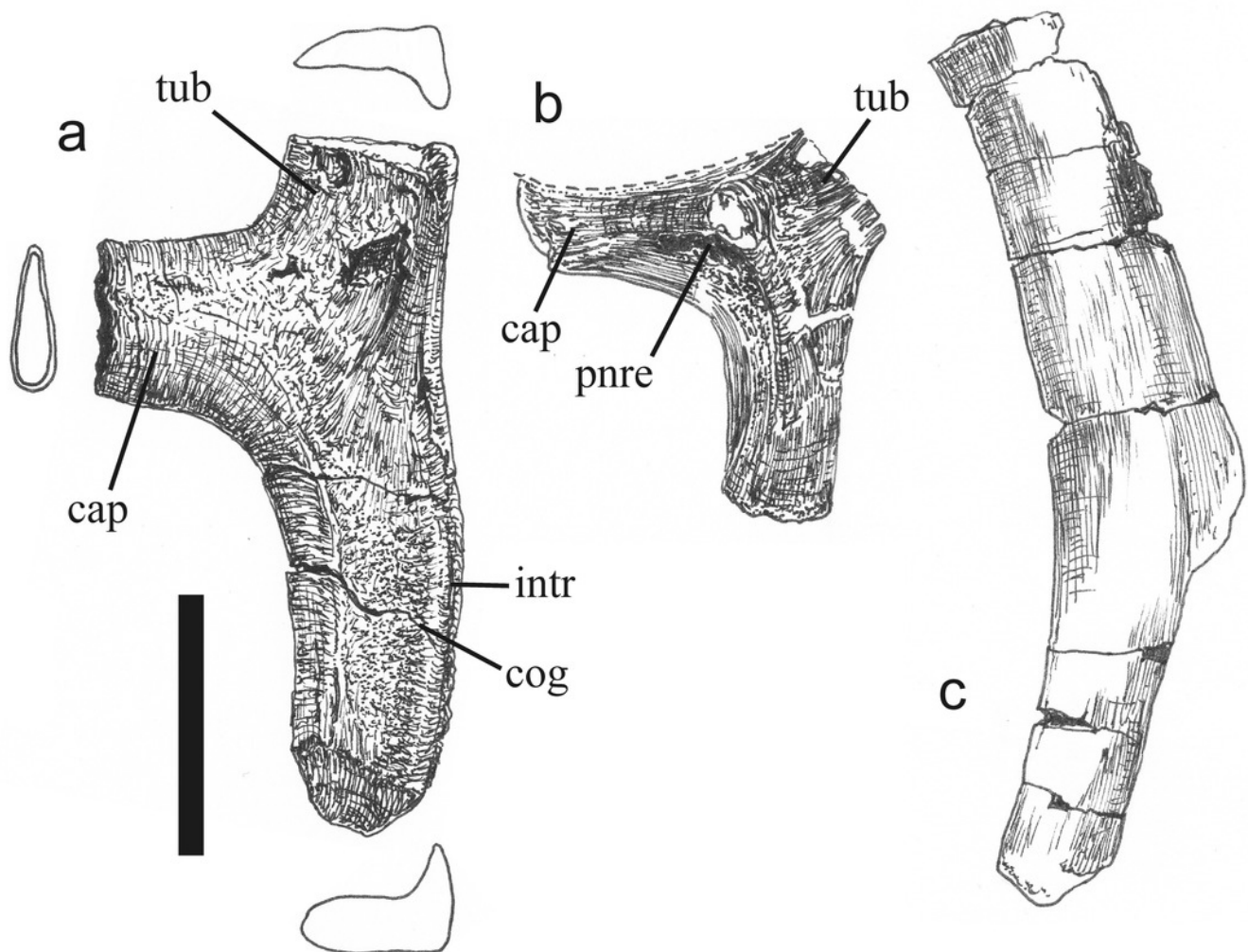




# Figure 15

Fig. 15 Scapulocoracoid of *E. lengi*.

**a** left coracoid in anterior view; **b** lateral view; **c** posterior view; **d** medial view; **e** left scapula in lateral view; **f** incomplete shaft and dorsal end of right scapula in lateral view. *acrp* acromion process, *cortu* coracoid tubercle, *doc* dorsal concavity, *epm* embayed posterior margin, *glef* glenoid fossa, *mec* medial concavity, *pvp* posteroventral process. Scale bars 30 mm.

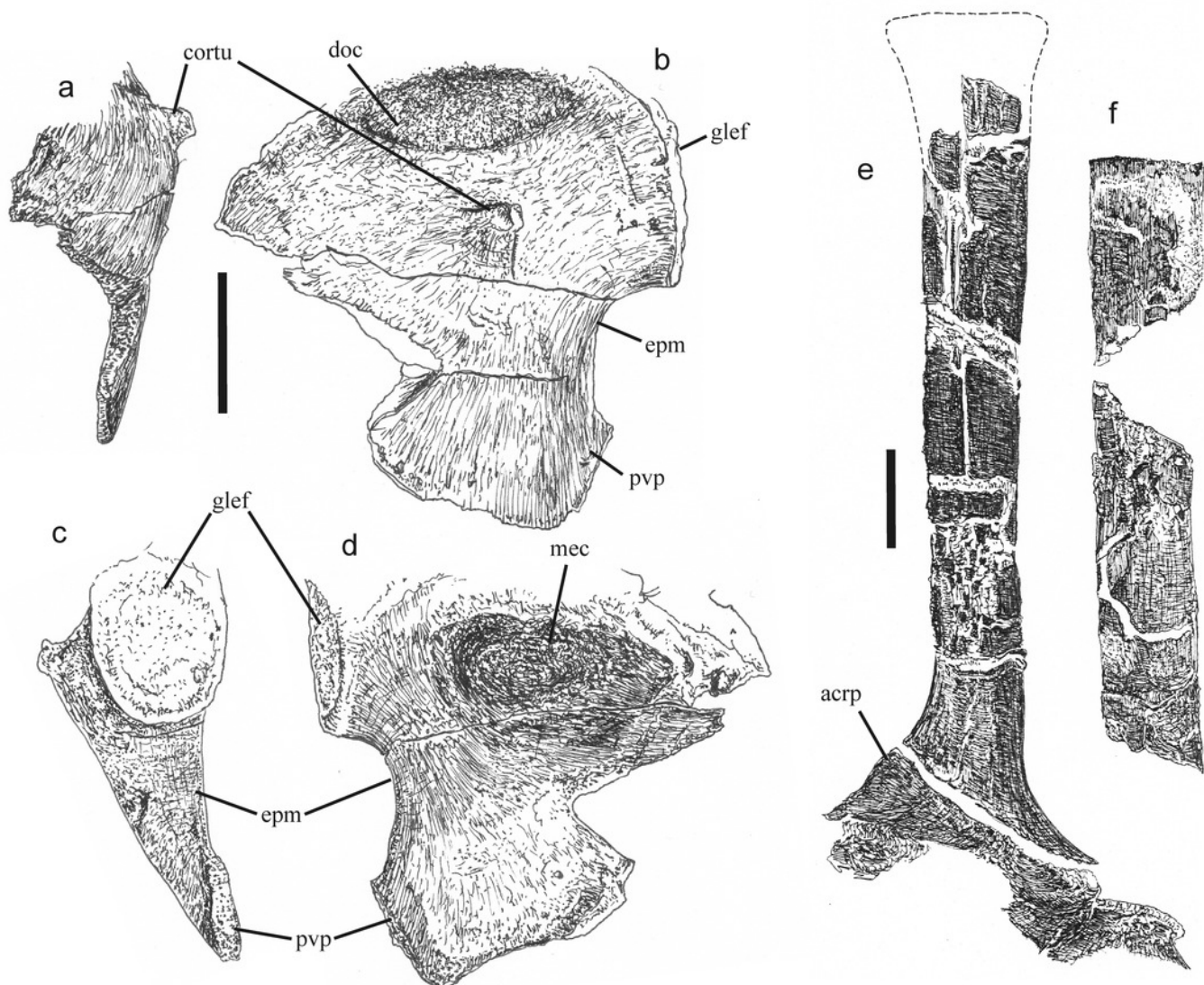


# Figure 16

Fig. 16 Right humerus of *E. lengi*.

**a** posterior view; **b** anterior view; **c** lateral view; proximal view; **d** distal view; **e** medial view; **f** distal view. *dpc* deltopectoral crest, *ent* entepicondyle, *grt* greater tubercle, *hh* humeral head, *lco* lateral condyle, *mco* medial condyle. Scale bar 30 mm.

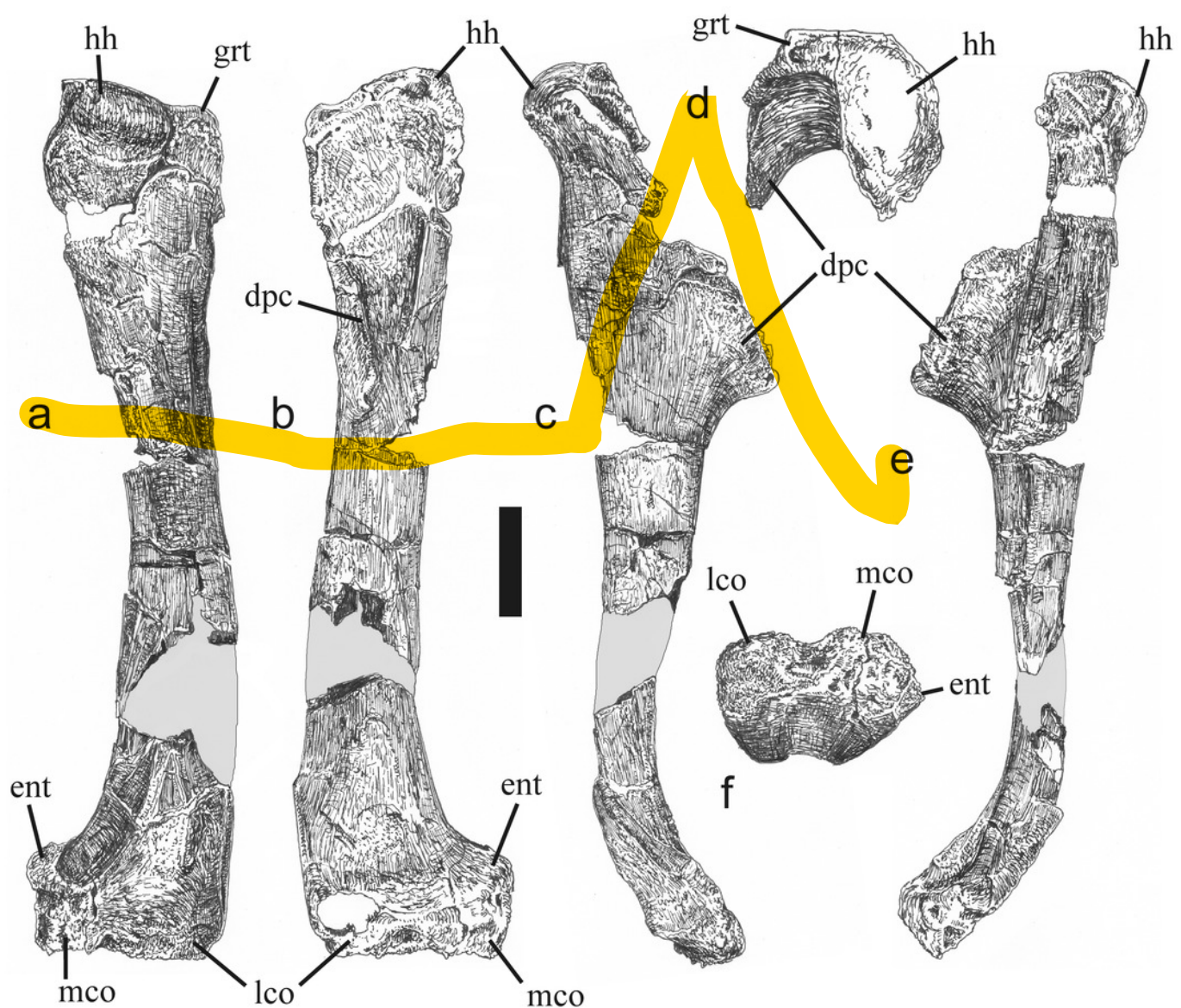


# Figure 17

Fig. 17 Partial left ulna and ?left radius of *E. lengi*.

**a** ?left radius in dorsal view; **b** in medial or lateral view; **c** proximal cross-section; **d** left ulna in medial view; **e** proximal cross-section; **f** distal cross section; **g** reconstructed forelimb anatomy of *E. lengi* showing inferred positions of known elements. *subco* subtriangular concavity, *vk* ventral keel. *Scale bar* 30 mm.

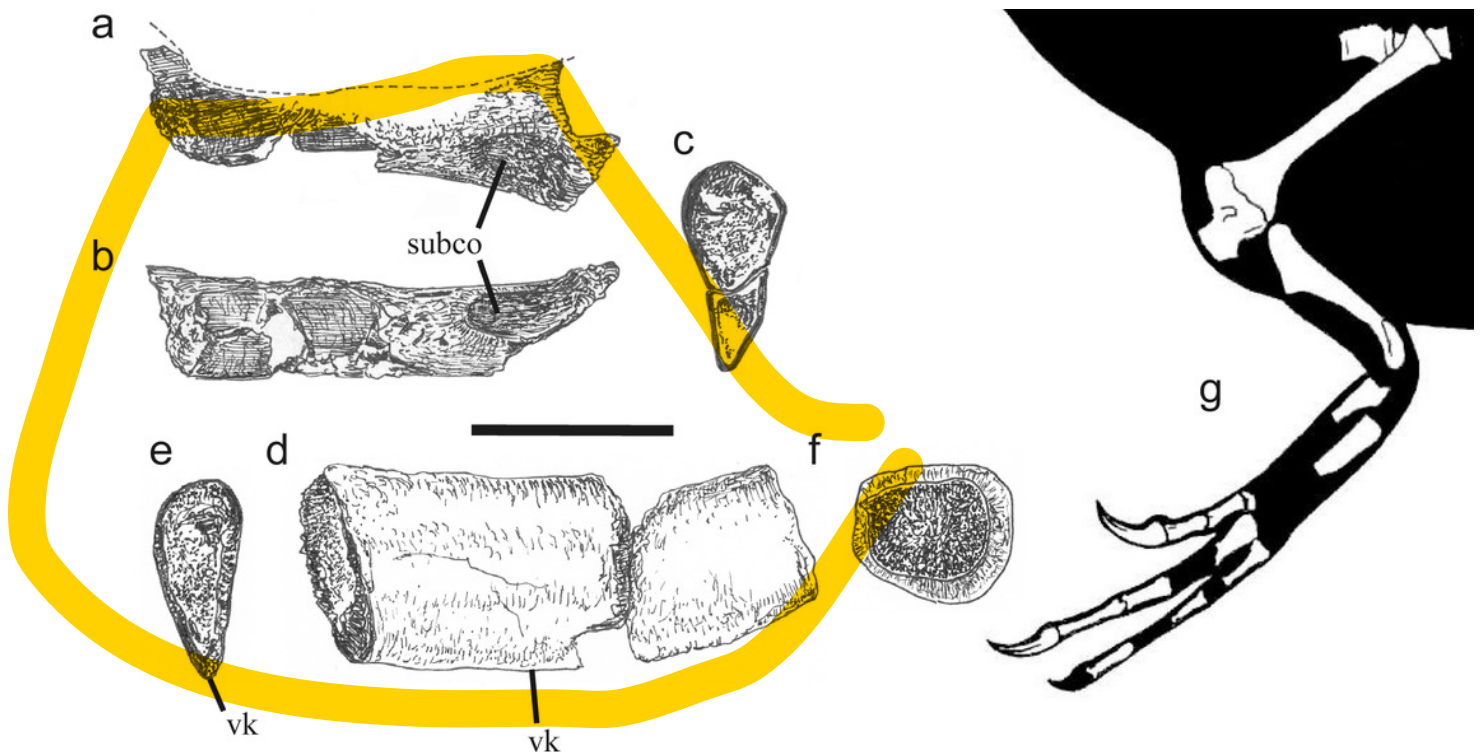


# Figure 18

Fig. 18 Distal carpal I and left metacarpal I of *E. lengi*.

**a** distal carpal 1 in proximal view; **b** distal view; **c** lateral view; **d** medial view; **e** dorsal view; **f** ventral view; **g** left metacarpal I in dorsal view; **h** ventral view; **i** distal view; **j** proximal view; **k** lateral view; **l** medial view. *artr* Articular surface for radiale; *clf* concave lateral facet (for distal carpal II?), *cmf* concave medial facet, *fmc* facet for metacarpal II, *lco* lateral condyle, *mco* medial condyle, *mes* medial surface. Scale bars 20 mm in a-f, 30 mm in g-l.

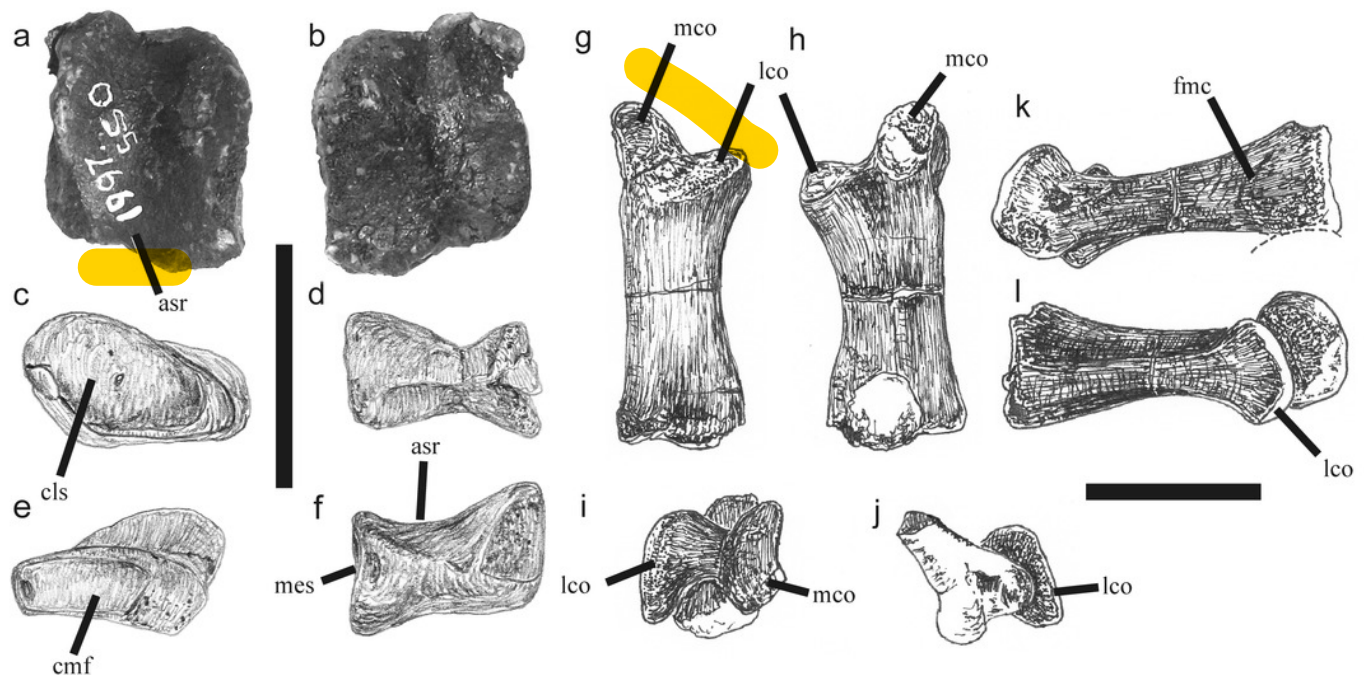


# Figure 19

Fig. 19 Manual phalanges of *E. lengi*.

**a** possible left manual phalanx I-1 in medial view; **b** dorsal view; **c** distal view; **d** lateral view; **e** dorsal view; **f** proximal view; **g** possible right phalanx II-1 in lateral view; **h** dorsal view; **i** distal view; **j** medial view; **k** dorsal view; **l** proximal view; **m** possible right manual phalanx II-2 in medial view; **n** proximal view; **o** lateral view; **p** possible manual phalanx III-1 in lateral or medial view; **q** dorsal view; **r** lateral or medial view; **s** ventral view; **t** proximal view; **u** possible left manual phalanx III-3 in medial view; **v** dorsal view; **w** distal view; **x** lateral view; **y** ventral view; **z** proximal view; **a'** possible pollex ungual in lateral or medial view; **b'** in ventral view; **c'** possible digit II ungual in lateral or medial view; **d'** in ventral view; **e'** metacarpals and phalanges arranged to show probable positions within the manus. Several phalanges are unknown (III-2, III-4). *clgr* claw groove, *dcon* dorsoproximal concavity, *dli* dorsal lip, *dol* dorsal lamina, *flt* flexor tubercle, *pdr* proximal dividing ridge. Scale bars 20 mm in a-d', 60 mm in e'.



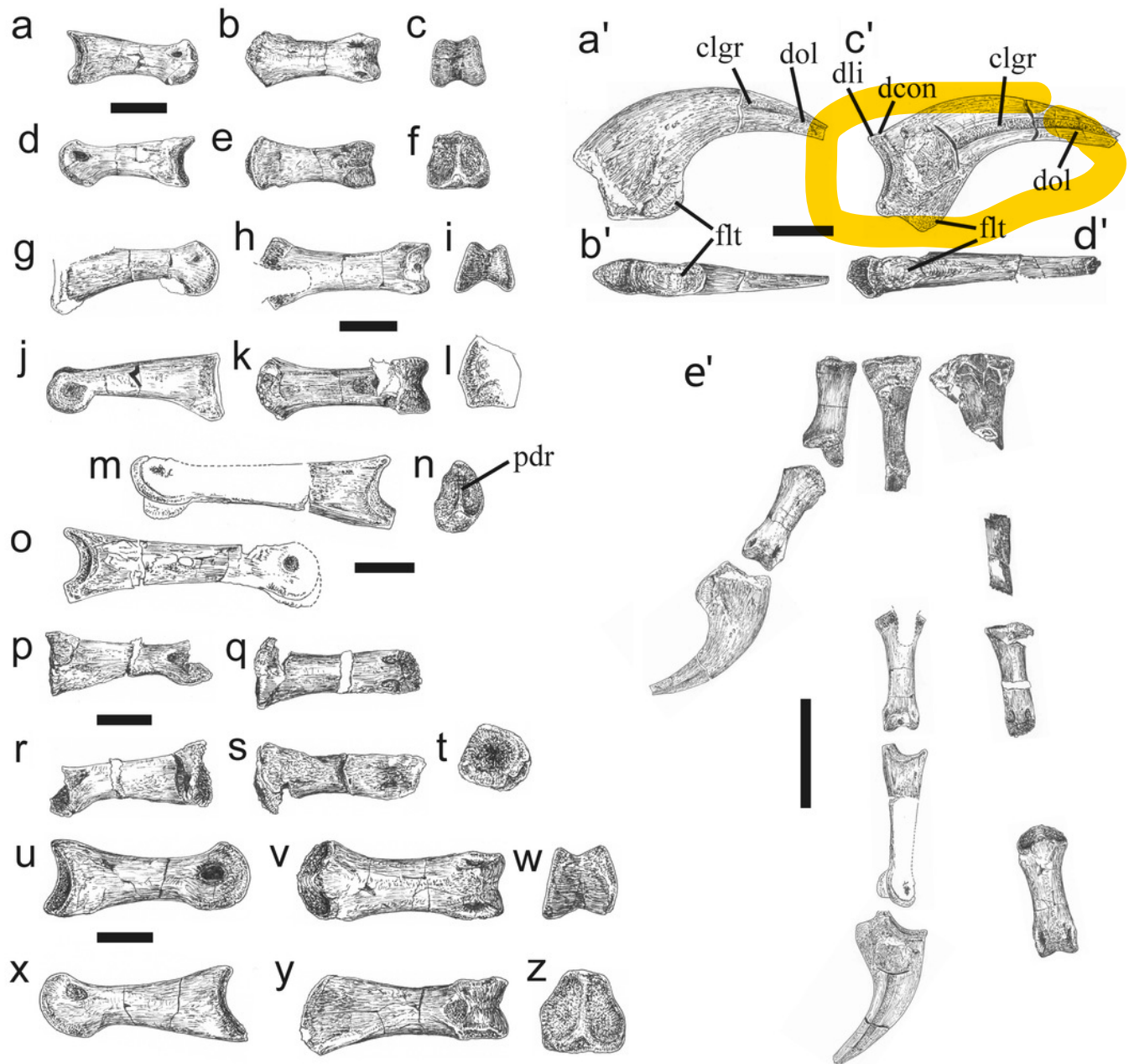




# Figure 20

Fig. 20 Segment of *E. lengi* left ilium representing the region dorsal and posterodorsal to the acetabulum.

**a** lateral view; **b** ventral view; **c** lateral view with median ridge outlined for clarity. *dm* dorsal margin, *frd* flat region dorsal to median ridge, *mr* median ridge. Scale bars 30 mm.

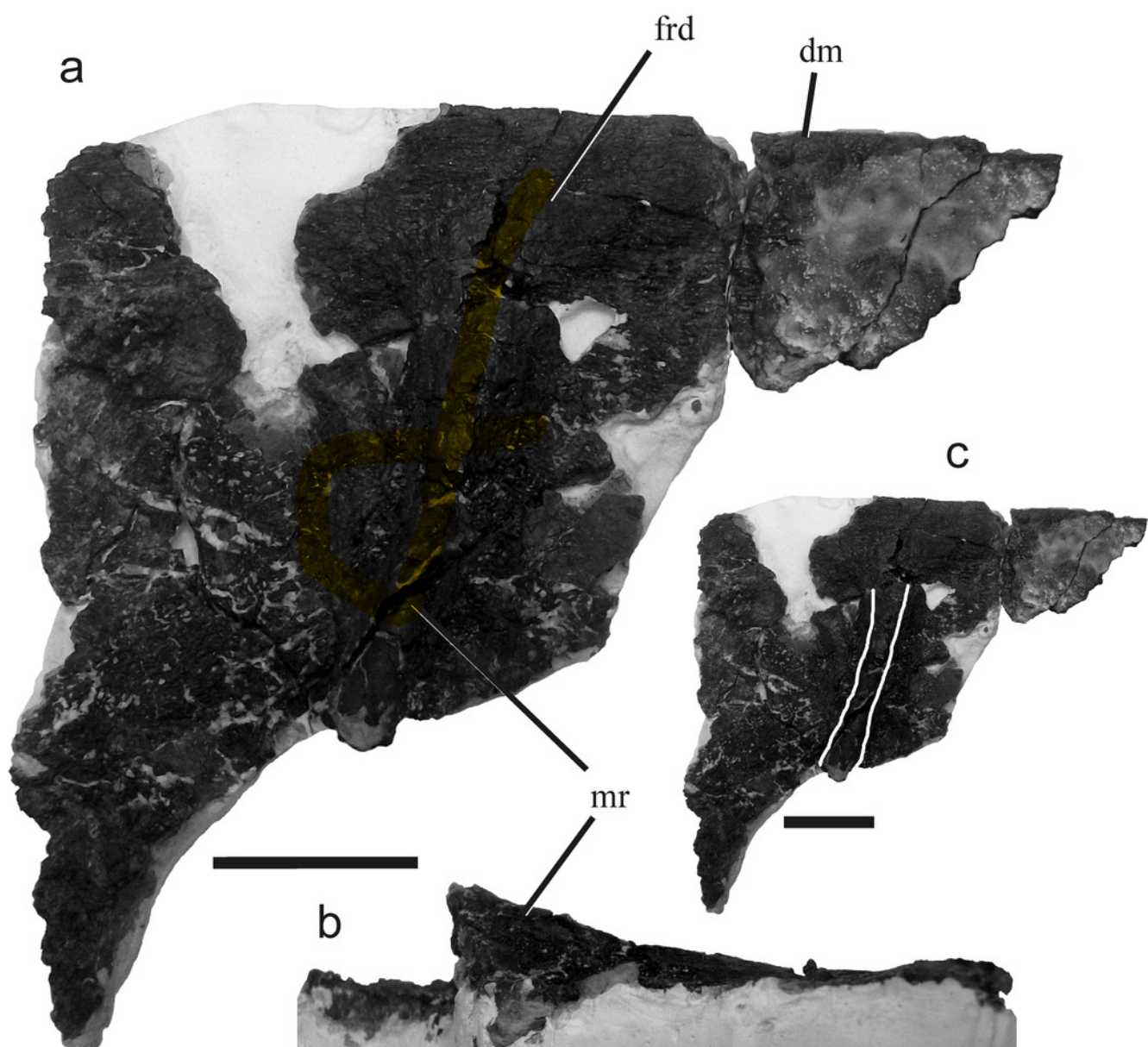


# Figure 21

Fig. 21 Incomplete left fibula and tibia of *E. lengi*.

**a** left tibia in posterior view; **b** lateral view; **c** proximal view; **d** anterior view of proximal end; **e** shaft of fibula in cross-section. *cncr* cnemial crest, *fcr* fibular crest, *fi* fibula, *tfor* tibial foramen, *lco* lateral condyle, *mco* medial condyle. *Scale bars* 30 mm.

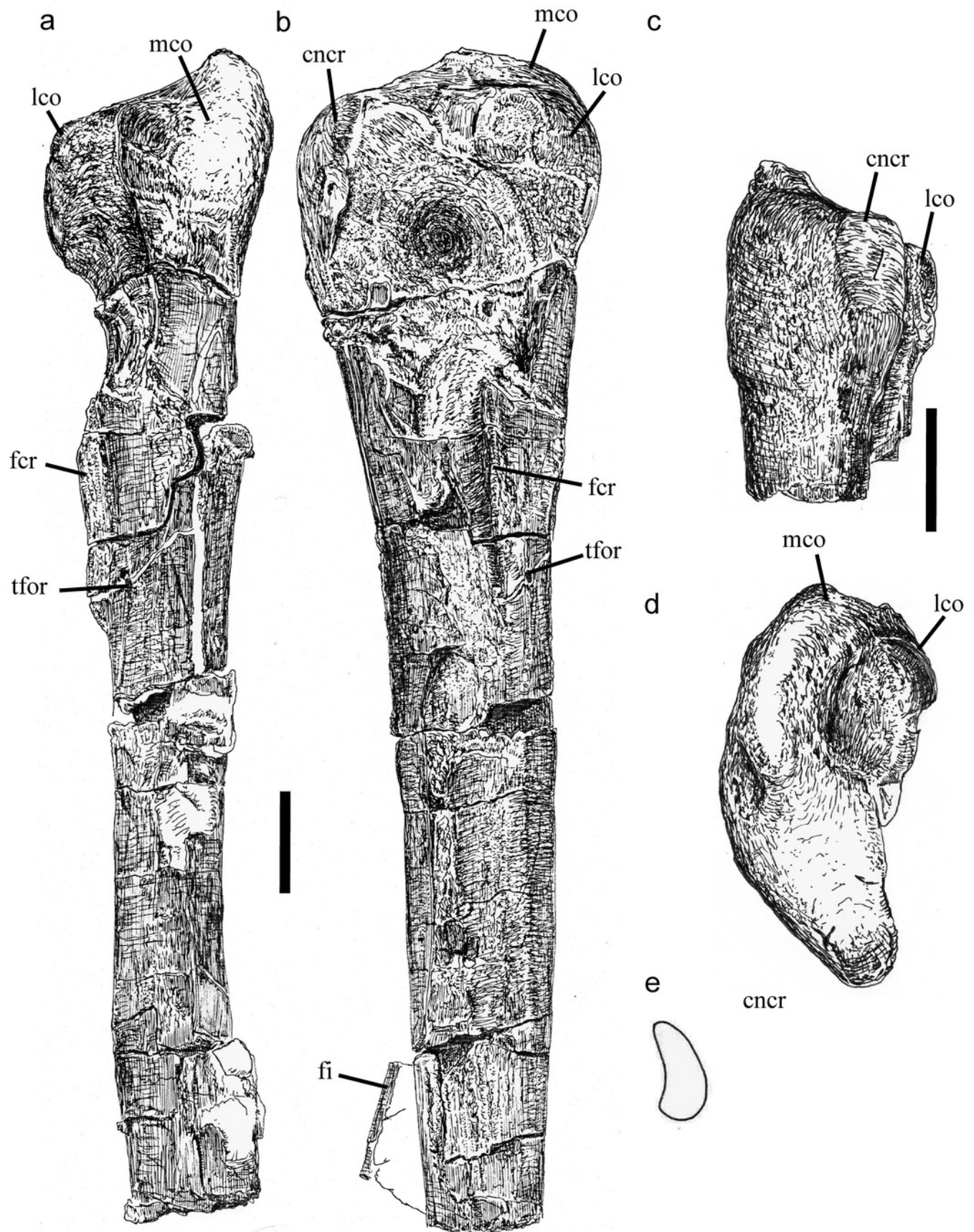


# Figure 22

Fig 22 Left tibia of *E. lengi*.

**a** distal end of left tibia in anterior view; **b** posterior view; **c** oblique anterodistal view; **d** complete tibia with all segments placed in their approximate original positions. *fma* flat medial area; *lach* lateral channel; *lash* lateral shoulder; *mm* medial malleolus. Scale bars 30 mm.

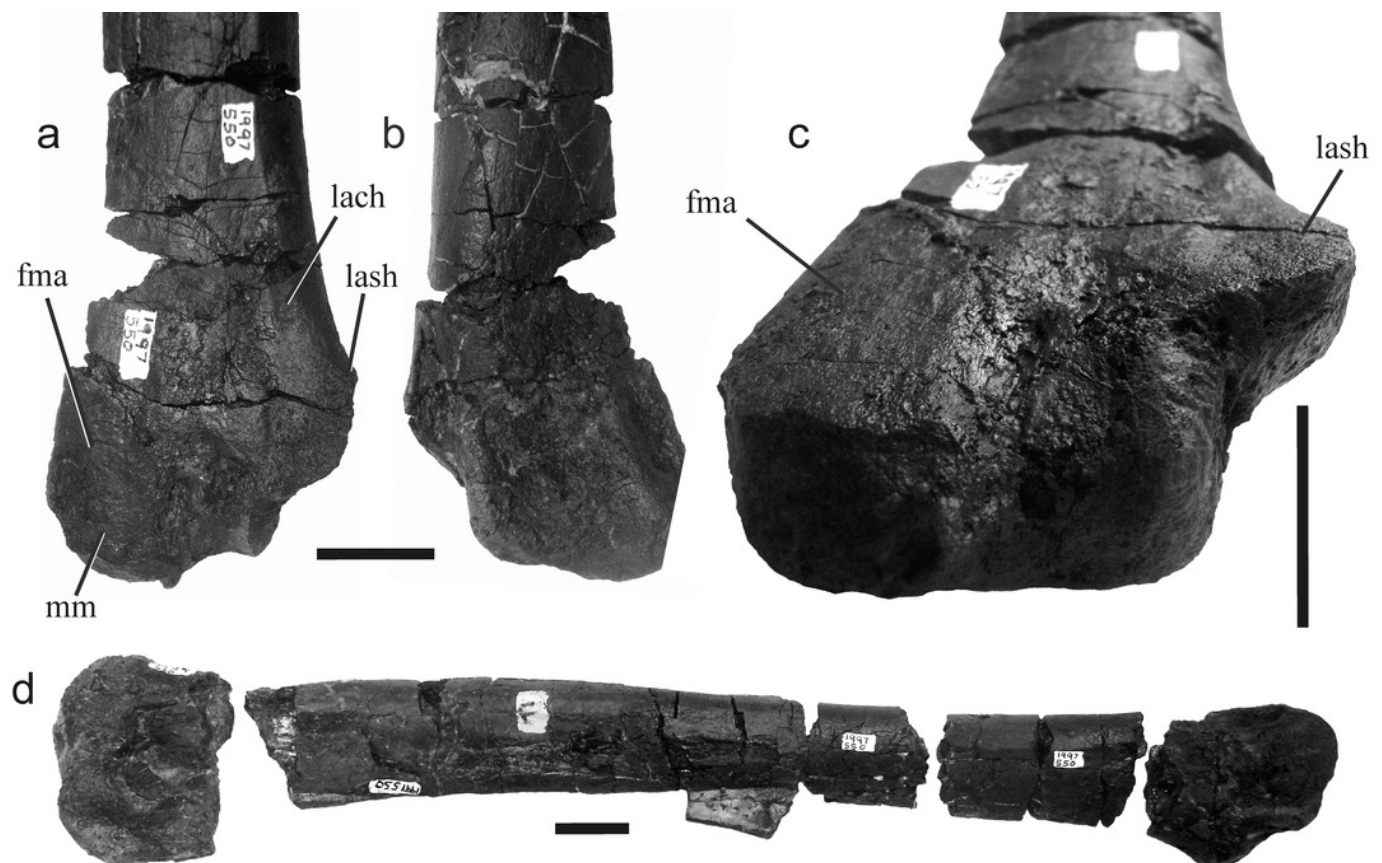


# Figure 23

Fig. 23 Metatarsals of *E. lengi*.

**a** right metatarsal II in anterior view; **b** lateral view; **c** posterior view; **d** medial view; **e** proximal view; **f** distal view; **g** distal end of left metatarsal III in posterior view; **h** lateral view; **i** anterior view; **j** medial view; **k** distal view; **l** left metatarsal IV in posterior view; **m** proximal end of left metatarsal IV in anterior view; **n** lateral view; **o** medial view; **p** proximal view. *antc* anterodistal concavity; *latc* lateral condyle, *medc* medial condyle, *mtfIII* facet for mt III. Scale bars 30 mm.

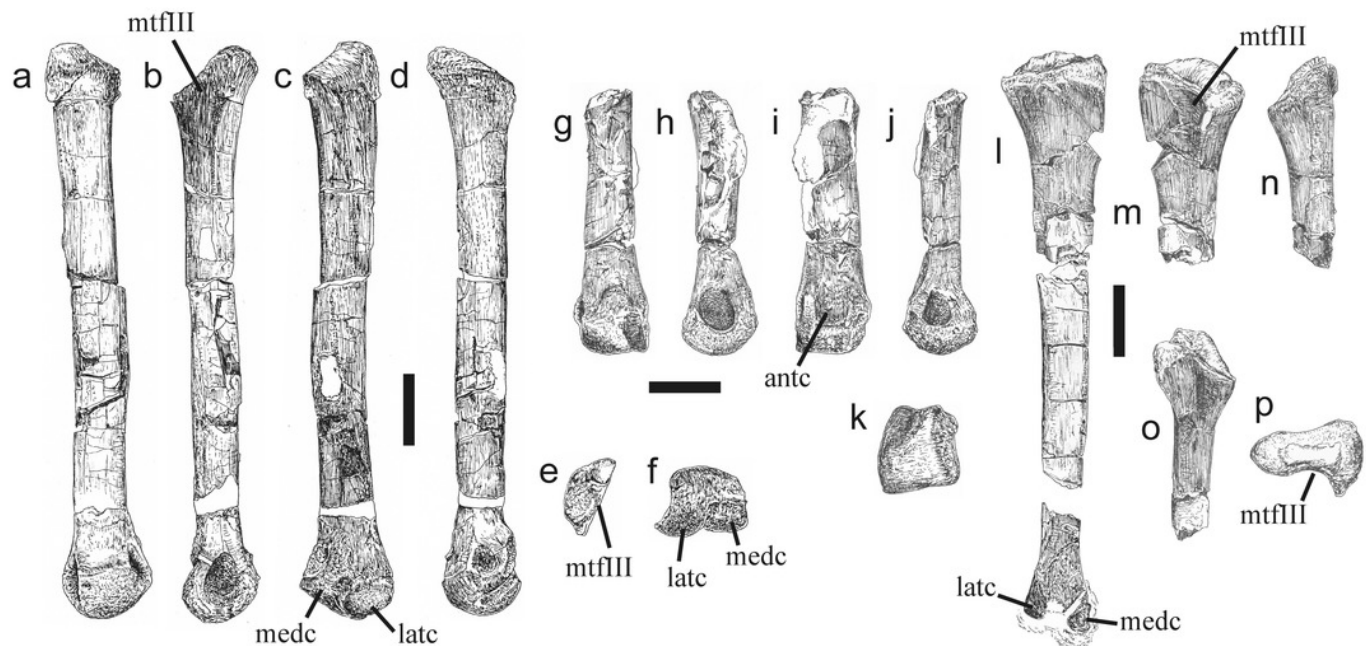


# Figure 24

Fig. 24 Pedal phalanges of *E. lengi*.

**a** probable III-1 in medial or lateral view; **b** dorsal view; **c** distal view; **d** medial or lateral view; **e** ventral view; **f** proximal view; **g** probable right II-1 in lateral view; **h** dorsal view; **i** ventral view; **j** distal view; **k** probable right IV-3 or IV-4 in lateral view; **l** dorsal view; **m** distal view; **n** medial view; **o** ventral view; **p** proximal view; **q** incomplete pedal ungual in lateral or medial view. *clgr* claw groove, *dorco* dorsal concavity, *prdp* proximodorsal process, *pdr* proximal dividing ridge. Scale bars 30 mm.

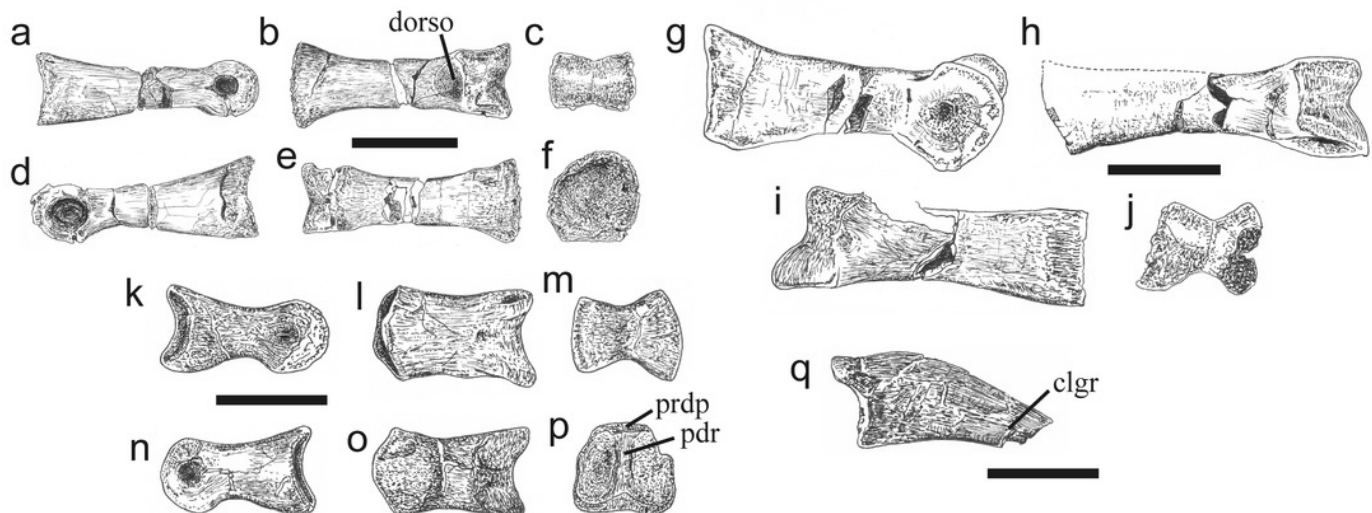




# Figure 25

Fig. 25 New skeletal reconstruction of *E. lengi*.

This reconstruction depicts only those elements preserved in the holotype. The exception is the palatine, which was not depicted because its appearance in lateral view could not be reconstructed. *Scale bar* 1 m.

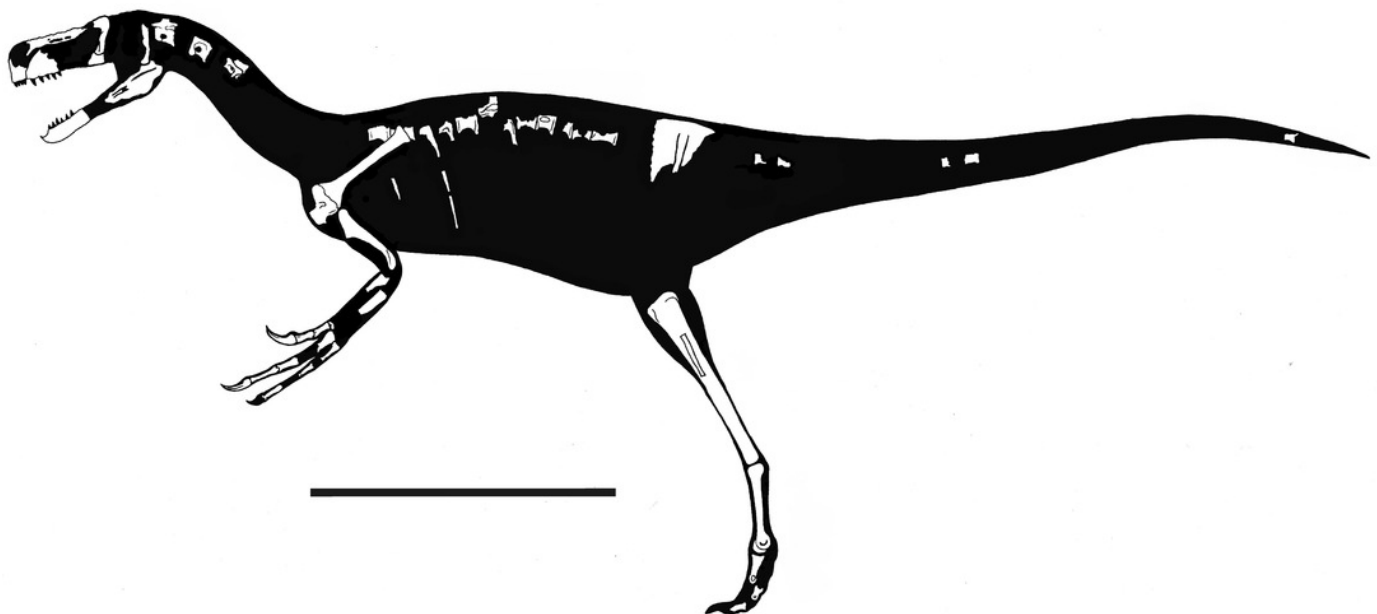


# Figure 26

Fig. 26 Montage showing selection of Lower Cretaceous theropod elements described from the Wessex Formation of the Isle of Wight.

**a** Holotype partial cervical vertebra of *Thecocoelurus daviesi* (NHMUK R181) in left lateral view; **b** right lateral view; **c** ventral view; **d** anterior view; **e** holotype sacrum of *Aristosuchus pusillus* (NHMUK R178) in left lateral view; **f** holotype pubes with pubic boot of *Aristosuchus pusillus* (NHMUK R178) in left lateral view; **g** pubic boot in ventral view; **h** one of the two holotype cervical vertebrae of *Calamosaurus foxi* (NHMUK R901) in anterior view; **i** right lateral view; **j** posterior view; **k** dorsal view; **l** ventral view; **m** isolated dorsal vertebra of *Baryonyx cf. walkeri* (UOP C001.2004) in anterior view; **n** left lateral view; **o** right lateral view; **p** posterior view; **q** holotype sacrum of *Ornithodesmus cluniculus* (NHMUK R187) in dorsal view; **r** right lateral view; **s** ventral view; **t** the so-called “*Calamosaurus* tibia” NHMUK R186 in anterior view; **u** posterior view; **v** isolated left coelurosaur femur MIWG 6124 in lateral view; **w** anterior view; **x** medial view; **y** isolated left coelurosaur tibia MIWG 5137 in medial view; **z** posterior view; **a'** lateral view; **b'** anterior view. *cncr* cnemial crest, *dp* diapophysis, *epi* epipophysis, *fc* fibular crest, *ft* fourth trochanter, *hyp* hyposphene, *ligfo* ligament fossa, *lco* lateral condyle, *mco* medial condyle, *mm* medial malleolus, *mp* metapophyses, *par* parapophysis, *pefo* pedicular fossa, *pnfos* pneumatic fossa, *spdl* spinodiapophyseal lamina, *vlg* ventrolateral groove, *vs* ventral sulcus. e-g modified from Owen (19876), m-p by Steve Hutt, q-s modified from Howse and Milner (1993). Scale bars 20 mm a-l, t-b'; 100 mm m-p.

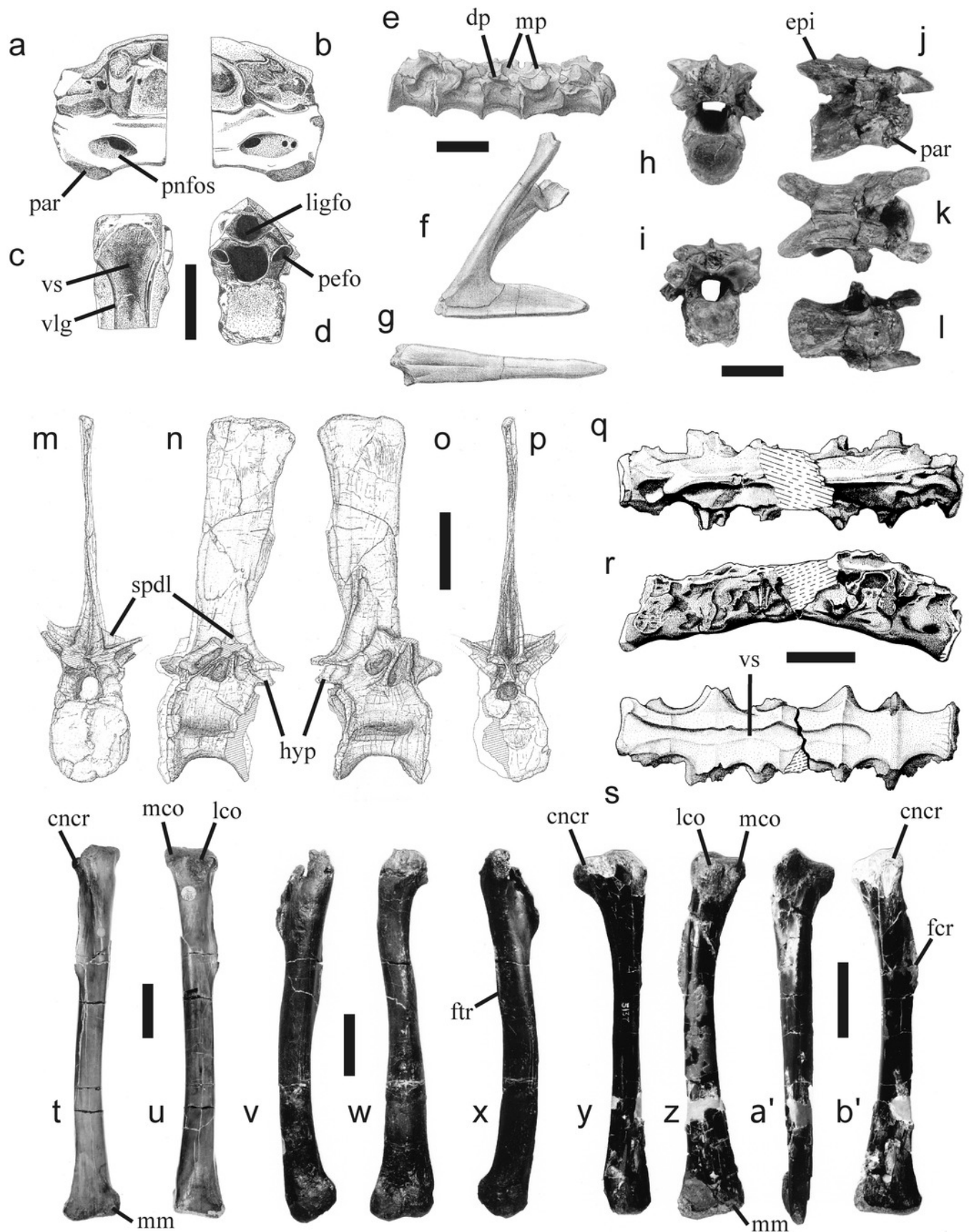


# Figure 27

Fig 27 Strict consensus topology of the shortest trees found by the analysis.

Numbers at nodes are Bremer Support values  $>1$ .

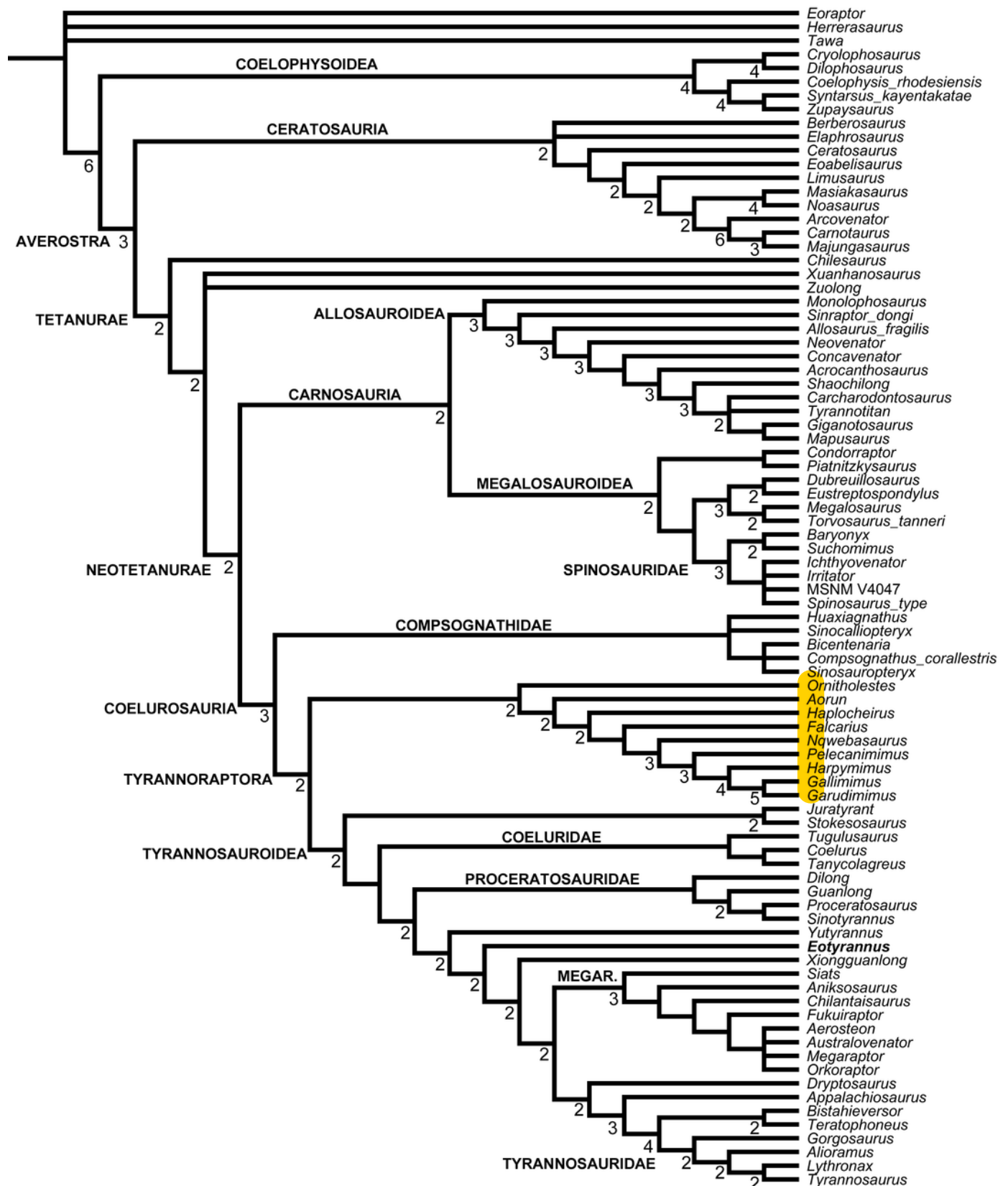


# Figure 28

Fig 28 Stratigraphically calibrated phylogeny of Tyrannosauroidae.

Geochronologic units modified from Carr and Williamson (2010). The black bars represent the possible stratigraphic ranges for taxa. Stratigraphic abbreviations: AA, Aalenian; AL, Albian; AP, Aptian; BA, Barremian; BAJ, Bajocian; BAT, Bathonian; BE, Berriasian; CA, Carnian; CAL, Callovian; CA, Campanian; CE, Cenomanian; CO, Coniacian; HA, Hauterivian; HE, Hettangian; J/K, Jurassic-Cretaceous boundary; KI, Kimmeridgian; MA, Maastrichtian; NO, Norian; OX, Oxfordian; PL, Pliensbachian; RH, Rhaetian; SA, Santonian; SI, Sinemurian; TI, Tithonian; TO, Toarcian; Tr/J, Triassic-Jurassic boundary; TU, Turonian; VA, Valanginian.

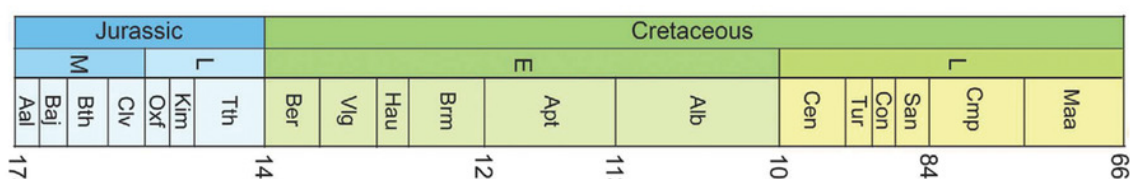
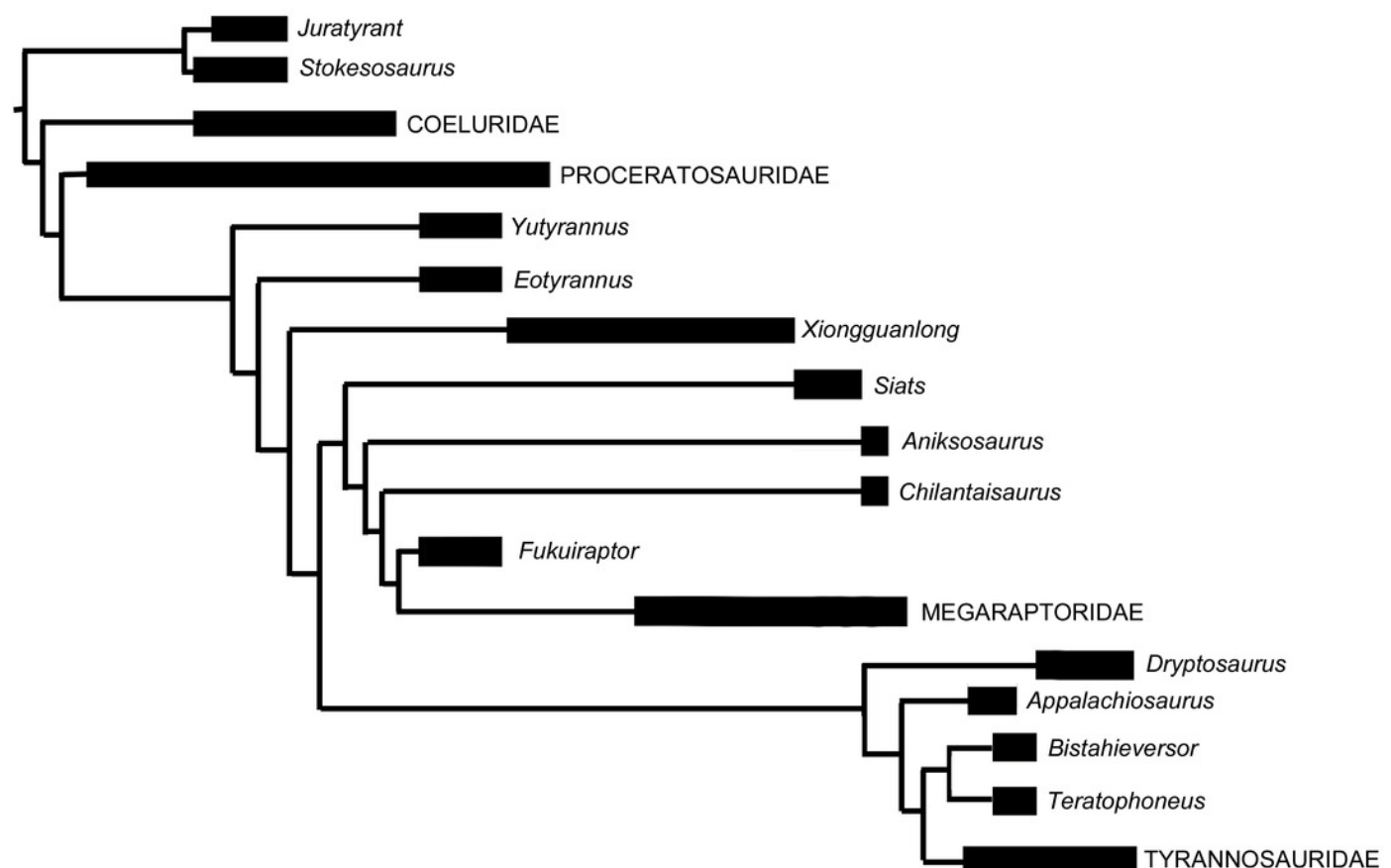




**Table 1** (on next page)

Table 1 Measurements (in millimetres) of the cranial elements of *E.lengi*.

Some measurements are approximate.

1	Premaxilla	
2	preserved height	44
3	height, body ventral to naris	c. 30
4	preserved length, body	36
5	mediolateral thickness, caudal end of body	10
6	height, most anterior interdental plate	2.5
7	length, most anterior interdental plate	2.5
8	<i>Maxilla</i>	
9	preserved length	95
10	preserved height	72
11	mediolateral thickness	c. 15
12	height, 4 <sup>th</sup> interdental plate	24
13	length, 4 <sup>th</sup> interdental plate	18
14	height, 5 <sup>th</sup> interdental plate	24
15	length, 5 <sup>th</sup> interdental plate	20
16	length, third alveolus	23
17	width, 3 <sup>rd</sup> alveolus	11
18	length, 4 <sup>th</sup> alveolus	22
19	width, 4 <sup>th</sup> alveolus	13
20	<i>Fused nasals</i>	
21	length	220
22	width, mid-length	33
23	maximum width	57
24	width, posterior end	43
25	maximum thickness	20
26	preserved length, dorsal border of right naris	15
27	depth of right naris at caudal end	15
28	<i>Lacrimal</i>	
29	preserved height	95
30	preserved length, dorsal end	c. 47
31	preserved length, ventral end	c. 30
32	length, mid-shaft	c. 15
33	<i>Palatine</i>	
34	preserved maximum length	88
35	maximum width, body	24
36	<i>Quadrate</i>	
37	maximum preserved height	82
38	width, across ventral condyles	40
39	<i>Left dentary</i>	
40	preserved length	147

41	height	40
42	length, 2 <sup>nd</sup> interdental plate	11
43	height, 2 <sup>nd</sup> interdental plate	12
44	length, 3 <sup>rd</sup> interdental plate	12
45	height, 3 <sup>rd</sup> interdental plate	15
46	<i>Right dentary</i>	
47	preserved length	130
48	height	46
49	length, 1 <sup>st</sup> interdental plate	c. 12
50	length, 2 <sup>nd</sup> interdental plate	18
51	height, 2 <sup>nd</sup> interdental plate	13
52	length, 3 <sup>rd</sup> interdental plate	c. 12
53	height, 3 <sup>rd</sup> interdental plate	17
54	length, 4 <sup>th</sup> interdental plate	c. 20
55	height, 4 <sup>th</sup> interdental plate	c. 17
56	height, 5 <sup>th</sup> interdental plate	c. 16
57	<i>Surangular</i>	
58	preserved length anterior half	116
59	width, anterior half	c. 1
60		

## Table 2 (on next page)

Table 2 Tooth measurements and denticle counts of selected teeth.

TCH, tooth crown height; FABL, fore-aft (mesial-distal) basal length, DSDI, denticle size difference index. All measurements (excepting DSDI) in millimetres.

1

	Total preserved length	TCH	FABL	Serrations per 5 mm, mesial carina	Serrations per 5 mm, distal carina	DSDI
pmx tooth 1	27	14	<i>c.</i> 5	-	-	-
pmx tooth 2	27	18	7	15	14	1.071
pmx tooth 3	51	<i>c.</i> 17	8	14	14	1.0
l dentary tooth	11	11	<i>c.</i> 8	17	14	1.214
lat tooth 1	59	<i>c.</i> 24	<i>c.</i> 12.5	-	16	-
lat tooth 2	50	<i>c.</i> 26	<i>c.</i> 14	-	-	-
lat tooth 3	23	23	<i>c.</i> 13	-	16	-
lat tooth 4	13	-	-	19	14	1.357
lat tooth 5	19	-	<i>c.</i> 12	-	14	-
lat tooth 6	36	-	15	-	22	-
lat tooth 7	>19	<i>c.</i> 19	-	<i>c.</i> 16	15	<i>c.</i> 1.067
lat tooth 8	26	26	<i>c.</i> 13	-	-	-
lat tooth 9	19	19	11	-	-	-

2

3

# **Table 3**(on next page)

Table 3 Measurements of preserved cervical neural arches of *E. lengi*.

All measurements in millimetres. Prezygs = prezygapophyses, n. a. = neural arch.



1

	Axial n. a.	2 <sup>nd</sup> cervical n. a
Neural arch length	50	72
Width, across prezygs	63	-
Width, space between prezygs	18	-
Height, neural spine	10	-
Length, neural spine	36	35

2

# **Table 4**(on next page)

Table 4 Measurements of preserved cervical vertebrae of *E. lengi*.

Centrum length measured along ventral mid-line. All measurements in millimetres. \* = estimated.

	Axial centrum	2 <sup>nd</sup> cervical centrum
Centrum length	40	37
Width of anterior articular surface	38	35*
Height of anterior articular surface	26	25*
Mid width of centrum		-
Width of posterior articular surface	20	-
Height of posterior articular surface	-	-

1

# Table 5 (on next page)

Table 5 Measurements of preserved dorsal vertebrae of *E. lengi*.

Centrum length measured along ventral mid-line. All measurements in millimetres. DV = dorsal vertebra. \* = estimated, as centrum incomplete. † = identification of this articular surface as anterior or posterior was arbitrary, and the identification was made for ease of tabulation.

	DV1	DV2	DV3	DV4	DV5	DV6	DV7
Centrum length	69	65	60	50	<i>c.</i> 50	-	-
Width, anterior articular surface	43	<i>c.</i> 45*	42	36†	<i>c.</i> 35†	39	54†
Height, anterior articular surface	37	-	38	42†	40†	<i>c.</i> 32	-
Mid width, centrum	22	30	25		19	-	-
Width, posterior articular surface	51	52	55	37†	<i>c.</i> 35†	-	50†
Height, posterior articular surface	<i>c.</i> 52	<i>c.</i> 50*	47	42†	-	-	-

1

**Table 6** (on next page)

**Table 6 Measurements of preserved** sacral and caudal vertebrae of *E. lengi*.

Length measured along ventral mid-line. All measurements in millimetres. CC = “cervical/caudal vertebra”: a specimen whose position within the vertebral column could not be determined with certainty (see text), CV = caudal vertebra, \*\* = measurements are preserved lengths because none of these vertebrae (except the sacral vertebra) are complete, \* = estimated, as centrum incomplete, † = identification of this articular surface as proximal or distal was arbitrary, and the identification was made for ease of tabulation.



	CC	sacral	CV1	CV2	CV3	CV5	CV6
Preserved length**	36	68	25	40	25	32	24
Width, proximal articular surface	32†	47	40†	37†	20†	-	-
Height, proximal articular surface	28*†	26	-	-	29†	-	-
Mid width, centrum	-	-	32	-	-	-	-
Width, distal articular surface	-	53*	-	-	-	25*	22
Height, distal articular surface	-	30*	-	-	-	22	-
Height, neural canal	-	-	-	-	-	6	6
Width, neural canal	-	30	-	-	-	5	5

1